418

BULK POLYMERIZATION OF ACRYLONITRILE

BULK POLYMERIZATION OF ACRYLONITRILE

By

LUIS HUMBERTO GARCIA RUBIO B.Sc.

A Thesis
Submitted to the Faculty of Graduate Studies
in Partial Fulfilment of the Requirements
for the Degree
Master of Engineering

McMaster University
May 1976

To my two Alicias

MASTER OF ENGINEERING (1976)
(Chemical Engineering)

McMASTER UNIVERSITY
Hamilton, Ontario

TITLE: BULK POLYMERIZATION OF ACRYLONITRILE

AUTHOR: LUIS HUMBERTO GARCIA RUBIO, B.Sc. Chemical Engineering
Universidad Nacional Autonoma de Mexico, Mexico

SUPERVISOR: Professor A.E. Hamielec

NUMBER OF PAGES: x, 169

ABSTRACT

This thesis reports on an experimental and theoretical study of the bulk polymerization of acrylonitrile to limiting conversions using 2,2' azobisisobutyronitrile initiator in the temperature range, 0°C to 120°C. Molecular weight averages and distributions were measured by gel permeation chromatography for polymers produced in the temperature range, 0°C - 120°C. A two-phase model which holds for the bulk polymerization of vinyl chloride was used in a preliminary attempt to explain the kinetic behaviour of the system. It appears that this model does not adequately describe the bulk polymerization of acrylonitrile.

ACKNOWLEDGEMENTS

The author wishes to express his gratitude to those who contributed to this work. He is particularly indebted to his research director, Dr. A.E. Hamielec, for his enthusiasm, interest and guidance throught the course of this study.

Dr. Niils Friss for his helpful advice and discussions. All his fellow graduate students for their help and cooperation. Mr. Dave Lowe for his conscientious help and cooperation. McMaster University and Petroleos Mexicanos for providing financial assistance.

Mrs. Lillian Mogensen for her careful and conscientious work in typing this dissertation.

TABLE OF CONTENTS

CHAPTER 1: INTRODUCTION

CHAPTER 2: MOLECULAR PROPERTIES OF POLYACRYLONITRILE

CHAPTER 3: PHYSICAL PROPERTIES OF POLYACRYLONITRILE

CHAPTER 4: MECHANISM OF BULK POLYMERIZATION OF ACRYLONITRILE

LIST OF FIGURES

PAGE

LIST OF TABLES

CHAPTER 1

INTRODUCTION

1 General

Acrylonitrile (AN) is an exceptionally versatile chemical and has been extensively studied (4,7,24,28). Among its properties, AN can be polymerized using free radical initiation. AN polymers have become very important commercially and have, therefore, been studied from almost every possible aspect, including polymerization kinetics, polymer characterization, degradation and processing. Despite these studies, many fundamental problems remain unsolved. For example, there are very few studies dealing with the molecular weight distribution of the homopolymer. There is a great discrepancy in the Mark Houwink constants for the viscosity-molecular weight relationship (24). A wide range of glass transition temperatures have also been reported (24). The kinetic behaviour for heterogeneous polymerization of AN is not fully understood and there is no model to date that predicts molecular weight distributions (MWD) and conversion histories over a wide range of conversions and temperatures.

This thesis reports on an experimental and theoretical study of the free radical bulk polymerization of acrylonitrile. For the first time, conversion histories up to limiting conversions are reported and analysed for 40°C, 60°C and 80°C. Molecular weight averages and distributions were obtained by gel permeation chromatography (GPC) for polymers produced in the temperature range 0°C - 120°C. Solubilities of the monomer in the polymer were measured gravimetrically, and the glass transition temperature estimated from the rate data, The theory of two-phase models is reviewed and the kinetic behaviour analysed.

The objective of this work was to provide experimental data to elucidate bulk polymerization kinetics of AN and to provide another step towards the understanding of other more important polymerization processes for AN, such as bulk, emulsion and suspension for homo and copolymerization. These reactions are also heterogeneous and it has been shown (2,29) that bulk polymerization can provide useful data for the modelling of polymerizations in other media.

1.1 Acrylonitrile Monomer (4,7,24,28)

Acrylonitrile monomer CH_2=CHCN is a colourless liquid with a rather penetrating characteristic odour. Its properties are summarized in Table 1-1. It is produced as a high grade chemical with practically no impurities and is usually stored in the presence of small concentrations of inhibitors. The most widely used are ammonia, ammonium carbonate and hydroquinone.(4) AN is very sensitive to light and excessive exposure causes it to darken and polymerize.

AN is a neurotoxin and both the liquid and vapour are toxic. Poisoning may result from inhalation of the vapour or adsorption through the skin. Care must be excerised when handling it.(4,7,24,28) Acrylonitrile or vinylcyanide was first reported by Moreau, 1893.(51) It is extremely important in synthetic fibers and plastics and is also

TABLE 1-1

PROPERTIES OF ACRYLONITRILE MONOMER

Appearance	Colourless liquid
Odour	Faintly pungent
Molecular weight	53.06
Freezing point	-83.55°C
Boiling point	77.3°C
Critical pressure	34.9 atm
Critical temperature	246°C
Flash point	0°C
Explosive limits in air	3.05 to 17% volume at 25°C
Density	0.8060 gr/cc
Vapour pressure at 0°C	40 mmHg
20°C	80 mmHg
40°C	200 mmHg
60°C	440 mmHg
80°C	815 mmHg
Refractive index	1.3888
Viscosity	0.31 centipoises (25°C)
Heat of polymerization	17.3 kcal/mol
Solubility	Miscible in most organic solvents including acetone, benzene, carbon tetrachloride, ether, ethanol, ethylacetate, ethylencyanohydrin, methanol toluene is partially soluble in water

used in a number of processes making use of the versatile cyanoethylation reactions. It can be obtained via a great variety of reactions (4,7).

1.2 Polymerization of Acrylonitrile

AN may be polymerized by any of the conventional techniques. Bulk, solution, emulsion, suspension slurry and even in the solid state. The process may proceed either by free radical or anionic mechanisms and it may be initiated chemically or with radiation sources.

1.2.1 Bulk Polymerization

It may appear at first sight that the simplest method of production of polyacrylonitrile is the polymerization in bulk, but this method suffers from some practical disadvantages. The reaction, autocatalytic in nature, is rapid and exothermic and when the degree of conversion is high, heat removal is very difficult, the reaction goes out of control and frequently ends with an explosion. This type of polymerization is not practiced in industry.

1.2.2 Solution Polymerization

When polymerized in solution, acrylonitrile behaves like a typical vinyl monomer and is industrially important because solutions for spinning and casting can be prepared directly from the reaction mixture after the polymerization is completed, avoiding the washing steps.

The polymerization rates show square root of the initiator concentration dependency (68), termination is mainly by combination (35) and transfer to monomer or to a transfer agent appears to control the MWD (60).

1.2.3 Polymerization in Aquous Medium

Emulsion polymerization, suspension and polymerization with the monomer dissolved completely in water overlap since acrylonitrile and water form a partially soluble system. In emulsion polymerization, catalysts soluble in water but insoluble in monomer are used, while the converse is true for suspension polymerization.

To produce polyacrylonitrile used in synthetic fiber production suspension polymerization with redox initiators or polymerization of acrylonitrile completely dissolved in water is used, whereas in most copolymerization cases, emulsion polymerization is used. (28)

Suspension polymerization and polymerization with the monomer completely dissolved in water follow very much the same pattern as with bulk polymerization. However in this case, the monomer is subdivided and therefore effectively cooled.

1.2.4 Slurry Polymerization

For this type of polymerization process the monomer is diluted in a substance which is a nonsolvent for the polymer. The general features of bulk polymerization are retained. Microscopical studies (48,68) have shown that the number of particles and its structure varies very much with the choice of diluent. The analogy of these systems with emulsion polymerization has been suggested (68) and the monomer adsorption by the polymer and extent of aggregation and swelling regarded as important factors in the polymerization process.

1.2.5 Anionic Polymerization

Acrylonitrile is one of the most reactive monomers toward anionic catalysts. In these systems, the propagating species is the $-CH_2-CHCN^-$ anion, propagation of this type is very susceptible to termination by proton donors. Therefore, most of the polymerizations are carried in aprotic solvents such as tetrahydrofuran, ethers, etc. The disadvantages encountered with anionic polymerization in general are: the heterogeneous characteristic of the reaction, meaning that the polymer is insoluble in most of the solvent systems, and the alkaline conditions favour the occurrence of cyanoethylation as side reaction. Since anionic polymerization can be conducted at low temperatures, cyanoethylation reactions can be avoided and those conditions would favour the formation of stereoregular polymer with narrow molecular weight distribution, but unfortunately, there is little information published at this point. (71)

1.3 Commercial Uses of Polyacrylonitrile (PAN)

The major industrial application of PAN homopolymer is in the fiber industry. The polymers are often prepared in heterogeneous systems and then dissolved in one of the appropriate solvents to give a solution from which fibers may be spun. Some processes employ homogeneous polymerizations giving a polymer solution suitable for spinning.

PAN is difficult to mold, it does not melt and flows only under severe conditions. To produce polymers with good molding characteristics acrylonitrile is usually polymerized in the presence of comonomers. Here is where the most important applications of AN are, because acrylonitrile is a substance which is capable of imparting unusual properties to polymeric materials, both by polymerization and copolymerization. Special characteristics of PAN include: hardness, heat resistance and slow burning, resistance to most chemicals and solvents, resistance to sunlight exposure, ability to form oriented fibers and films, and reactivity toward nitrile group reagents, for example, polyacrylic acid or polyamide can be obtained by acid or alkaline hydrolysis of polyacrylonitrile.

1.4 Copolymers of Acrylonitrile

Among the more important copolymers of AN are: acrylonitrile-butadiene, acrylonitrile-vinyl chloride, acrylonitrile-styrene, acrylonitrile-butadiene-styrene.

1.4.1 Graft Copolymers

Graft copolymers of PAN have received much attention. A considerable part of this arose in efforts to make a satisfactory basic polymer for fiber production. It seemed possible that by segregating the basic constituents in a chain grafted to the main backbone, the deleterious effects of the bases on the polymer colour would be reduced. An example is the acrylonitrile-vinyl chloride graft copolymer used in the modacrylic fibers. Three basic techniques are used: the first one utilizes a chain transfer in a free radical reaction to produce active centers on a preformed polymer from which chains of a second polymer may be grown, the second relies on activating the preformed polymer by high energy radiation and the third involves the use of ceric ions. (7)

1.4.2 Acrylonitrile-Butadiene

Most of these rubbers are based on copolymers containing 15-55% acrylonitrile, and by varying the methods of compounding, a wide range of rubbers may be produced. Properties which can be enhanced by the appropriate method of fabrication are abrassion resistance low compresion set, low coefficient of friction, low-temperature flexibility, oil resistance, non addition to metal and good electrical conductivity. Therefore, nitrile rubbers are specially useful for seals, solvent resistant bases, soles, flexible joints and adhesives.

1.4.3 Acrylonitrile-Vinylchloride

This copolymer is used in the manufacture of modacrylic fibers to give a fiber which is flame resistant but they have poor colour and light stability (1).

1.4.4 Acrylonitrile-Styrene

Acrylonitrile-styrene copolymers are thermoplastic polymers of increasing commercial importance, they are strong, rigid and transparent. AN resins have an excellent balance of physical and chemical properties. Retain most of the transparency of general purpose polystyrene, they can withstand more impact, and exposure to a wider range of chemicals without degradation.

1.4.5 Acrylonitrile-Butadiene-Styrene (ABS)

ABS polymers are thermoplastic polymers produced either by blending styrene-acrylonitrile copolymer resins with butadiene based elastomers or by grafting styrene and acrylonitrile onto polybutadiene. They exhibit an extraordinarily desirable combination of mechanical thermal, chemical and electrical properties as well as easy processing.

CHAPTER 2

MOLECULAR PROPERTIES OF PAN

Molecular properties are those class of properties associated with the arrangements of atoms in the molecules themselves. They are created during synthesis, but once the polymer has been formed, they cannot be changed by processing without bond breaking. These properties are: chain configuration, branching and molecular weight distribution.

2.1 Chain Configuration

It is believed that polymerization of acrylonitrile takes place by head to tail mechanism (28):

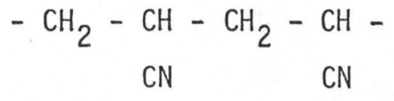

$$-\mathrm{CH_2}-\underset{\mathrm{CN}}{\mathrm{CH}}-\mathrm{CH_2}-\underset{\mathrm{CN}}{\mathrm{CH}}-$$

The infrared spectra of AN polymers generally do not contain absorption bands characteristic for ketenimine units, showing therefore that nitrile groups do not participate in polymerization processes. In some anionic processes, addition 1,4 has been reported. (28)

Syndiotactic conformation is generally accepted. Stereoregularity for polymers produced at several temperatures has been studied by Murano and Yamadera (73), using high resolution NMR spectroscopy. They conclude that almost all polyacrylonitriles have the syndiotactic part predominantly and that the syndiotactic placement probability increases as the polymerization temperature decreases.

2.2 Branching

Polyacrylonitrile is considered essentially linear (27) although long chain branching has been reported for the high molecular weight fractions. (58) X-ray data on PAN do not permit a definitive conclusion concerning its structure. The abnormal behaviour in molecular weight determinations has been related to association. (58)

2.3 Molecular Weight Distribution

Despite numerous studies which have been reported for PAN (24), the reliability of $\overline{M}n$ and $\overline{M}w$ values remains in doubt. Relatively little work has been published on the molecular weight distributions.

The measurements for both, the averages and the distributions, are characterized by a surprising lack of agreement; variations of more than 100% have been reported. (45) The molecular weight measurements are strongly influenced by polymer-solvent and polymer-polymer interactions. It has been shown that PAN associates. (11) Evidence of association has been provided by light scattering and electron microscopy. (11,58) Strong Zimm plot distortion has been encountered (25,58) and correlated with the presence of microgel or branching, therefore fractionation by addition of a nonsolvent is difficult and inhomogeneity in the fractions is considered the main source of discrepancy. (41) One of the best known viscosity-molecular weight relations for PAN is that published by Cleland and Stockmayer (27). Using unfractionated samples of polymers produced in solution at low conversion, the molecular weights were measured by light scattering, the relation obtained is:

$$[\eta] = 2.33 \times 10^{-4}\overline{Mw}^{0.75}$$

The weight averages were transformed into viscosity averages assuming the most probable distribution, that is, transfer reactions control the MWD. Giving the final relation:

$$[\eta] = 2.43 \times 10^{-4}\overline{Mv}^{0.75}$$

These relations are claimed to be applicable over the range DP 150 - 1320.

Onyon (54,55) reported two molecular weight-viscosity relations derived from that of Cleland and Stockmeyer:

$$[\eta] = 3.92 \times 10^{-4}\overline{Mn}^{0.75}$$

$$[\eta] = 3.20 \times 10^{-4}\overline{Mn}^{0.75}$$

The first one is for polymers formed by transfer or disproportionation and the second one is for polymers formed by combination.

These relations are claimed to be applicable for unfractionated polymers over the range DP 1770 - 10^4.

Bamford, et.al. (9) derived a MWD equation for polymers produced by transfer or combination:

$$[P_r] = \Delta M \frac{k_{tc}[R^\circ]}{k_p[M]} (1 - \xi)\, \xi^n \{\beta + \frac{1}{2}\, r(1 - \xi)$$

where

$$\xi = \frac{K_p[M]}{k_p[M] + k_{fs}[S] + k_{tc}[R^\circ] + k_{fc}[FeCl_3]}$$

$$\beta = \frac{k_{fs}[S] + k_{fc}[FeCl_3]}{k_{tc}[R^\circ]}$$

and substituting into the equation for ideal specific viscosity

$$[\eta] = KMo^{\alpha} \int_{1}^{\infty} [Pr]r^{1+\alpha}dr$$

obtained the expression:

$$[\eta] = K_1\overline{Mn}^{\alpha}\, f(\beta)$$

where

$$f(\beta) = \frac{(\beta + \frac{1}{2})^{\alpha}}{(\beta + 1)^{\alpha}}\{\beta + 1 + \frac{\alpha}{2}\}$$

The limiting values of $f(\beta)$ are unity (when $\beta = \infty$, exclusive transfer, or equivalent) and $(2 + \alpha)/2^{1t\alpha}$ ($\beta = 0$, exclusive combination).

The weight average molecular weight to number average molecular weight ratio is given by

$$\frac{\overline{Mw}}{\overline{Mn}} = \frac{(2\beta + 3)(\beta + \frac{1}{2})}{(\beta + 1)^2}$$

From the polydispersity ratio and the equations for intrinsic viscosity the following relations were obtained:

$$[\eta] = 5.74 \times 10^{-4} f(\beta)\overline{M}n^{0.733}$$

$$[\eta] = 5.74 \times 10^{-4} F(\beta)\overline{M}w^{0.733}$$

where

$$F(\beta) = \frac{\beta + 1 + \frac{\alpha}{2}}{(\beta + 1)^{1-\alpha}(2\beta + 3)^{\alpha}}$$

in the limiting case for molecular weights controlled by transfer:

$$[\eta] = 5.74 \times 10^{-4}\overline{M}n^{0.733}$$

by combination:

$$[\eta] = 4.72 \times 10^{-4}\overline{M}n^{0.733}$$

in both cases, the following is reported a good approximation

$$[\eta] = 3.46 \times 10^{-4}\overline{M}w^{0.733}$$

over the range DP 50 - 550.

Bisschops (22) using DMF/Heptane solvent system, fractionated PAN polymers and the intrinsic viscosities were measured in DMF at 25°C. The molecular weights were determined by the sedimentation-diffusion method.

The relation obtained over the range DP 904 - 5100 is

$$[\eta] = 1.66 \times 10^{-4}\overline{M}w^{0.81}$$

Krigbaum and Kotliar (45) attempted to explain the differences encountered in the literature. Light scattering, osmometry and sedimentation were used. The solvents were DMF, deionized DMF, 0.5M LiBr/DMF, 1.0M KI/DMF, fractionated and unfractionated polymers were used. The fractions were obtained from DMF with heptane as nonsolvent and the measurements were done at several temperatures.

The following conclusions were drawn:

(i) the water content in DMF affects considerably the osmometry measurements and favours aggregation.

(ii) the pH of the solution seems to be important. Deionized solutions which are basic showed erratic behaviour and great difference appeared between solutions prepared with deionized DMF and deionized solutions.

(iii) The difference between the values of Cleland and Stockmeyer and those of Bisschops are due to a systematic error in the light scattering measurements.

The following relation is proposed which compromises between the relations of Cleland and Bisschops.

$$[\eta] = 1.55 \times 10^{-4}\overline{M}w^{0.8}$$

Kobayashi (41) studied the variations on the second virial coefficient (A2) diffusion constant (Do) and intrinsic viscosity with molecular weight for fractionated polymers. The fractions were obtained from DMF with benzene as nonsolvent and the light scattering measurements were performed in DMF at 35°C giving the following relation:

$$[\eta] = 2.78 \times 10^{-4}\overline{Mw}^{0.76}$$

The possible causes of discrepancy were analyzed and attributed mainly to inhomogeneity in the fractions. His results agree partially with those of Bisschops in the molecular weight range 2.8×10^4 to 57.5×10^4.

In a series of subsequent publications, Kobayashi (42) and Fujisaki and Kobayashi (32) studied the molecular weight-intrinsic viscosity relation over the temperature range 35°C - 50°C for fractionated polymer in several solvents. The solvent nonsolvent system used was Dimethyl sulfoxide/Toluene, the molecular weights were measured by light scattering. In DMF, the following relations were obtained.

$$[\eta] = 3.17 \times 10^{-4}\overline{Mw}^{0.746} \quad \text{at } 35°\text{C}$$

for the molecular weight range $9 \times 10^4 - 76 \times 10^4$, and

$$[\eta] = 3.0 \times 10^{-4}\overline{Mw}^{0.752} \quad \text{at } 50°\text{C}$$

over the range $4 \times 10^4 - 102 \times 10^4$.

The intrinsic viscosity variations with temperature were also analyzed. A complex behaviour was observed for the intrinsic viscosity-molecular weight relation and no further conclusions were drawn.other than intrinsic viscosity decreases with increasing temperature.

Inagaki (34) analyzed, using light scattering in DMF samples of fractionated polymers prepared at low temperatures and at 60°C. For polymers prepared at 60°, the relation obtained is in agreement with that of Cleland and Stockmeyer. For the polymers produced at low temperature, the following relation was obtained at 20°C over the molecular weight range $7 \times 10^4 - 30 \times 10^4$:

$$[\eta] = 1.77 \times 10^{-4}\overline{Mw}^{0.78}$$

Peebles (58) reported a strong Zimm plot distortion for the high molecular weight range and his results were not in agreement with either Stockmeyers or Bisschops' equation. In a more recent publication (59), Peebles proposed another intrinsic viscosity molecular weight equation for polymers produced in ethylene carbonate by azo catalysts. The molecular weights were determined by light scattering in DMF for unfractionated polymers. The equation for intrinsic viscosity in DMF at 25°C is

$$[\eta] = 6.98 \times 10^{-4}\overline{Mw}^{0.645}$$

for the molecular weight range $0.824 \times 10^5 - 23 \times 10^5$.

Intrinsic viscosities for two polymers of different molecular weights were measured at 60° and 0°C. Two opposite effects were observed. An increase in the polymer-solvent interaction as shown by an increase in α, and a decrease in polymer-polymer repulsion by a decrease in K_θ, both which occur with an increase in temperature. The increasing flexibility overrides the expansion coefficient and hence viscosity decreases with increasing temperature.

Chiang and Stauffer (26) determined the weight average molecular weight of unfractionated AN polymers prepared in solution by a free radical initiator and an organometallic catalyst, by light scattering measurements in DMF, DMSO and DMAc at 25°C, and in DMSO at 140°C. The results in DMSO at 140°C gave relations in agreement with that of Cleland and Stockmeyer. High molecular weights were obtained for the polymers produced with the organometallic catalyst when measured in DMF at 25°C. The apparent decrease in molecular weight from 25°C to 140°C is an indication of association. They concluded that aggregation is not present in PAN produced by free radical polymerization. The aggregates cannot be removed by centrifugation or ultrafiltration and when present even in small concentrations, affected substantially the molecular weight measurements. The increase in turbidity to a maximum followed by a sudden drop and the small increase in intrinsic viscosity of a sample heated over a period of time are considered conclusive in favour of aggregation. No degradation is assumed, intrinsic viscosity is only slightly affected by aggregation over a wide temperature range (25°C - 140°C) and that DMSO appears to be preferable to DMF as solvent for light scattering measurements because PAN samples are more stable in DMSO.

Cha (25) studied the MWD of PAN and copolymers of AN carring a sulfonate group by GPC. Two solvents were used, DMF and 0.1M LiBr/DMF. No association was reported but strong effects due to the polarity and ionization of the polymers, concluding that valid GPC results could only be obtained by swamping out the electrostatic effect, This can be achieved by adding an electrolyte such as LiBr to the carrier solvent. The polydispersity reported for PAN is 3.86 for the GPC measurements, and 2.2 for light scattering and osmometry measurements.

Kenyon and Mottus (38) determined the molecular weights of AN copolymers by GPC in DMF and LiBr/DMF solvents at 55°C. Unimodal chromatograms were obtained for polymers in LiBr/DMF whereas some bimodal character was observed in DMF. This is attributed to an interaction between the dipoles of the polymer and the dipoles of the solvent which could lead to a form of association. Intrinsic viscosities were found nearly the same in both solvent systems which indicates that the salt has a small effect on the molecular size. To calibrate the GPC, a fractionated copolymer containing approximately 10% VA was characterized. The viscosity average molecular weights were determined using the Cleland and Stockmayer equation and the weight average molecular weights calculated from the Lanzing-Kraemer distribution. Reasonable agreement was observed for molecular weights determined by PVC calibration and by an AN copolymer of known distribution. PVC and AN copolymers seem to have close to the same behaviour in DMF solvents where the polarities can be assumed close. The hydrodynamic volume theory was applied using polystyrene narrow standards but no agreement was found. The molecular-weight-viscosity relation obtained for AN/vinyl copolymers in LiBr/DMF at 55°C is

$$[\eta] = 1.42 \times 10^{-5} \overline{M}_w^{0.9636}$$

The large exponent obtained suggests that GPC is much more sensitive to dipolar effects than is viscosity. Such a large value would indicate a possible change in shape and therefore the hydrodynamic volume theory would not be expected to hold.

In this study, the molecular weight averages and distributions were determined by GPC in 0.05M LiBr/DMF solvent at 25°C (see Chapter 4), for PAN produced in bulk with azo initiator over the temperature range 0°C - 120°C. The intrinsic viscosities for the polymers were in agreement with previous values reported for the same polymerization process. (69) The calibration curve was obtained from a well characterized AN copolymer and from PVC standards (Fig. 4-6). The solutions were heated and reinjected, but the results showed no indication of aggregation. The weight average and number average molecular weights varied slightly with conversion, being practically constant over a wide temperature range (25°C - 100°C) showing a slight maximum near 60°C (13,21) (Figs. 4-30 to 4-32). The polydispersity ratios are close to 2.2 through most of the reaction (25), increasing at high temperature (Figs. 4-33, 4-34). The nearly constant polydispersity ratio at different temperatures is an indication that the polymer is linear or practically unbranched. The fact that its value is close to 2 indicates that transfer reactions are important in controlling the MWD (1), as it has been reported previously (27,56,58). The hydrodynamic volume theory was tested using narrow polystyrene standards and the intrinsic viscosity-molecular weight relations available. Good agreement was found using the relation reported by Fujisaki and Kobayashi.(32)

From the results reported here and in the literature, the following conclusions may be drawn.

The discrepancies in the intrinsic viscosity molecular weight relation are due mainly to poor efficiency of the fractionation method. Therefore the agreement obtained using the equation of Fujisaki and Kobayashi is not surprising since their fractionation procedure seems to be more effective, and the measurements were done at higher temperatures where no abnormal behaviour for PAN solutions has been reported. Another source of discrepancy appears to be the use of unfractionated polymers produced at different conditions with different processes. Differences in the MWD would cause large errors in the molecular weight determinations. Finally, abnormal behaviour of PAN solutions at temperatures close to room temperature will account for the "aggregation" reported.

CHAPTER 3

PHYSICAL PROPERTIES OF POLYACRYLONITRILE

These are the class of properties associated with the physical behaviour of the polymer. They depend on the molecular properties but can be altered by processing. Examples of those properties are:

3.1 Crystallinity

In comparison with many polymers not much is known about the microstructure of PAN. Ordinarily, PAN exhibits good lateral order but is poorly ordered along the chain axis (23), that is, it possesses a high degree of directional crystallisation in the solid state. (65) Two types of intermolecular bonds have been considered in the association of PAN. Hydrogen bonds (Fig. 3-1a) and the formation of a CN dipole pair bond (65) (Fig. 3-1b).

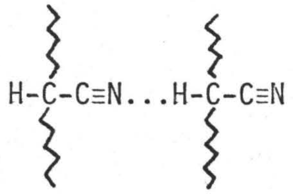

Fig. 3-1a

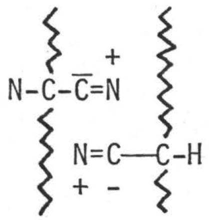

Fig. 3-1b

It is probable that both hydrogen and dipole CN pair bonds form between the polymer molecules as the results obtained for the glass transition temperature appear to show. (6,13)

3.2 Glass Transition Temperature

The glass transition temperature (Tg) is determined by the freedom of molecular motion. This mobility depends on the internal stiffness of the chain and on the strength with which the neighbouring chains hold together. These factors depend also on stereoregularity and are given by the chemical structure of the chain. The molecular weight has also some influence and in the molecular weight range of 100,000, a slow decrease in Tg with decreasing molecular weight may be observed.(22) Most of these properties are not well defined for PAN and therefore, the wide range in temperatures reported is not unexpected. (24)

The glass transition temperature of acrylonitrile homo and copolymers has been studied by variations of dielectric dispersion, density, linear thermal expansion and refractive index.(12,33,46,63) The temperatures reported for the homopolymer lie in the range 85°C - 140°C. In this study, Tg was determined from rate data (Fig. 4-16). The value obtained (110°) is in agreement with the value obtained by Howard (33) for amorphous PAN from linear thermal expansion studies, with Krigbaum and Tokita (46) which obtained a value of 104°C from melting point depression studies and with Kogura et al. (43) which reported four transition points (90°C, 110°C, 120°C and 140°C) by infrared absorption spectrophotometry.

3.3 Crystalline Melting Temperature

This is defined as the melting temperature (Tm) of the crystalline domains of the polymer, and it is a strong function of stereoregularity and crystallinity. The crystalline melting temperature for PAN can not be measured by direct techniques because polymer decomposition is too rapid at elevated temperatures. Using a melting point depression technique, Krigbaum and Tokita reported a value of 319°C for Tm. (46)

3.4 Solubility (24)

PAN is a relatively insoluble polymer. The known solvents are generally polar solvents and include the following organic compounds: N-N Dimethylformamide, N,N-dimethylacetamide, N,N-diethylacetamide, dimethylsulfone, dimethylsulfoxide, ethylenecarbonate, propylenecarbonate, nitrophenols, γ-butyrolactone and succionitrile. In addition, concentrated solutions of very soluble salts such as LiBr, $ZnCl_2$, NaCNS, $Ca(CNS)_2$, $NaClO_4$, quaternary ammonium salts, molten quaternary ammonium salts, solutions of the latter in organic nitriles including acrylonitrile, and concentrated nitric and sulfuric acids are also solvents.

No theta solvent has been reported for PAN.

3.5 Aggregation

It has been known for some time that PAN molecules form aggregates and that these entities dissolve very slowly. As mentioned before, the presence of these aggregates leads to difficulties in measurements using dilute PAN solutions. (22,26,50,58) It has been suggested from analysis on the molecular weights that very few large aggregates are present (11,46) and the microgel formed is very stable and cannot always be removed by centrifugation. (26,58) Heat treatment has been suggested to break the aggregates. (14-17,26) It is interesting to note that Chiang and Stauffer (26) reported a sharp drop on turbidity by heating a solution of PAN produced with organometallic catalysts in DMF to 140°C for six hours and no degradation was observed. Whereas in this study, heat treatment was applied at 120°C to free radical PAN dissolved in DFM. After one hour, the degradation was considerable (see Appendix 9-3.) This seems to indicate that the PAN produced by Chiang and Stauffer has a high degree of stereoregularity.

Rate constants for aggregation in DMF/Benzene have been measured (4) and the results reported indicate that association is mainly caused by formation of CN dipole pair bonds (Fig. 3-1b).

3.6 Chemical and Thermal Stability

Because of the fact that nitrile groups in the PAN molecules do not participate in the chain formation, they retain their activity. A number of polymer-analogous reactions can therefore be carried out with PAN. Thus, for example, a polyamide or polyacrylic acid can be obtained by acid or alkaline hydrolisis.(28) A water soluble polymer containing carboxy, amide and nitrile groups can be obtained by the alkaline hydrolisis of PAN. An acrylonitrile-acrolein copolymer can be obtained by carrying out a Stephen reaction with PAN. (4,28)

The general stability of PAN is not very high. It is soluble in sulfuric acid and unstable toward other mineral acids, alkalies, formic acid, anyline and pyridine, but is resistant to the action of organic acids, alcohols and most of the common organic solvents.

When heated at 80°, PAN becomes discoloured (even with the exclusion of air). It first becomes yellow, then brown and finally dark brown and black. As the colour gets darker, the mechanical strength decreases. A cyclization process is hypothesized to occur according to the following scheme.

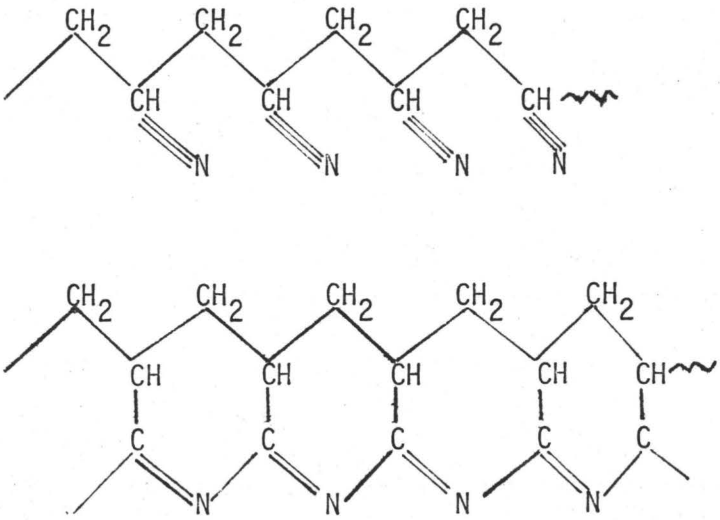

if oxygen is present $+nO_2$

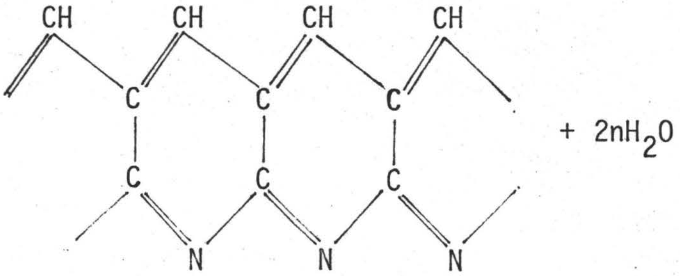

Fig. 3-2

It cannot be demonstrated that the arrangement of the ring units in the chain of cyclized PAN as it is described by the above formulas is true for the whole polymer chain. Rather this formula represents a more or less long segment of the chain. (71) This cyclization reaction is used to produce a flame resistant fabric ("Black Orlon" DuPont) in which this ladder type structure seems to play an important role in its thermal stability.

The cyclization reaction has been reported for temperatures as low as-80°C which is below AN glass transition temperature. (71) Therefore PAN does not soften or melt and cannot be processed by methods used for thermoplastic materials and is not associated with the evolution of volatile products. Recently (19) thermal degradation studies have been reported in the temperature range 200° - 850°C. A micropyrolysis technique was used. The kinetics of thermal degradation and the laddering stabilization process are discussed in this paper.

CHAPTER 4

MECHANISM OF BULK POLYMERIZATION OF ACRYLONITRILE

Bulk polymerization of acrylonitrile is a typical example of what is known as "precipitation polymerization". Other examples are the bulk polymerizations of vinyl chloride and vinylidene chloride. These systems have the following general characteristics:

1. The reaction is heterogeneous, meaning that the polymer is insoluble in the monomer. Since there is no solvent in bulk polymerization, polymer precipitates during the reaction.
2. The reaction is autocatalytic. The rate increases with conversion up to a given conversion where it reaches a maximum, then starts to drop and finally a limiting conversion less than 100% is reached.
3. Transfer to monomer controls the molecular weight distribution for PVC and appears to do so for PAN as well.

4.1 General

The polymerization in bulk of acrylonitrile has been studied extensively. (7-10,68,69) Despite this, the mechanism is still a matter of controversy.

The main features of the bulk polymerization of AN are discussed in this section and the models proposed discussed in the following chapter.

Polymerization is initiated readily by light, by azo and peroxi compounds, by ionizing radiation, or in general, by any source of free radicals. The monomer is quite stable and uncatalyzed thermal polymerization is negligible. Oxygen is a very strong inhibitor of the reaction.

The sudden appearance of a haze signals the beginning of polymerization with polymer precipitating. Ordinarily, the haze does not extend uniformly through the tube but appears as a cloud along the axis of the tube beginning near the bottom. Turbidity increases rapidly and particles can be seen with the unaided eye. As the reaction proceeds further, the suspension begins to coagulate, and the slurry gradually increases in thickness. At approximately 50% conversion, the reaction mixture is a hard coarse, white solid. Particles are fairly densely packed aggregates porous to nitrogen. (48, 68) They are several thousands angstroms across and comprise many small particles of diameter, 100 to 1000 Å or more. (68) As the reaction proceeds further, the monomer seems to disappear in a solid mass of polymer. Towards the end of the reaction (limiting conversion) the polymer forms a dense white solid.

A large amount of heat (17 Kcal/mole) is given off during the polymerization, (68) and the character of the slurry and the solid polymer is such that heat is not easily transferred. Unless the sample is small and the rate of polymerization small, the temperature is likely to rise rapidly and lead to an uncontrolled reaction.

A typical conversion-time curve exhibits a short period of acceleration followed by a nearly constant rate and then followed in turn by a rate rapidly diminishing to zero. The acceleration period is sometimes reported to persist to quite high conversions.

4.2 Experimental

4.2.1 Reagents

The initiator 2-2' azobisisobutironitrile (AIBN) (Eastman Organic Chemicals) was recrystallised twice from absolute methanol. The solvent for GPC analysis was N-N Dimethylformamide (Chinook Chemicals Ltd) technical grade. The monomer acrylonitrile practical grade was obtained from J.T. Baker Chemical Co. The analysis provided by J.T. Baker is given in Table 4-1. Lithium Bromide (Fisher) purified grade was used as electrolyte in the carrier solvent.

4.2.2 Apparatus and Procedure

Polymerization was carried out in 10 inch long glass ampoules of different diameters (Fig. 4-1). Type 2 and 3 are the conventional straight tube ampoules and were used for two different levels of conversion. A capillary ampoule was also used to examine whether isothermal conditions prevailed by having the reaction conducted in ampoules having different surface area to volume ratios. Type 1 were used to prepare the GPC solutions "in situ" for conversion and MWD analysis. The general procedure was as follows.

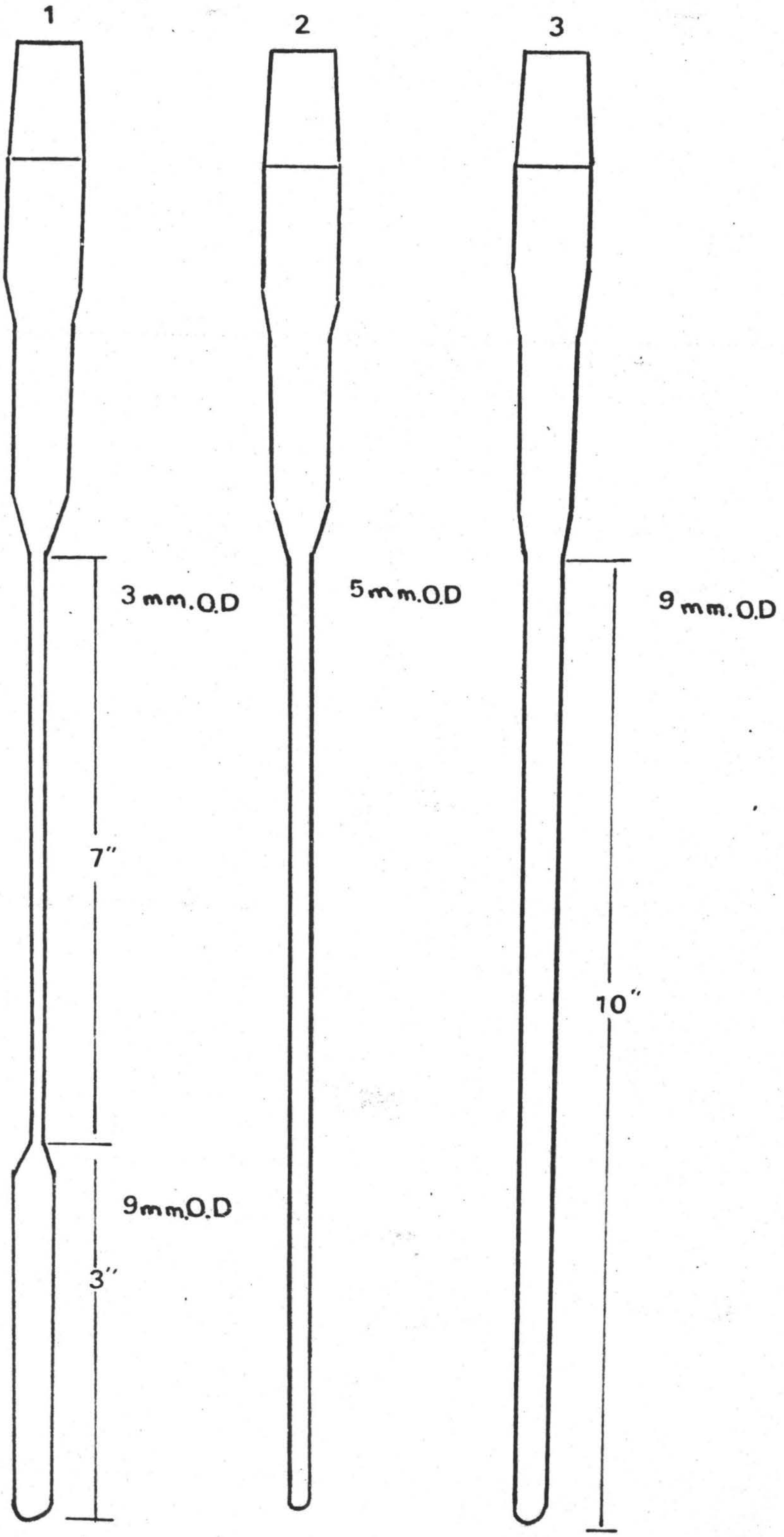

Fig. 4-1: Ampoule reactors

TABLE 4-1

Specifications for Acrylonitrile

Property	Value
Water %	0.05
HCN, ppm	2.
Aldehydes as CH_3CHO, ppm	25.
Divinyl acetilene, ppm	3.
Cyanobutadiene, ppm	3.
Methyl vinyl ketone, ppm	<100.
Peroxides as H_2O_2, ppm	0.3
Ammonia, ppm	65 - 85
Iron as Fe, ppm	0.1
Copper as Cu, ppm	0.1
Acetone, ppm	300.
Non volatile matter (100 - 150°C), ppm	50.
Distillation range at 760 mmHg, °C	74.5 - 79

1. Preparation: Because AN is very stable and does not polymerize in the presence of oxygen, batches of monomer initiator solutions were prepared and stored at low temperatures (- 5°C) in the dark. No polymerization or change in colour was observed throughout this study. It has been reported that successive purifications had no effect on the rate curves. Therefore the monomer was used directly, without any washing or distilling prior to polymerization.

   The ampoules were washed with water, flushed with THF (tetrahydrofurane) and dried overnight at 50 °C. Finally, the ampoules were flamed with the oxy-methane torch, flushed with THF and dried with the flame. A plug was used to prevent moisture pickup while the ampoules were being cooled.

2. Filling Procedure: The solutions were warmed at 20°C. The volumes were measured using volumetric pipettes and stored in liquid nitrogen.

3. Degassing: Because oxygen is a powerful inhibitor (68) it is necessary to degas the reactant samples by vacuum treatment. The vacuum line used was a standard high vacuum apparatus. It consisted of a rotary backing pump, a mercury diffusion pump, a McLeod gauge, a cold trap and eight valved standard taper joints. The schematic diagram is shown in Fig. 4-2. The complete degassing procedure follows:

   i) The filled reaction ampoule was connected to the vacuum

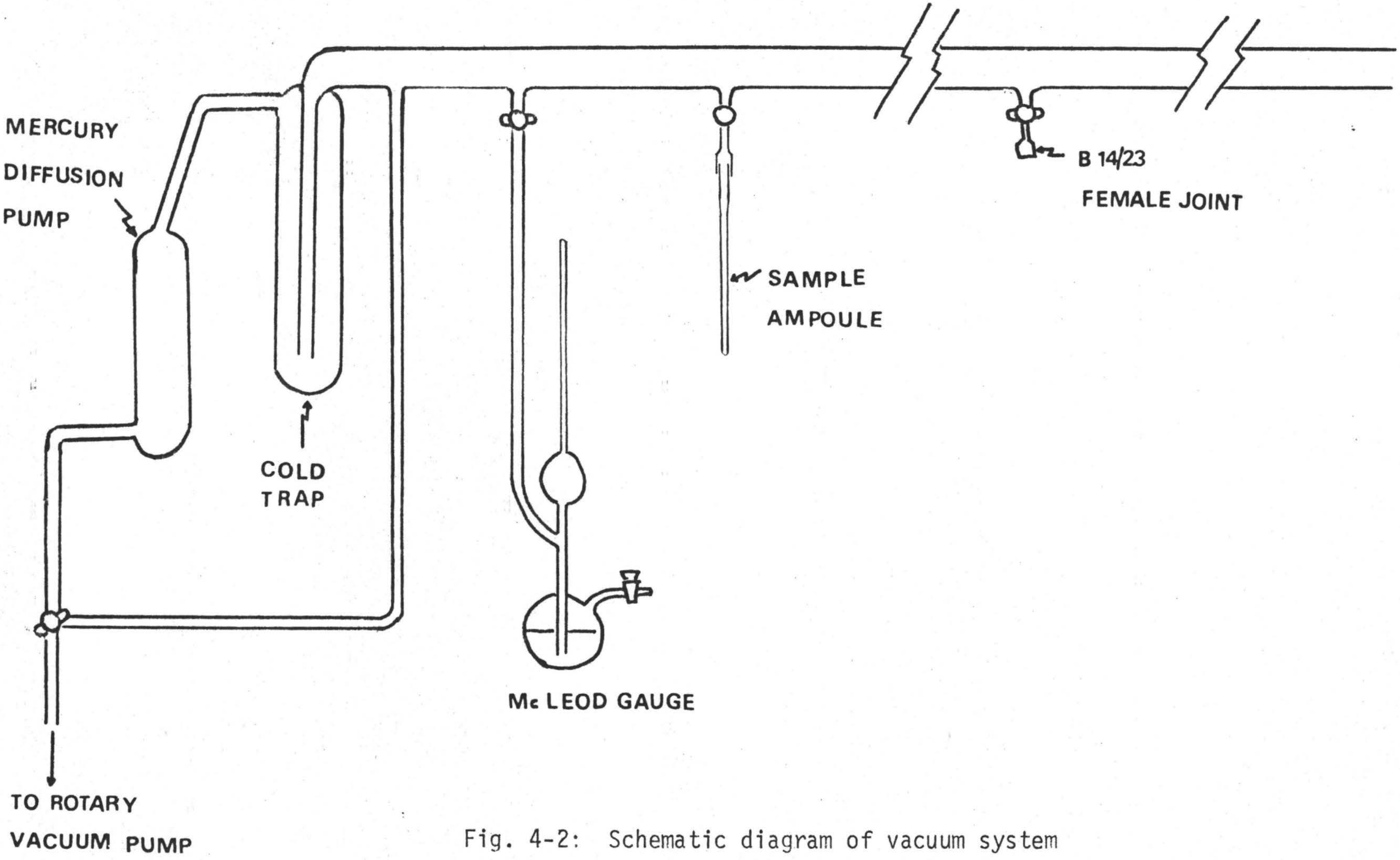

Fig. 4-2: Schematic diagram of vacuum system

manifold, and immersed in liquid nitrogen.

ii) Fifteen minutes later, the valve connecting the ampoule to the vacuum line was opened and the reactant ampoule was evacuated for 15 minutes.

iii) The valve was then closed, liquid nitrogen removed, allowing the frozen samples to warm up to room temperature during which the dissolved gases escaped from the reactant. Cracking of the glass ampoules due to expansion of the reactant was prevented by warming the frozen ampoules with icy water immediately after the removal of surrounding liquid nitrogen (whenever warm water was used to speed up the process, polymerization started).

iv) The flasks of liquid nitrogen were put back again to freeze the ampoules.

v) Fifteen minutes later, the valves were open again. The ampoules were evacuated for five minutes and the whole process repeated five times.

The pressure was tested with the McLeod gauge every second freeze-thaw cycle, making sure that a vacuum of the order of 10^{-6} was attained.

vi) At the end of the fifth cycle, the ampoules were sealed off from the vacuum line, while the monomer was still under liquid nitrogen by applying the oxy-methane torch to the ampoule just below the ground glass joint.

vii) The sealed ampoules were stored in liquid nitrogen ready for polymerization.

4. Ampoule Reactions: The ampoules to be polymerized were immersed in icy water for five minutes prior to the bath immersion. This was done to avoid cracking of the ampoules due to a sudden expansion of the reactant. No polymerization was observed during this process.

The ampoules were immersed suspended by a copper wire in a water bath maintained to ± 0.01°C by a mercury thermoregulator and an electric heater. After reaction for a certain period, an ampoule was quickly removed and quenched in liquid nitrogen. Rapid action and accurate timing were necessary in immersion and quenching.

4.2.3 Analytical Techniques

For the measurement of conversion, two analytical techniques were used:

The first one involves the use of the GPC in an attempt to measure conversion and MWD at the same time. The samples were prepared in type 1 ampoules filled with 0.3 cc of monomer-initiator solution. Once polymerized, the ampoules were open at the narrow end and a solution of DMF/10 ppm Hydroquinone was added to the reaction mixture. The solution formed was transferred into a volumetric flask. The ampoules were flushed several times with the same DMF/Hydroquinone solution and the volumes completed to 100 cc having at the maximum conversion, a concentration of polymer equal to 0.24 wt%.

The solutions were injected in a Waters model ALC-201 GPC using DMF as carrier. The injections were done at room temperature and at a flow rate of 2.5 cc/min. A train of three styragel columms were used ($2 \times 10^3/700$ Å, $5 \times 10^3/10^4$ Å and $2 \times 10^6/700$Å) which gave reasonable separation and fairly good analysis time (45 minutes). The GPC was calibrated using DMF/Hydroquinone solutions with different polymer-monomer mixtures and measuring the respective areas under the chromatograms. The calibration curves are shown in Figs 4-3 and 4-4. A typical chromatogram obtained with this set of columns is shown in Fig. 4-5.

There are two main problems in using this method, namely: the long dissolution time and the impurities. The impurities present in the carrier solvent such as water are very difficult to control (DMF is hygroscopic) and are included in the monomer peak. Therefore, high purity DMF with low water content must be used. The samples cannot be stored for a long time. After a few days erratic results were obtained. Also the polymer takes several days to dissolve at 40°C which made the analysis very tedious.

This method was therefore not used as a standard technique for measuring conversions and was used only to verify the gravimetrical results particularly at low conversions.

The second technique used is a basic gravimetric technique. The ampoules were taken from the liquid nitrogen bath, opened at one end and placed into an icy bath. At the beginning, they were washed

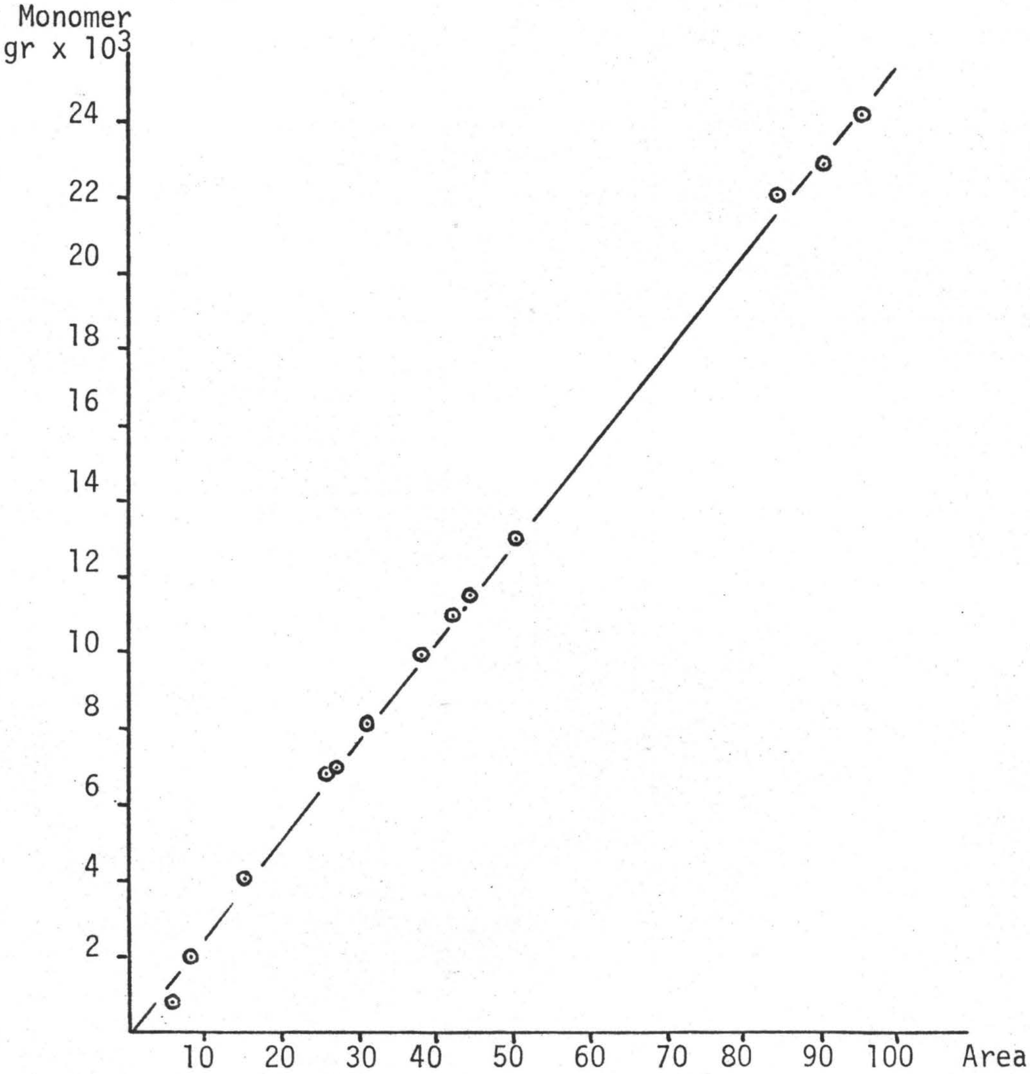

Fig. 4-3: Monomer calibration curve

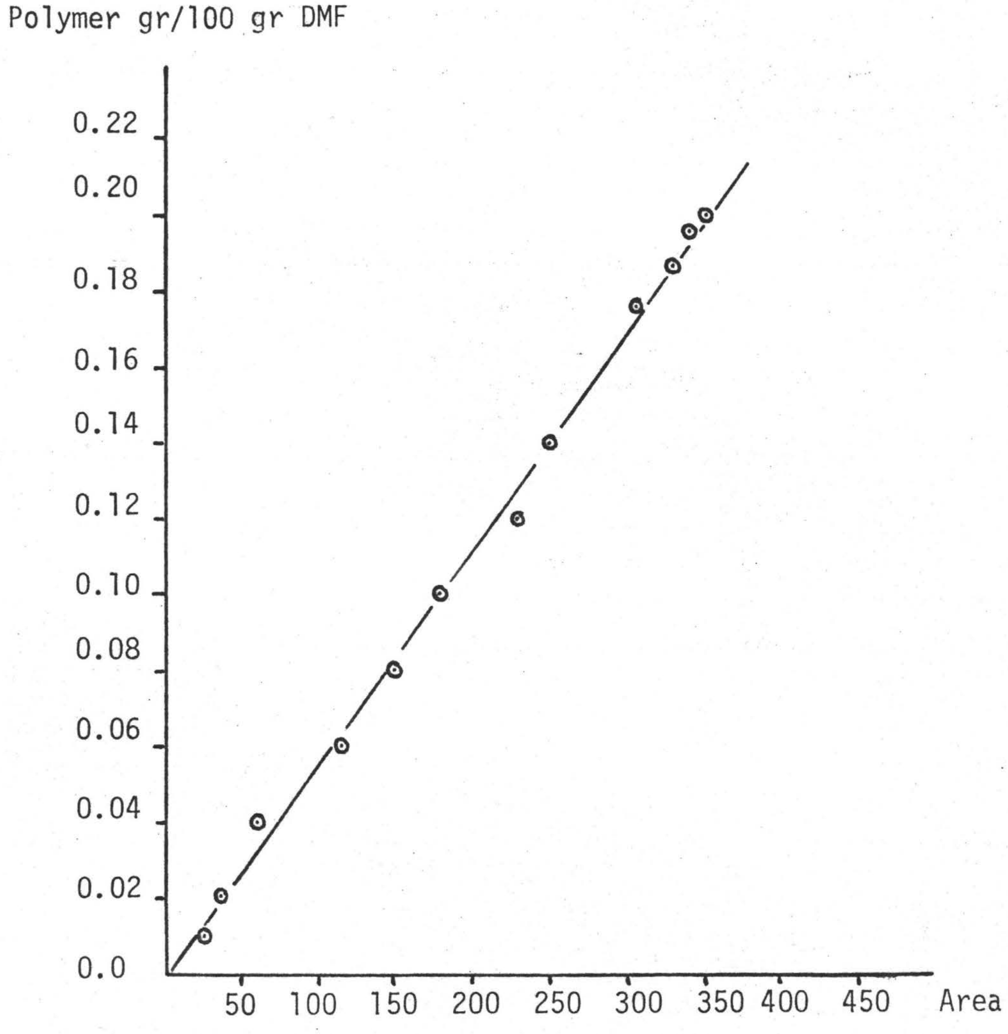

Fig. 4-4: Polymer calibration curve

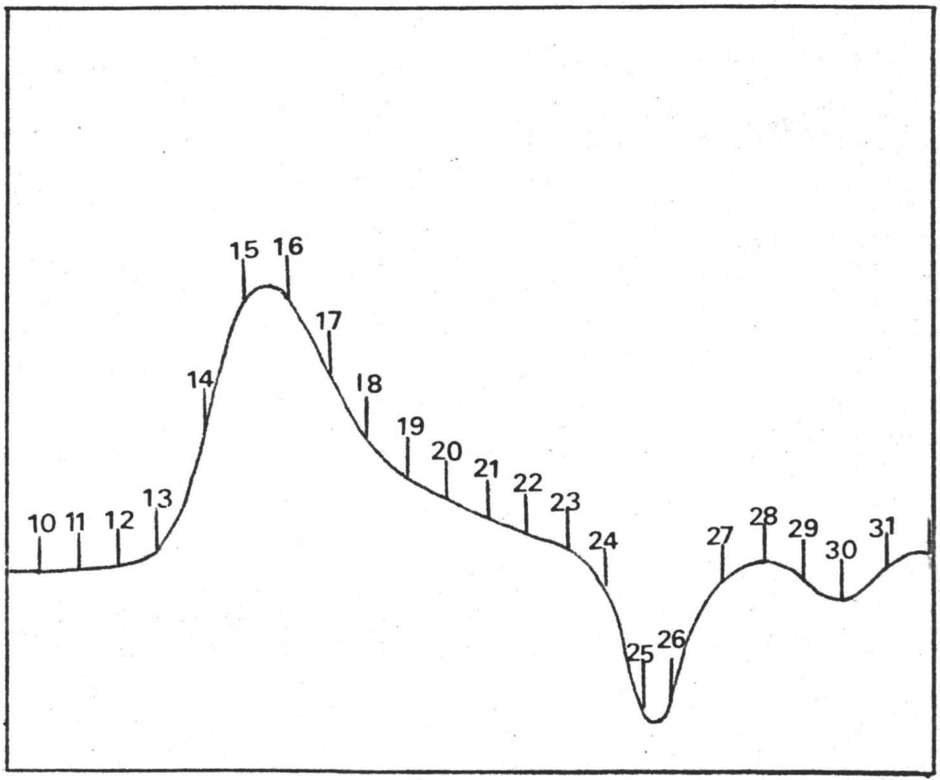

Fig. 4-5: Typical GPC response for conversion measurements

with a methanol/10 ppm hydroquinone solution to inhibit any further polymerization but the polymer was discoloured when dried. Therefore, samples washed with hydroquinone solution and without it were compared. No difference was observed but that no discolouration was present in samples washed with pure methanol. The polymer was washed and decanted three times, transferred to pre-weighed weighing bottles and dried over night at 40°C.

4.2.4 Molecular Weight Distribution

For MWD and averages, the GPC operating conditions were: DMF/ 0.5M LiBr as carrier solvent, measurements were done at room temperature and at a flow rate of 2.5 cc/min. A train of five columns was used. These columns were:

Deactivated Porasil	2500 Å
Deactivated Porasil	1500/800 Å
Deactivated Porasil	800/200 Å
Styragel	2000/700 Å
Styragel	100/20 Å

This column combination gave very good resoltution at intermediate molecular weights. A note of caution here: solutions with polymer concentrations above 0.5 wt% caused plugging of the column end fittings and were therefore avoided although lower attenuation was required and base line drifting more pronounced.

A linear effective calibration curve (30) was obtained using a sample of A-16 reference polymer provided by A.S. Kenyon of Monsanto Co. St. Louis, Mo., U.S.A. This polymer contains 94% acrylonitrile and

6% styrene. It has been characterized by viscosity and osmotic molecular weights. The following molecular weights were used:

$\overline{M}n$ by osmotic pressure = 38800

$\overline{M}v$ by viscometry using the relation $[\eta]_{25°}^{DMF} = 2.43 \times 10^{-4} Mv^{0.75}$

$\overline{M}w$ (calculated) from Lansing-Kraemer dist. = 117000

In using this calibration technique, several fundamental assumptions were made. The true calibration curve is linear and the corrections for axial dispersion are small. If this true as it appears to be, this method corrects automatically for axial dispersion. The linear calibration curve was obtained in the form

$$M(v) = D_1 \exp(-D_2 V)$$

Two more calibration curves were obtained using PVC and polystyrene standards. The PVC standards were supplied by T. Provder of Monsanto Co. and the polystyrene narrow standards are from Waters Associates, Framingham, Mass.

PVC Standards

PVC1	$\overline{M}w$ = 132,000	$\overline{M}n$ = 54,000
PVC2	$\overline{M}w$ = 118,000	$\overline{M}n$ = 41,000
PVC3	$\overline{M}w$ = 68,000	$\overline{M}n$ = 25,500

A linear effective calibration curve was obtained for PVC standards, and for polystyrene standards, the hydrodynamic volume theory was applied using the relations after Fujisaki and Kobayashi (32) and Kenyon (39).

Polystyrene Standards

Sample	$\overline{M}w$	$\overline{M}n$	EV
PS1	104.14	104.14	46.5
PS2	600.	545.	46.5
PS3	2030.	1845.	45.75
PS4	5000.	4600.	45.0
PS5	10,300.	9700.	43.5
PS6	19,850.	19,650.	42.0
PS7	21,000.	19,800.	41.75
PS8	51,000.	49,000.	38.5
PS9	98,200.	96,200.	36.0
PS10	200,000.	188,680.	33.5
PS11	411,000.	392.000.	31.5
PS12	670,000.	582,610.	29.5
PS13	860,000.	747,830.	29.0
PS14	$1.8x10^6$	$1.5x10^6$	27.0
PS15	$2.145x10^6$	$1.78x10^6$	26.5
PS16	$4.0x10^6$	-	25.0
PS17	$7.2x10^6$	-	24.5

The peak positions were taken as $(\overline{M}nx\overline{M}w)^{0.5}$. The calibration curves are shown in Fig. 4-6.

4.2.5 Intrinsic Viscosities

Intrinsic viscosities of several polymers were measured to compare the values obtained with those reported in the literature.

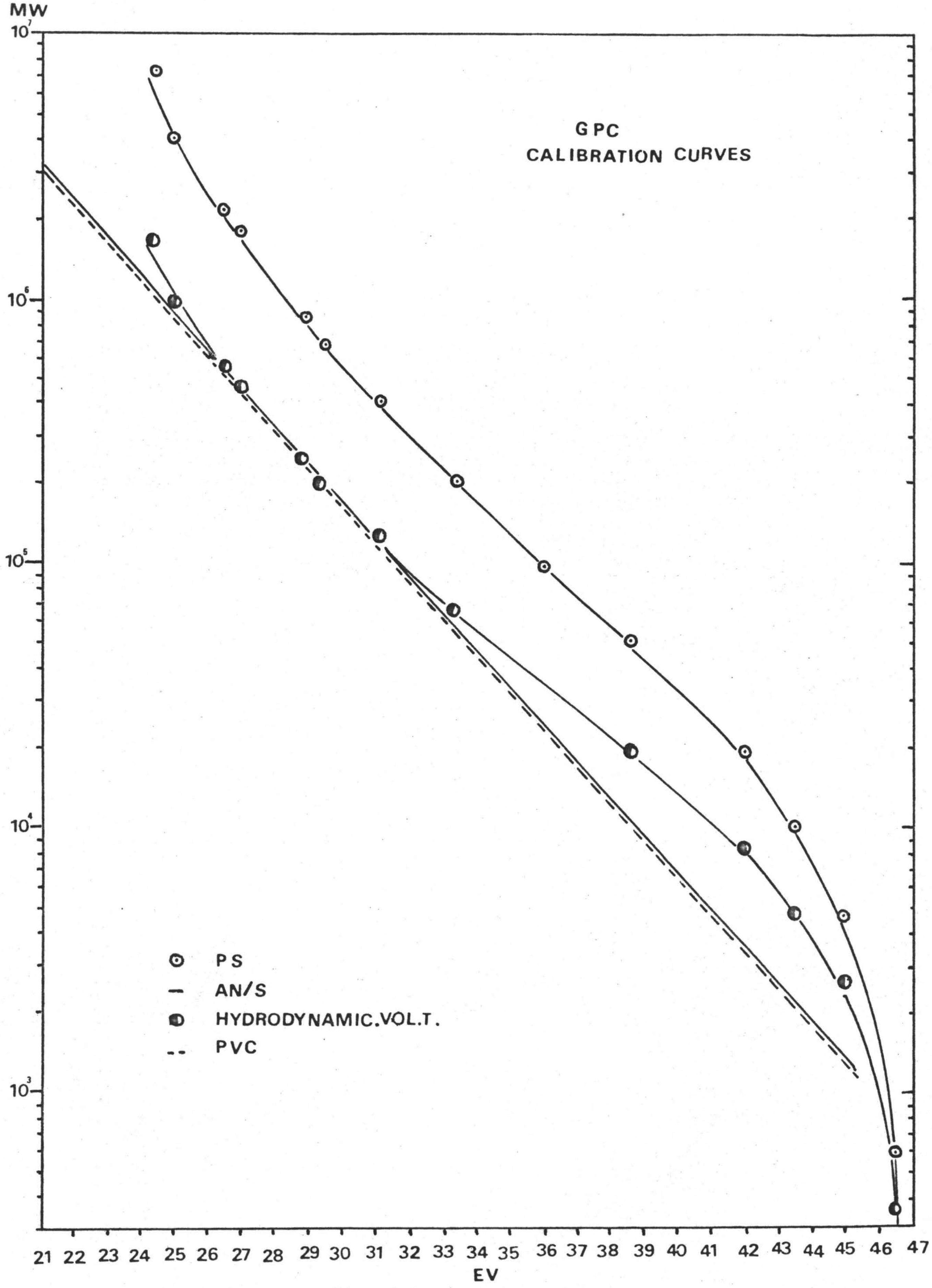
MW
10^7
10^6
10^5
10^4
10^3
GPC
CALIBRATION CURVES
PS
AN/S
HYDRODYNAMIC.VOL.T.
PVC
21 22 23 24 25 26 27 28 29 30 31 32 33 34 35 36 37 38 39 40 41 42 43 44 45 46 47
EV

Fig. 4-6

Solutions were prepared at 0.25 wt% in DMF. A two cc pipette was used to transfer the solution to a No. 75 Cannon viscometer. The samples were diluted three times in the viscometer by adding 2 cc of DMF in each dilution step. Flow times were measured in a bath controlled to 25 ± 0.05°C. The readings were taken several times to ensure the validity of the results, and were compared with times for the solvent. The flow time for the solvent was greater than 100 sec and no corrections were applied. A plot of $\ln \eta r/c$ vs. and η_{sp} vs. c and the intrinsic viscosities were determined by extrapolating to c = 0. Results are shown in Table 4-2.

TABLE 4-2

Intrinsic Viscosities

Sample	$[I]_o$wt%	T°C	X	$[\eta]$
S_1	0.075	60	0.40	9.025
S_2	0.075	60	0.92	12.5
S_3	0.025	60	0.17	9.4
S_4	0.025	60	0.80	12.9

4.2.6 Solubility of the Monomer

To obtain an estimate of the solubility of the monomer in the polymer over the temperature range 0°C - 80°C, a gravimetric technique described in Appendix 9-4 was used.

The solubility of the monomer in the polymer appears to be fairly constant with temperature.

The results are reported in Appendix 9-4. No speculations concerning the shape of the curve are anticipated since the variance is comparatively high.

4.2.7 Experimental Condtions

Difficulties were encountered in setting the experimental conditions which would allow maximum polymer quality in terms of discolouring and maximum yields, meaning limiting conversions. The values reported in the literature proved to be too high or too low. Finally, the following experimental scheme was set for which polymer discolouring was minimum and limiting conversions were obtained:

Polym. Temp °C	Initiator Cons. range wt%
0	2.0
25	2.0
40	0.20 - 2.00
50	0.1
60	0.01 - 0.20
70	0.1
80	0.005 - 0.05
100	0.1
120	0.1

About 300 successful polymerization experiments are reported covering the above levels and including replicates. Approximately 40 samples were analysed by GPC for MWD and averages including replicates, which gave for analysis near to 120 chromatograms.

4.3 Results

4.3.1 Reproducibility

Since ampoules of different surface to volume ratio were used for polymerizations at basically two conversion levels, 0 - 50% and 50% - X_f, replicates were taken randomly along the conversion-time curve at 60°C and 0.05 wt% initiator concentration to account for any underlying effect of the ampoule diameter on the experimental error. There is no evidence of such effect and the variance can be assumed constant. The 95% confidence interval for these conditions is: $\overline{X} \pm 0.008$ where $\overline{X}$ is the replicate's mean. Two typical reproducibility curves are shown in Figs 4-1 and 4-8. The individual 95% confidence intervals for replicates at 60°C are shown in Figs. 4-9 to 4-11.

The reproducibility of MWD data included two separate considerations. The GPC reproducibility and the MWD and averages reproducibility with conversion. The latter was not significant. The major variance was observed for the GPC replicates. The GPC reproducibility was verified by two methods: averaging $\overline{M}_N$ and $\overline{M}_W$ and comparing the normalized heights for several injections of the same polymer and by adding the heights from replicate chromatograms and from this calculating the

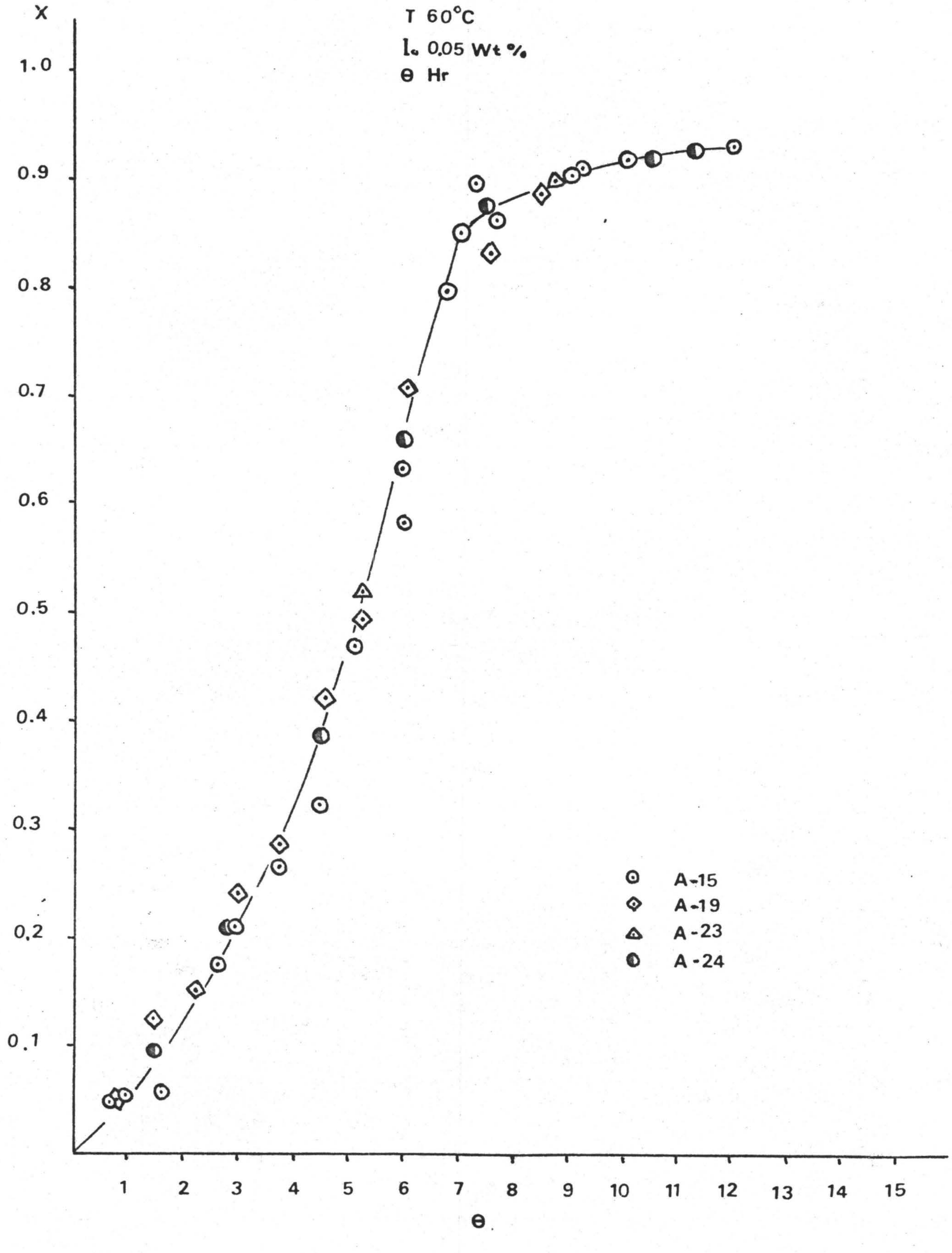
X
T 60°C
I₀ 0.05 Wt %
θ Hr
1.0
0.9
0.8
0.7
0.6
0.5
0.4
0.3
0.2
0.1
1
2
3
4
5
6
7
8
9
10
11
12
13
14
15
θ
A-15
A-19
A-23
A-24

Fig. 4-7

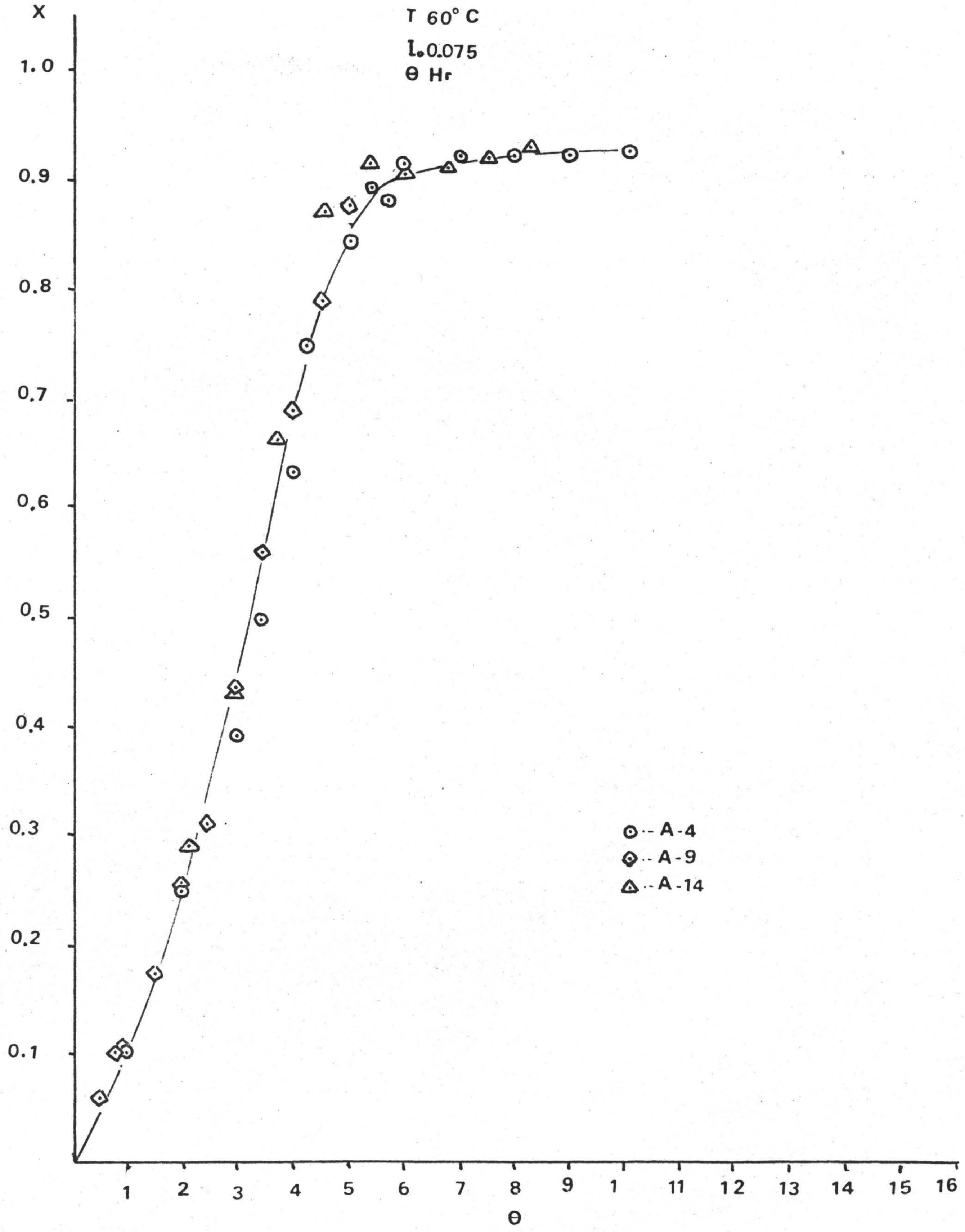
X
T 60° C
I₀0.075
θ Hr
1.0
0.9
0.8
0.7
0.6
0.5
0.4
0.3
0.2
0.1
1
2
3
4
5
6
7
8
9
1
11
12
13
14
15
16
θ
⊙ -- A-4
◈ -- A-9
△ -- A-14

Fig. 4-8

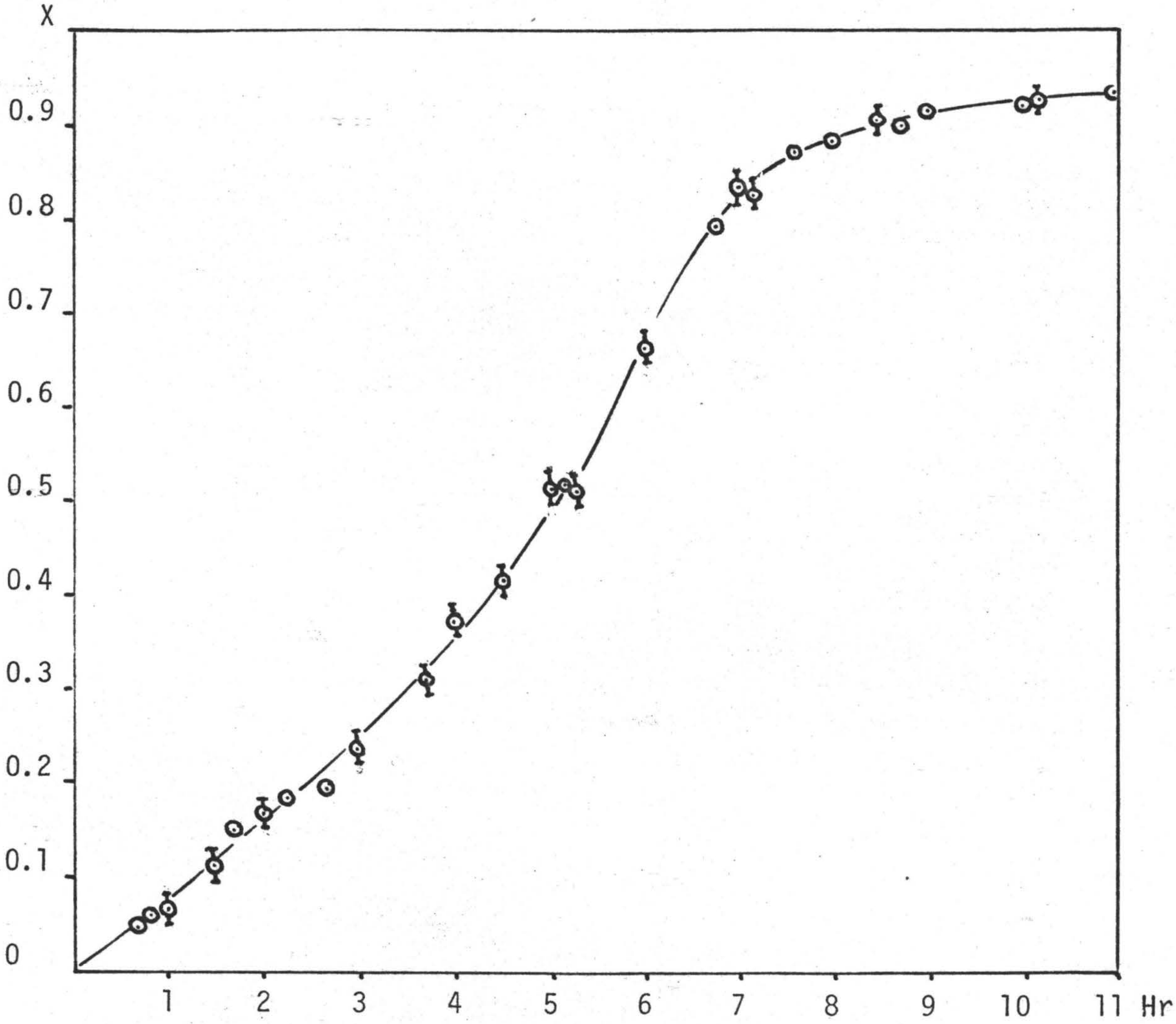

Fig. 4-10: Individual 95% C.I. for replicates at 60°C and 0.05 $[I]_0$ wt%.

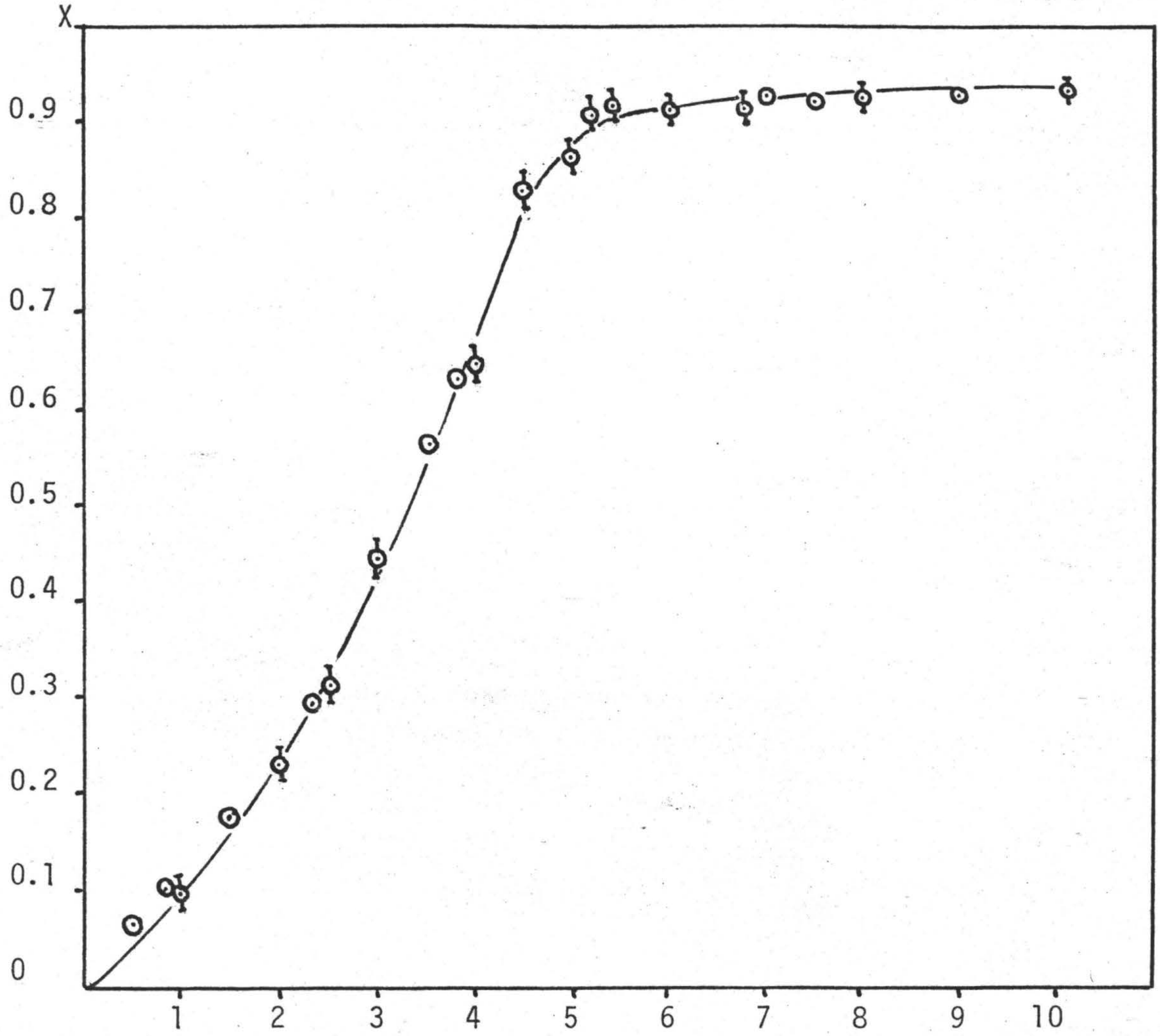

Fig. 4-9: Individual 95% C.I. for replicates at 60°C and 0.075 $[I]_0$ wt%.

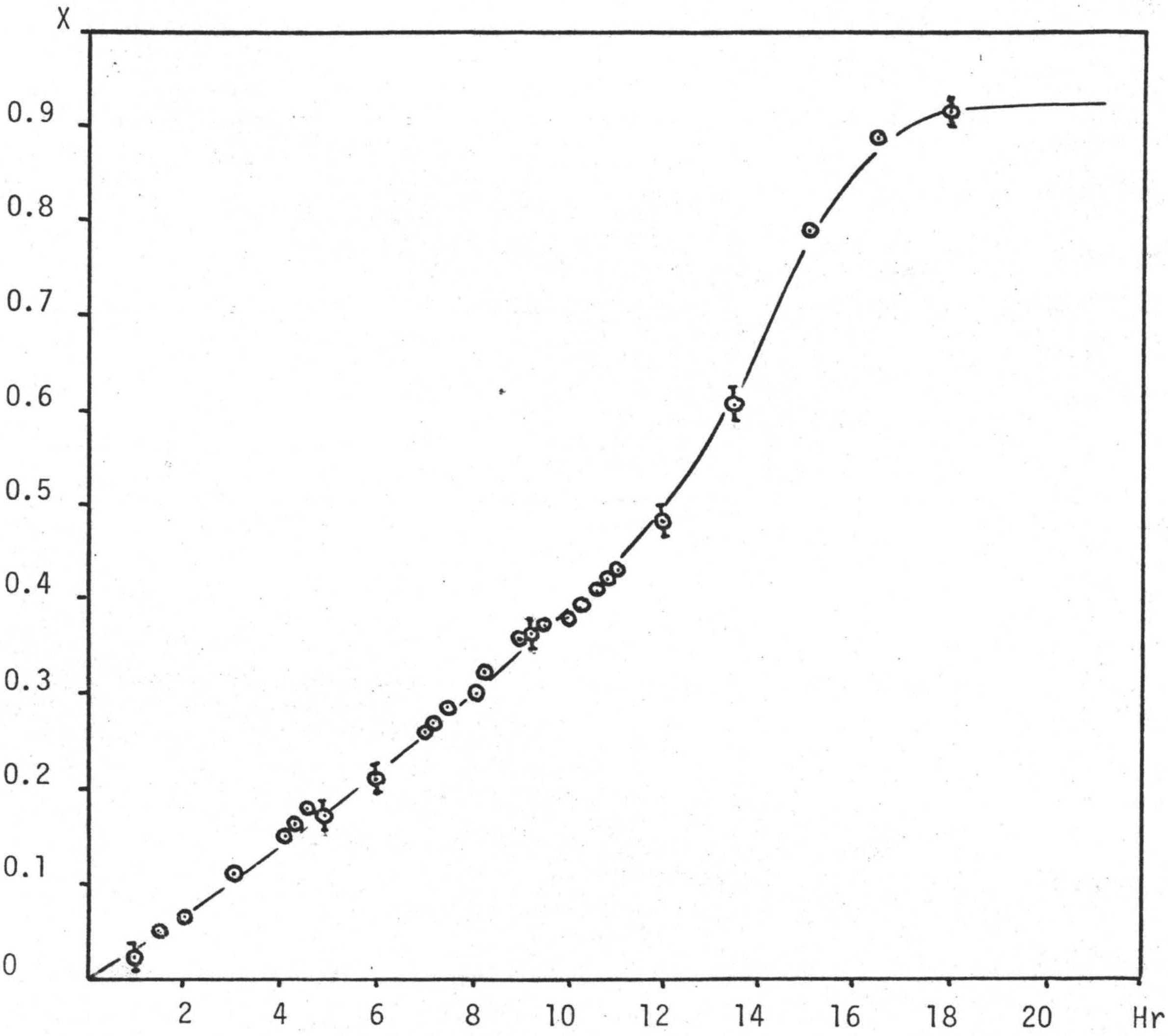

Fig. 4-11: Individual 95% C.I. for replicates at 60°C and 0.025 $[I]_0$ wt%.

MWD. The 95% confidence interval for the replicates is: $\hat{M}_N \pm 0.128 \times 10^5$ and $\hat{M}_W \pm 0.21 \times 10^5$. The reproducibility of gravimetrically determined conversions and GPC determined MWD and averages were considered satisfactory. Details of the statistical analysis of the data are given in Appendix 9-1.

4.3.2 Isothermal Conditions

As mentioned earlier, the heat of reaction for PAN is very high, therefore, small ampoules with high surface to volume ratio were used, particularly at high conversions (above 50%) where the polymer is almost solid. Type 3 ampoules were used for conversions below 50% and type 2 for polymerizations from 50% on.

No difference among the three types of ampoules was observed for conversion measurements. At high conversions, discolouring was present in type 1 ampoules. In types 2 and 3, discolouration was observed only when the samples remained in the bath for a long period of time after the limiting conversion was reached. A slight drop in molecular weight was observed for these high conversion runs.

4.3.3 Conversion Results

Figures 4-12 to 4-15 show conversion versus time curves for the temperature levels 40°C, 60°C and 80°C at several initiator concentrations. The curves represented have the same sigmoidal shape characteristic of vinyl chloride bulk polymerization. Almost in every case, there is an acceleration period and after reaching a maximum, the rate continually decreases. The extent of this acceleration period and the position of the maximum rate vary with initiator concentration. This is an important difference with the vinyl chloride system because the latter shows an acceleration period followed by a constant or nearly constant rate. A further acceleration is observed at the onset of the gel effect, reaching then, a maximum and then continually decreasing. (1)

The limiting conversion is independent of the initiator concentration for sufficiently high initiator concentrations but it varies with the polymerization temperature. It has been suggested (31) that the limiting conversion is a direct result of a polymerizing solution reaching its glass transition point; therefore if a plot of limiting conversion versus polymerization temperature is extrapolated to 100% conversion, the glass transition temperature of the polymer should be obtained. Such a plot is shown in Fig. 4-16. The temperature obtained is 110°C in agreement with values reported previously. (43, 46) If not enough initiator is present so the limiting conversion can be reached, the rate drops constantly and a limiting value smaller than the actual limiting conversion is obtained. This is the case for the curves shown in Fig. 4-15. Useful information can be obtained from these curves such as the initiator efficiency if k_d is known and a model is available, or the actual value of k_d. For the decomposition rate constant for AIBN.(54)

$$k_d = 2.67 \times 10^{15} \exp\{- 31,100/RT\} \ (\sec^{-1})$$

Reasonable agreement was found for times estimated from the curves.

4.3.4 Molecular Weights

In Fig. 4-17, a typical GPC response for a molecular weight determination is shown. The MWD's for the polymerization temperature range 0°C - 120°C are shown in Figs. 4-18 to 4-26. The cummulative chromatograms at different conversions are shown in Figs. 4-27 to 4-29. These plots show a slight variation of the peak position indicating therefore, that although transfer to monomer appears to control the MWD, termination reactions have some contribution. This can be discussed further by looking at the molecular weight averages and their variation with conversion, temperature and initiator concentration. The variation of molecular weight averages is shown in Figs. 4-30 to 4-32. An increase in $\overline{M}_n$ and $\overline{M}_w$ is observed with conversion. It is more significant with increasing initiator concentration. A drop in molecular weight in the vicinity of limiting conversions is attributed to some degradation. To ensure maximum conversion, the samples remained in the bath for long periods of time. This is more significant for polymerizations at 80°C where because of the high polymerization temperature, the degradation process might be present before the limiting conversion was reached.

The polydispersities as shown in Fig. 4-33 are constant through most of the reaction at almost every temperature increasing towards 2.5 at low conversions and low polymerization rates, indicating a greater contribution from bimolecular termination.

Figure 4-34 shows the variation of molecular weight and polydispersity ratios with polymerization temperature. The molecular weight curves can be divided into three regions. An increasing molecular weight with increasing temperature region in the temperature range 0°C - 20°C, a fairly constant molecular weight (with perhaps a slight maximum between 50°C and 60°C) with increasing temperature in the temperature range 20°C - 90°C and finally, a monotonical decrease in molecular weight for polymerization temperatures above 80°C. The polydispersity ratio curve can be divided in two regions: a nearly constant polydispersity over the temperature range 0°C - 80°C and a monotonical increase for temperatures above 80°C. A note of caution here. The variations with respect to polymerization temperature shown in Fig. 4-32 were taken at different conversions for data is not available for all conversions over the whole temperature range. The conversion range 5 - 20% is for all but that at 100°C, where samples were prepared at 92% conversion (see Appendix 9-1). The strong maximum observed by Bamford and Jenkins (9) could be due to the assumption that molecular weights were independent of conversion. Thomas and Pellon (69) observed a maximum in intrinsic viscosity over the same polymerization temperature region. The polymers used were obtained between 40 and 50% conversion and the maximum is less pronounced.

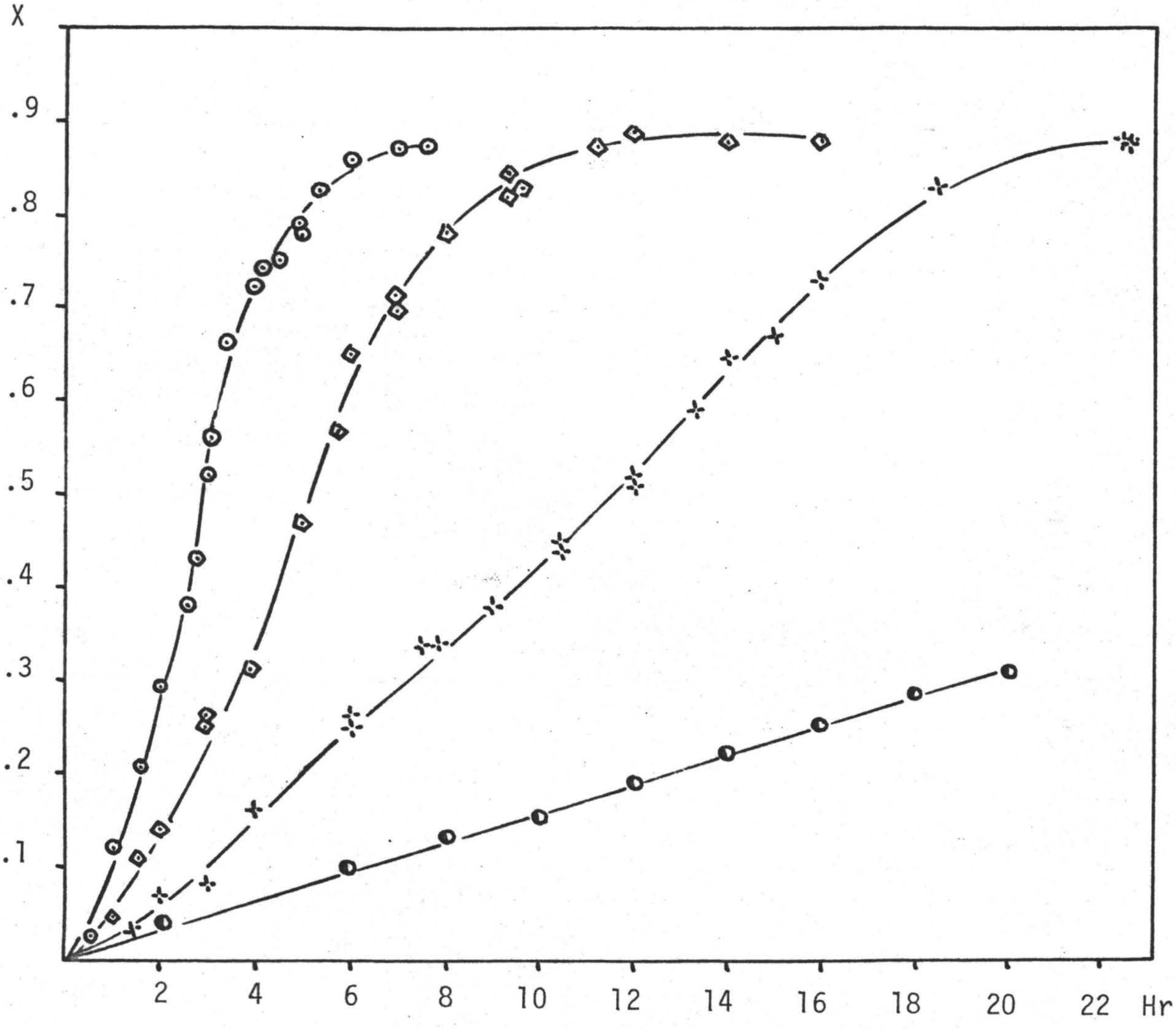

Fig. 4-12: Conversion histories for polymerizations at 40°C ⊙ 2.0 $[I]_o$ wt%, ◇ 1.0 $[I]_o$ wt%, ✢ 0.5 $[I]_o$ wt%, ● 0.2 $[I]_o$ wt%.

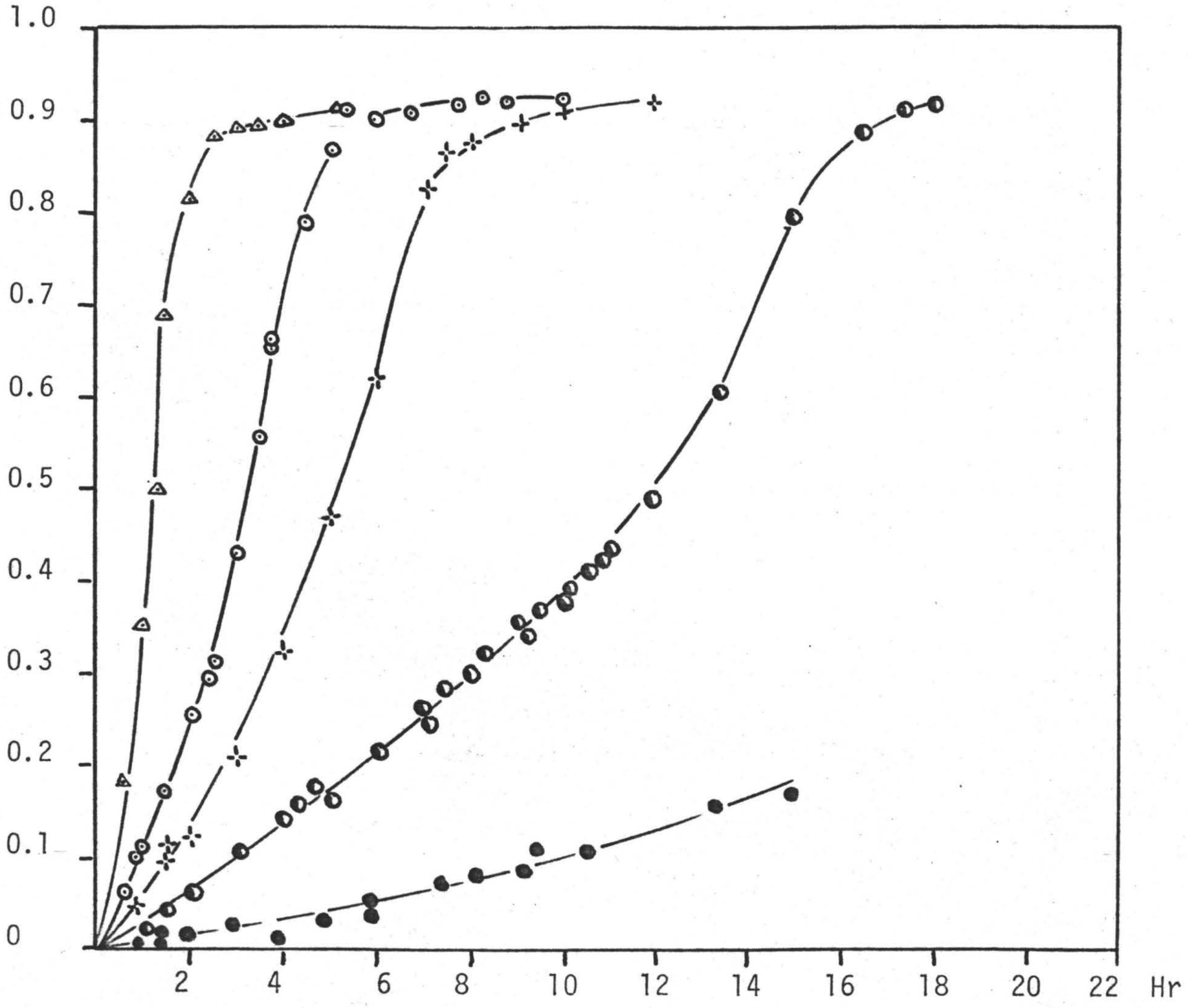

Fig. 4-13: Conversion Histories for polymerizations at 60°C, △ 0.20 $[I]_o$ wt%, ⊙ 0.075 $[I]_o$ wt%, ✢ 0.050 $[I]_o$ wt%, ◐ 0.025 $[I]_o$ wt%, ● 0.010 $[I]_o$ wt%.

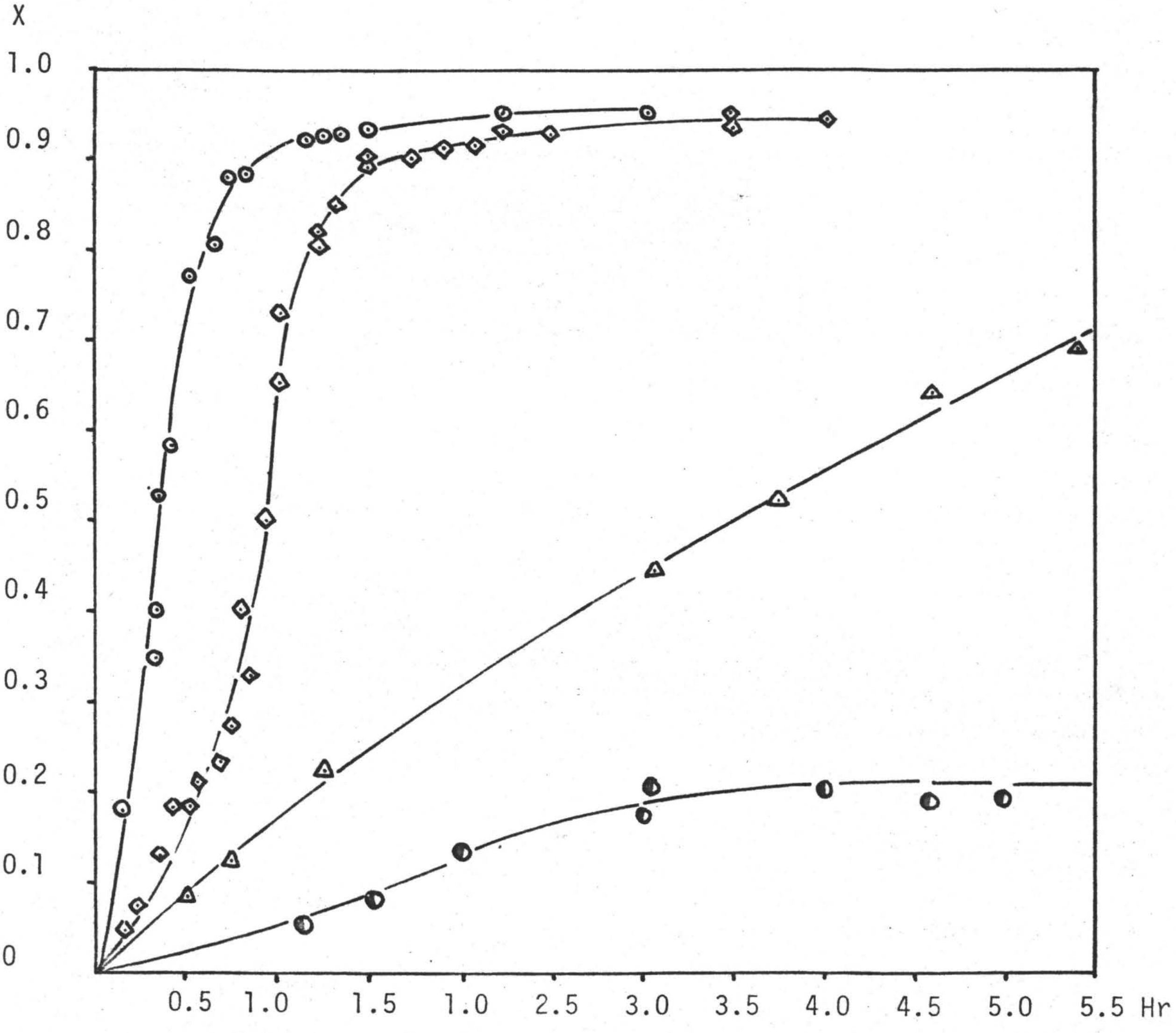

Fig. 4-14: Conversion histories for polymerizations at 80°C.

⊙ 0.05 $[I]_0$ wt%, ◈ 0.025 $[I]_0$ wt%, ▲ 0.010 $[I]_0$ wt%,

◐ 0.005 $[I]_0$ wt%.

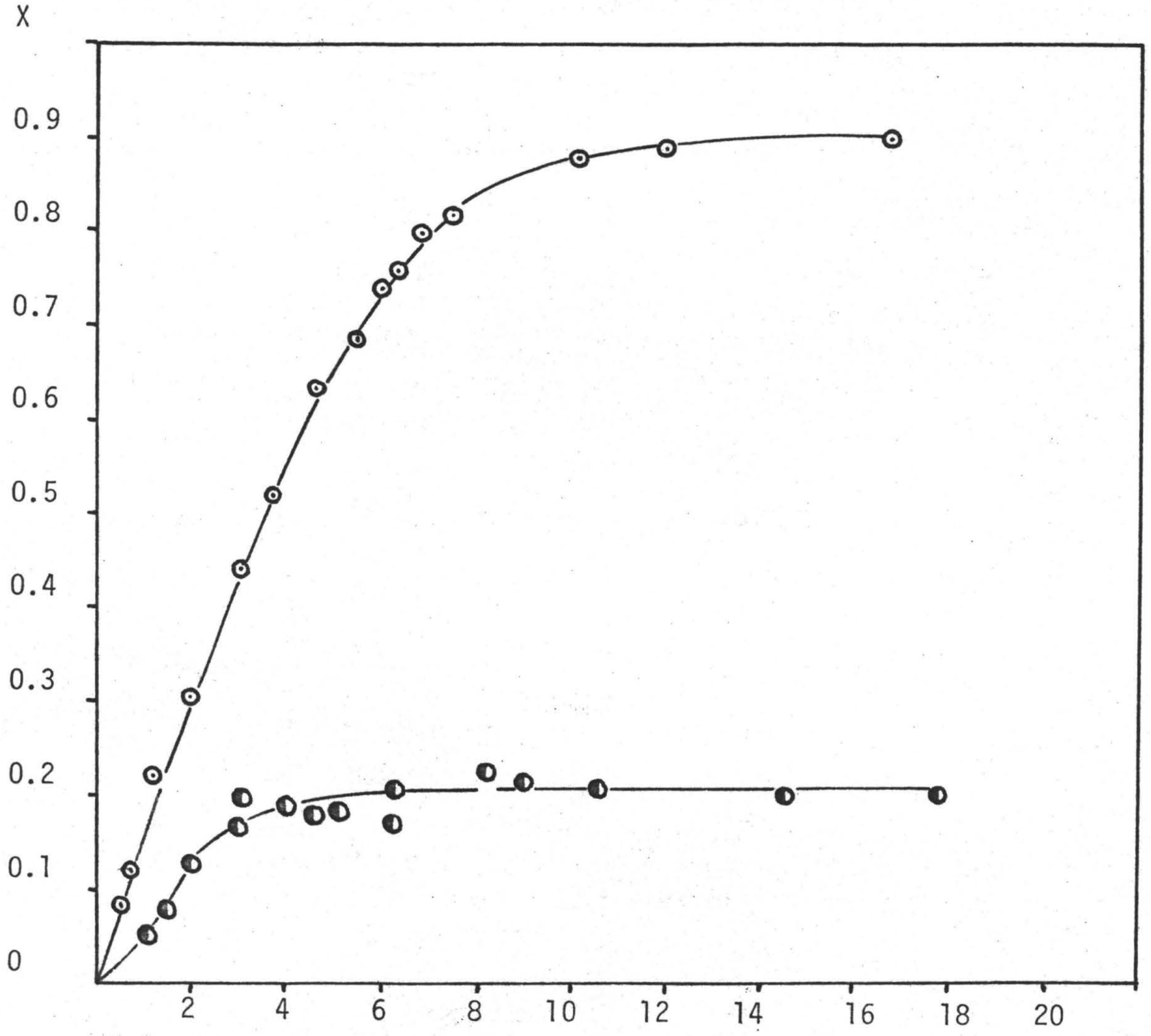

Fig. 4-15: Conversion histories for polymerizations at 80°C

⊙ 0.010 $[I]_o$ wt%, ◐ 0.005 $[I]_o$ wt%.

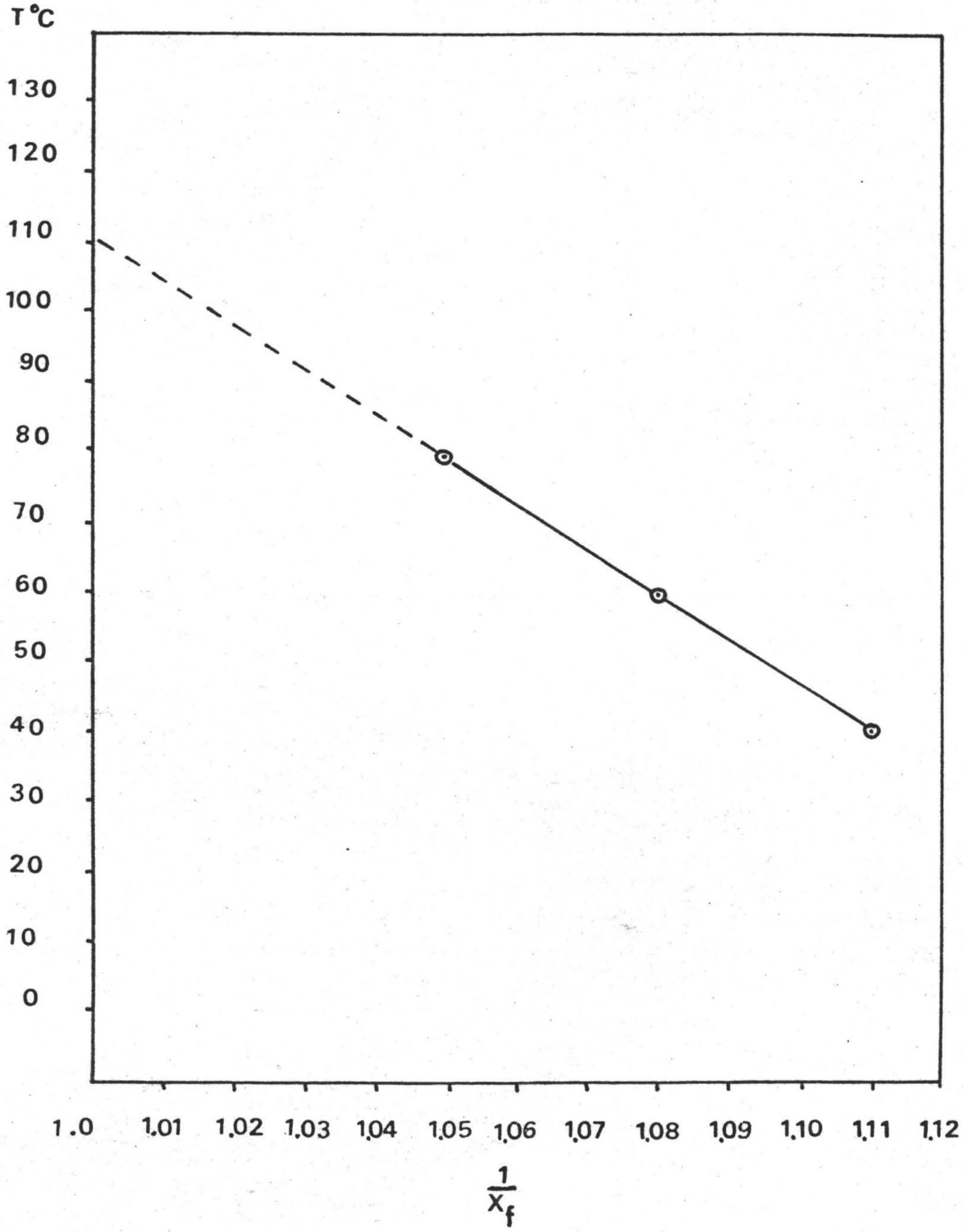

Fig. 4-16: Glass transition temperature estimated from limiting conversion data.

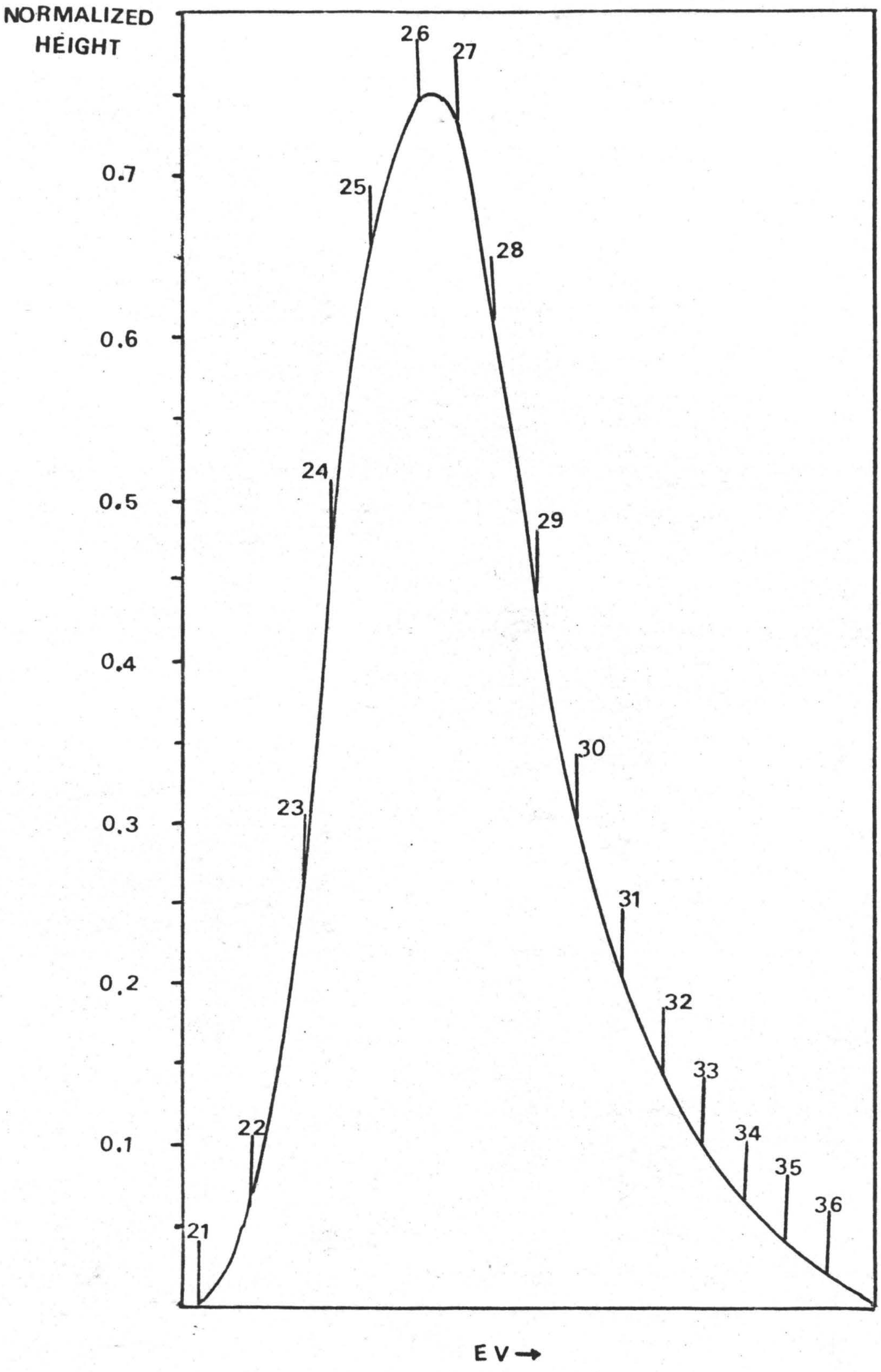

Fig. 4-17: Typical GPC response for MWD determinations.

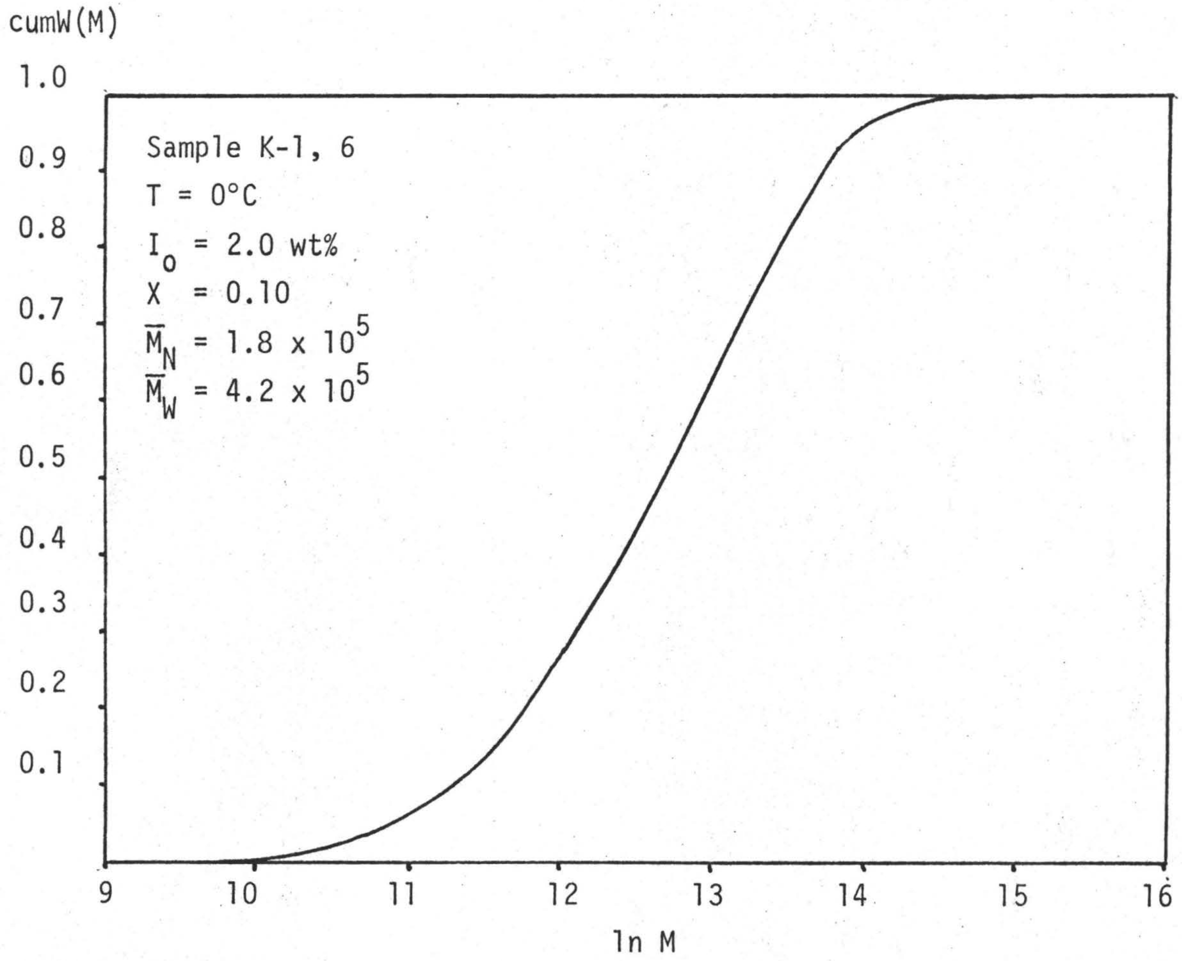

Fig. 4-18: Cumulative MWD.

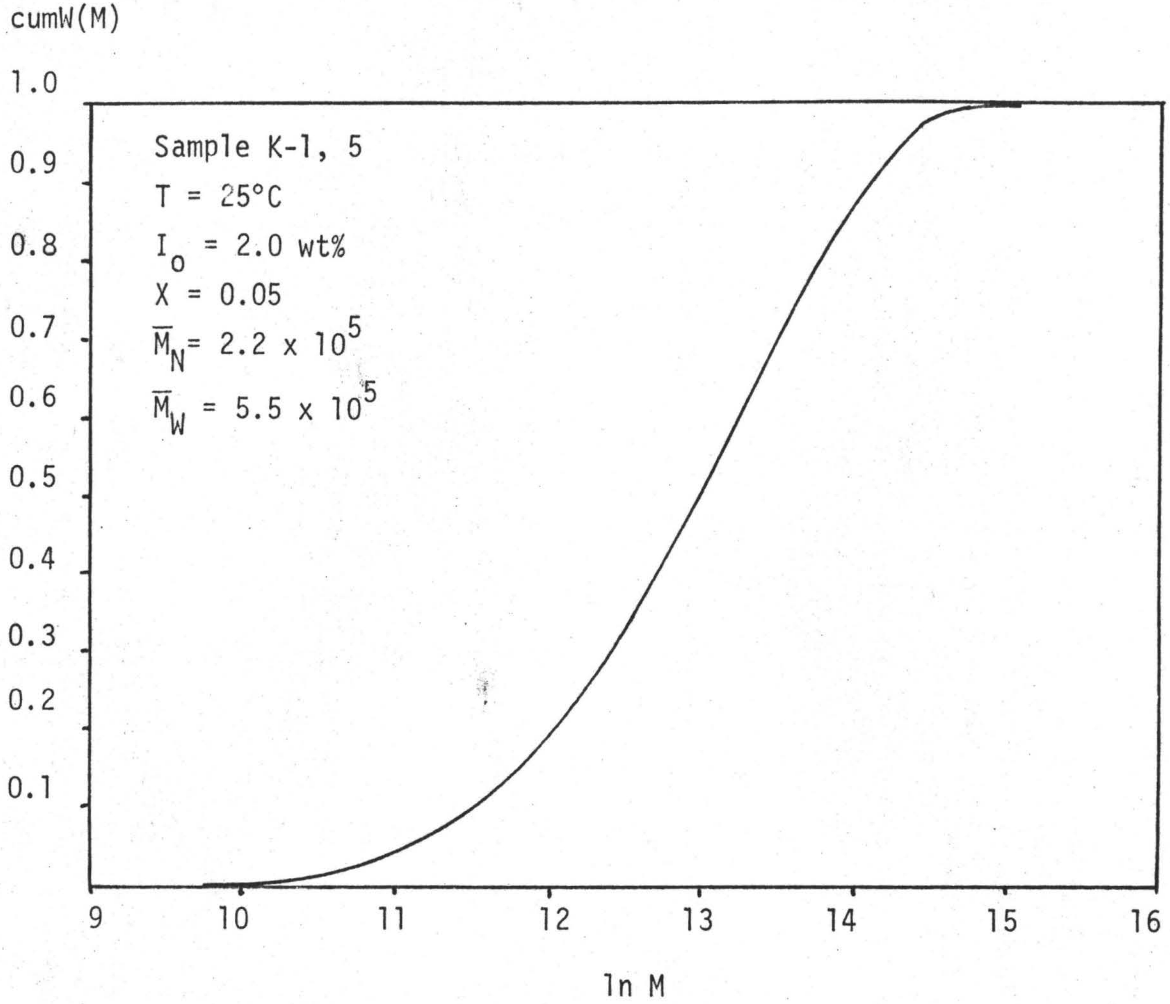

Fig. 4-19: Cumulative MWD.

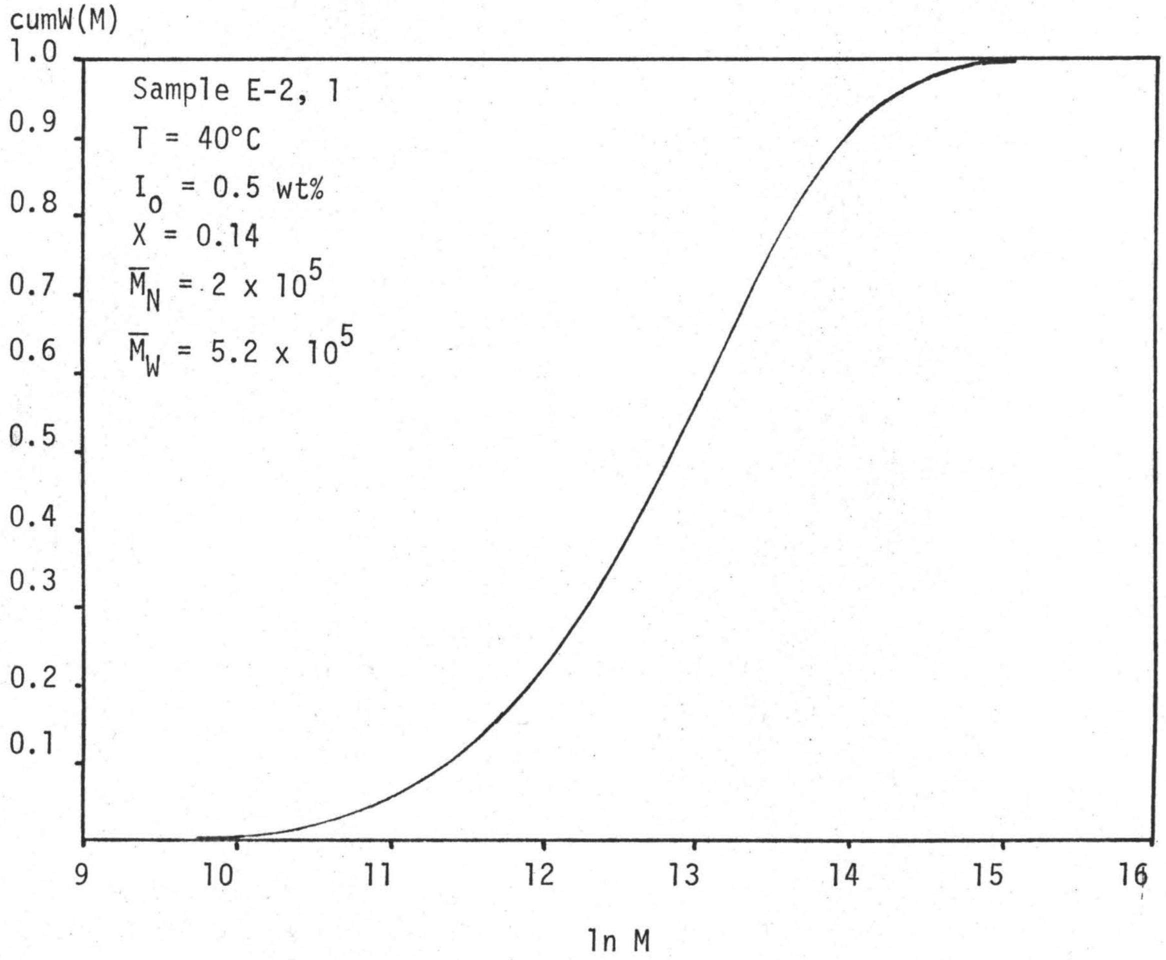

Fig. 4-20: Cumulative MWD.

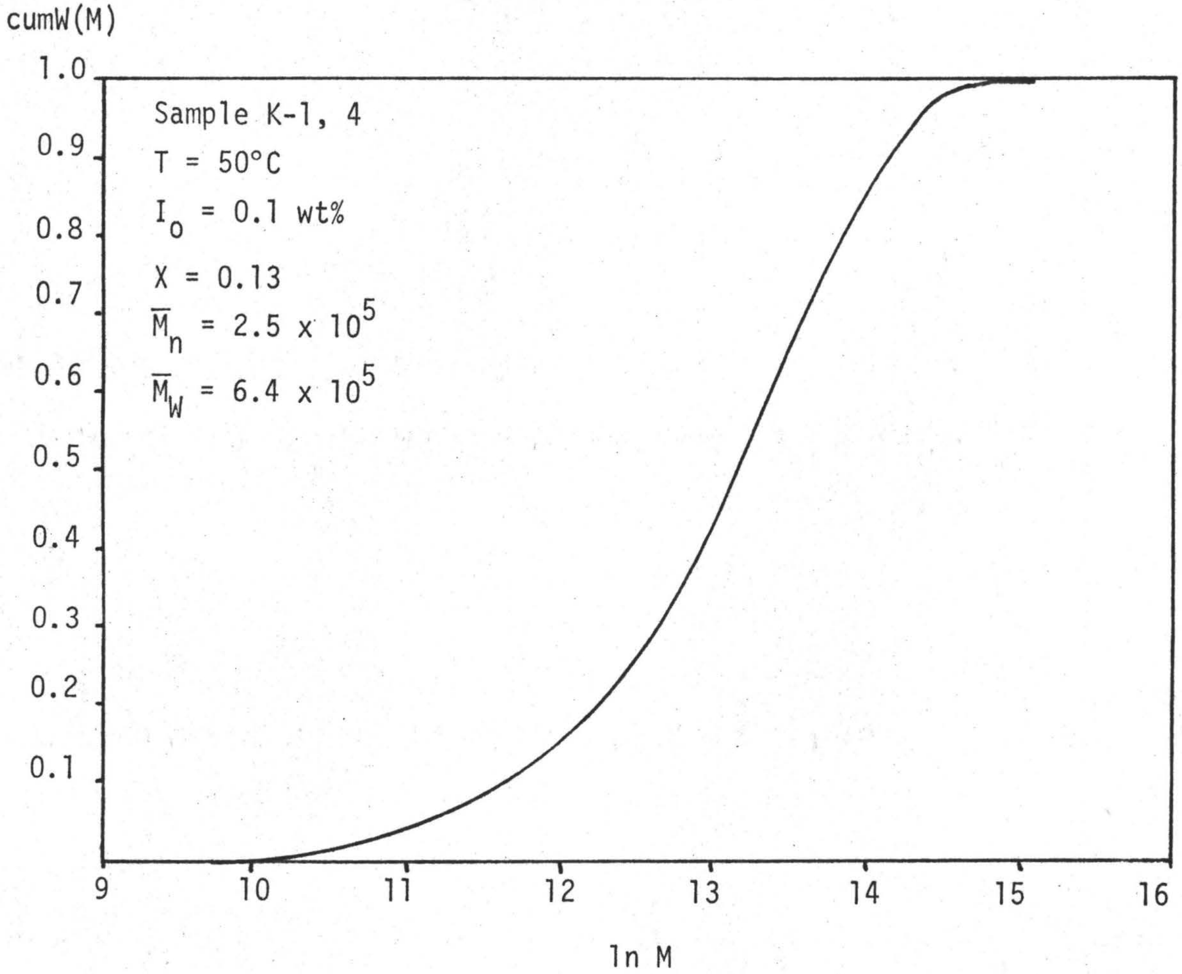

Fig. 4-21: Cumulative MWD.

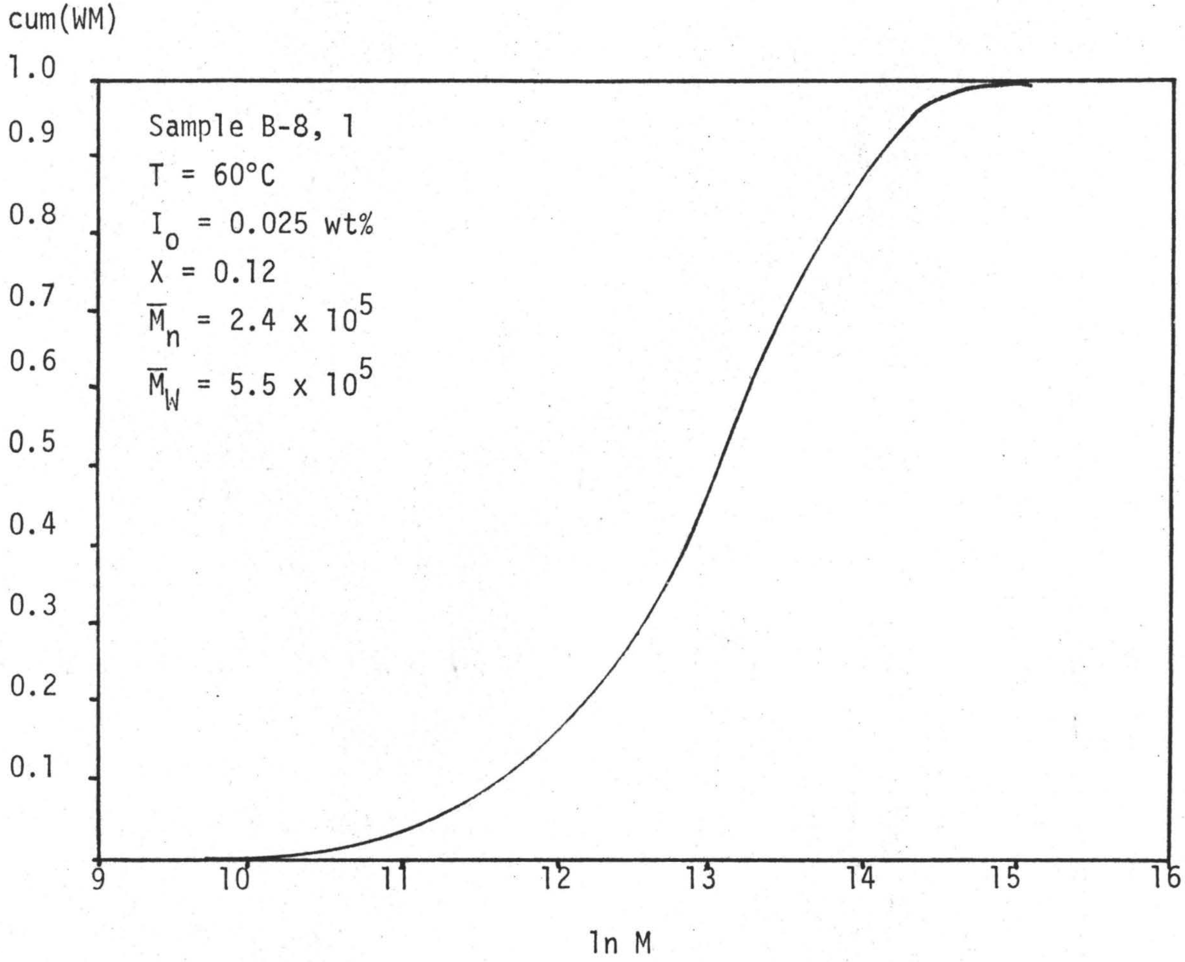

Fig. 4-22: Cumulative MWD.

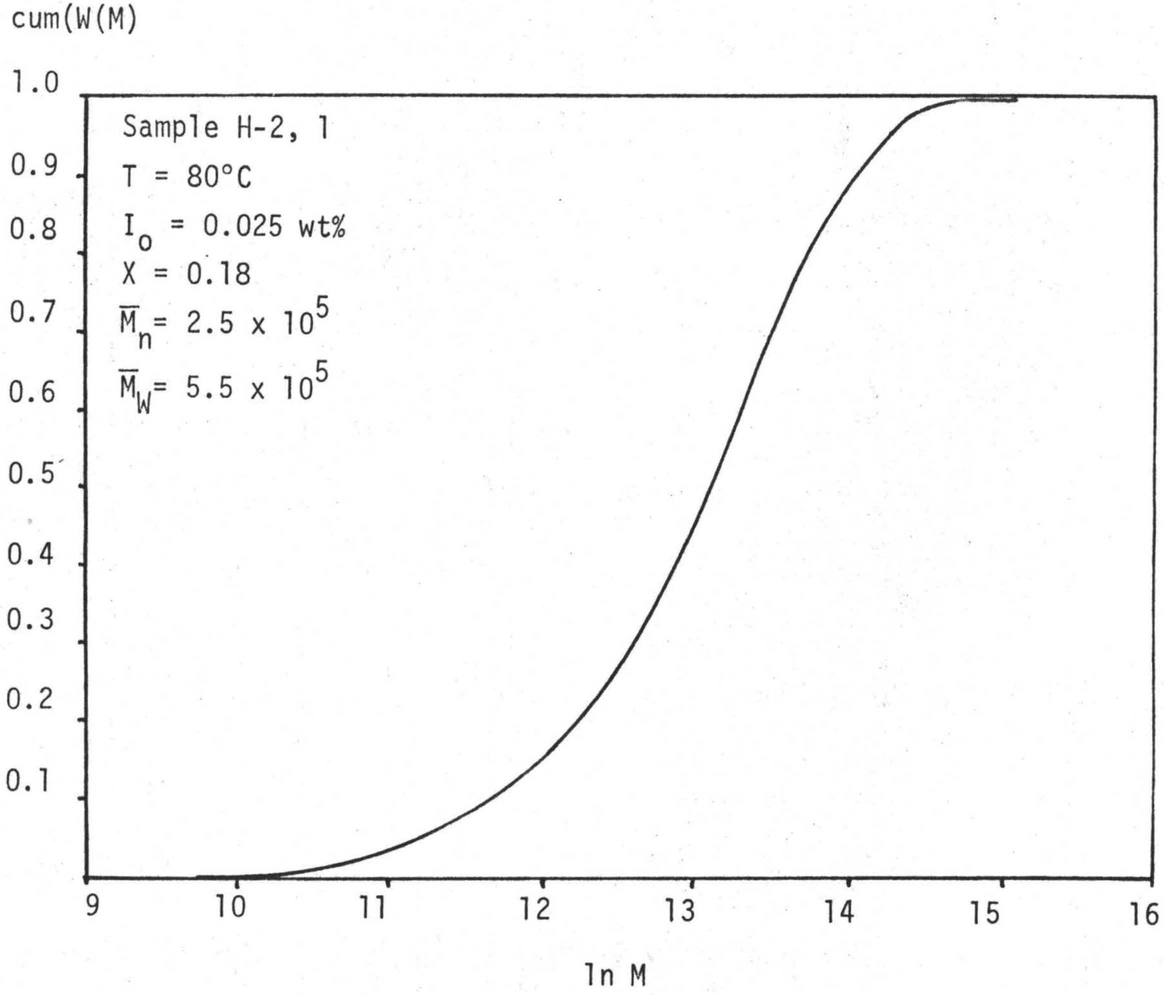

Fig. 4-24: Cumulative MWD.

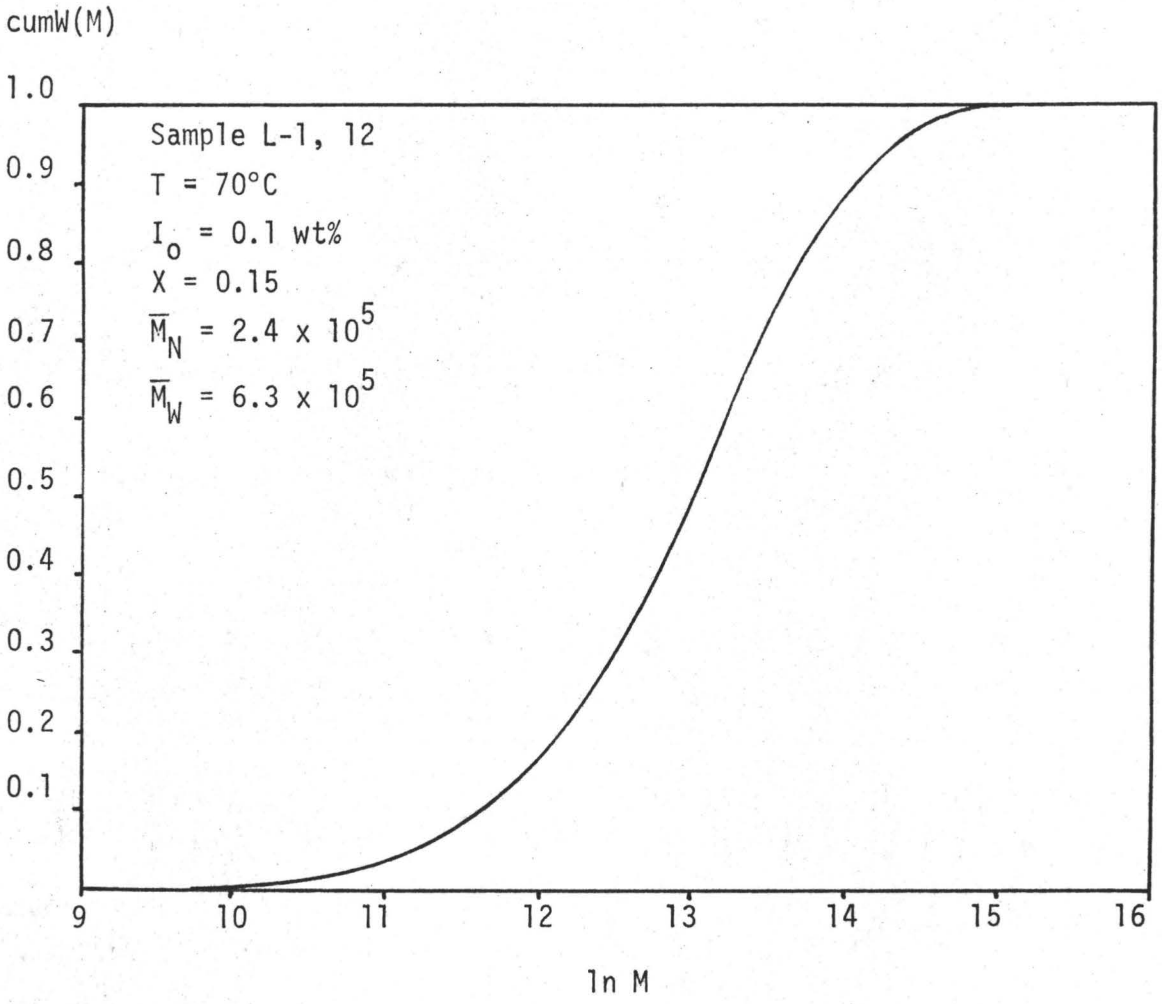

Sample L-1, 12

$T = 70°C$

$I_o = 0.1$ wt%

$X = 0.15$

$\overline{M}_N = 2.4 \times 10^5$

$\overline{M}_W = 6.3 \times 10^5$

Fig. 4-23: Cumulative MWD.

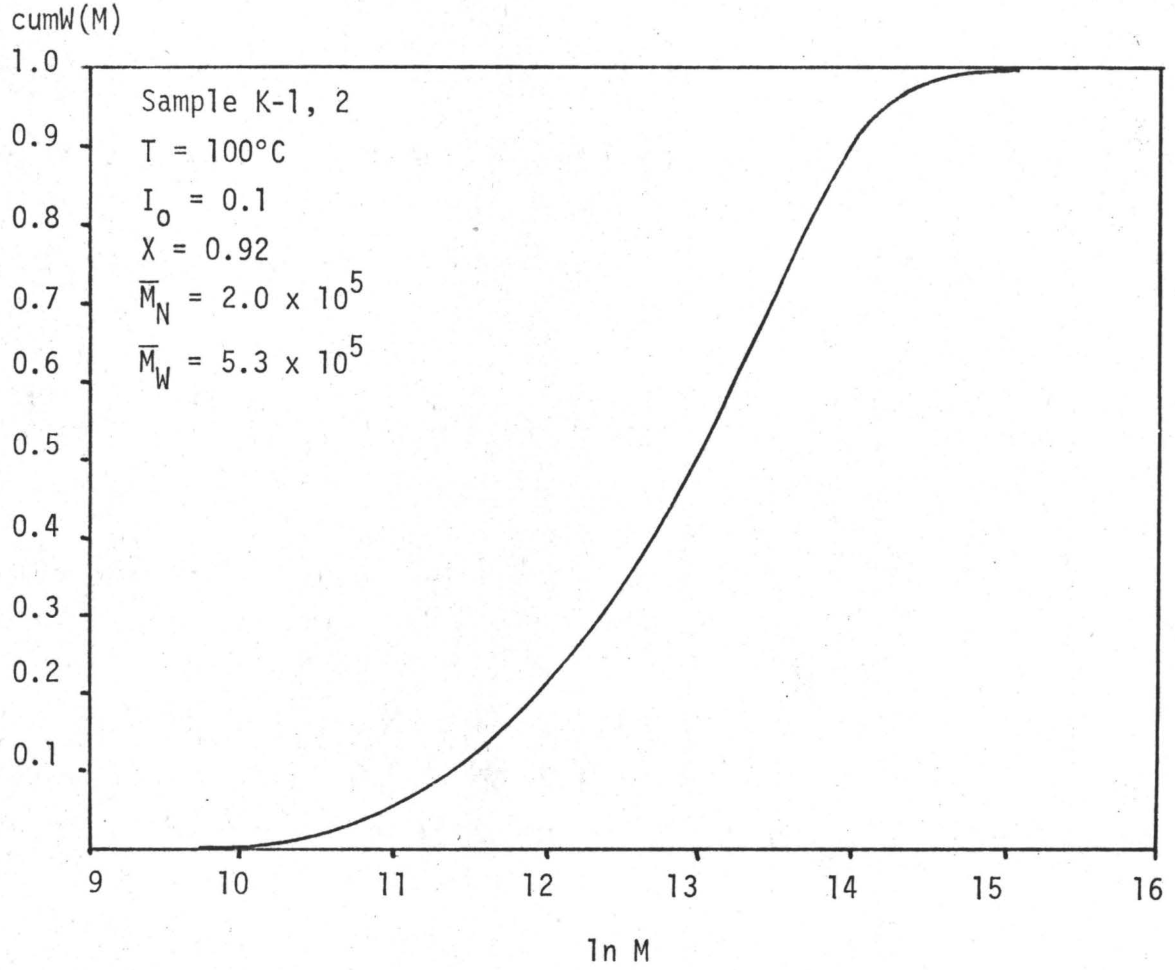

Fig. 4-25: Cumulative MWD.

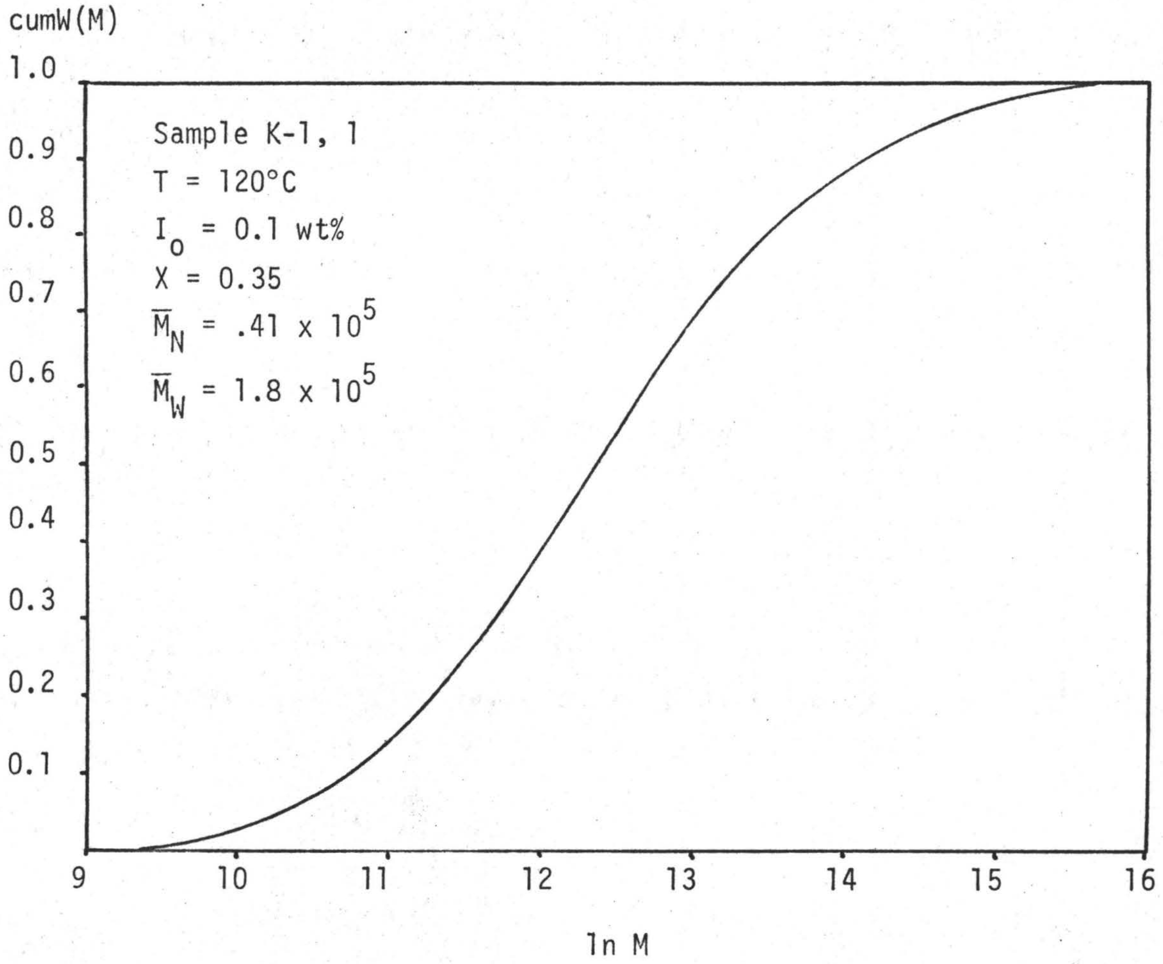

Fig. 4-26: Cumulative MWD.

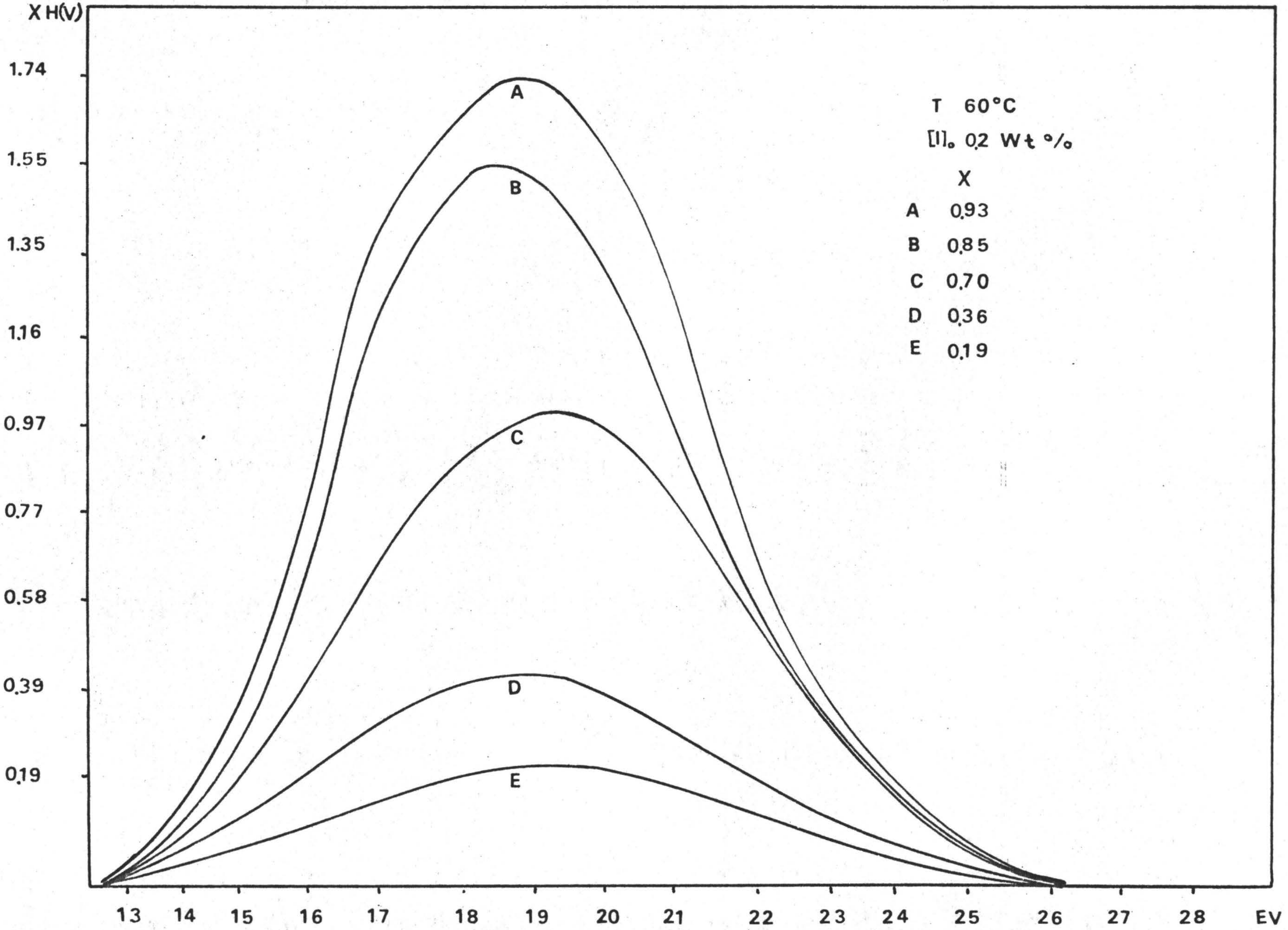

Fig. 4-27: Cumulative Chromatograms.

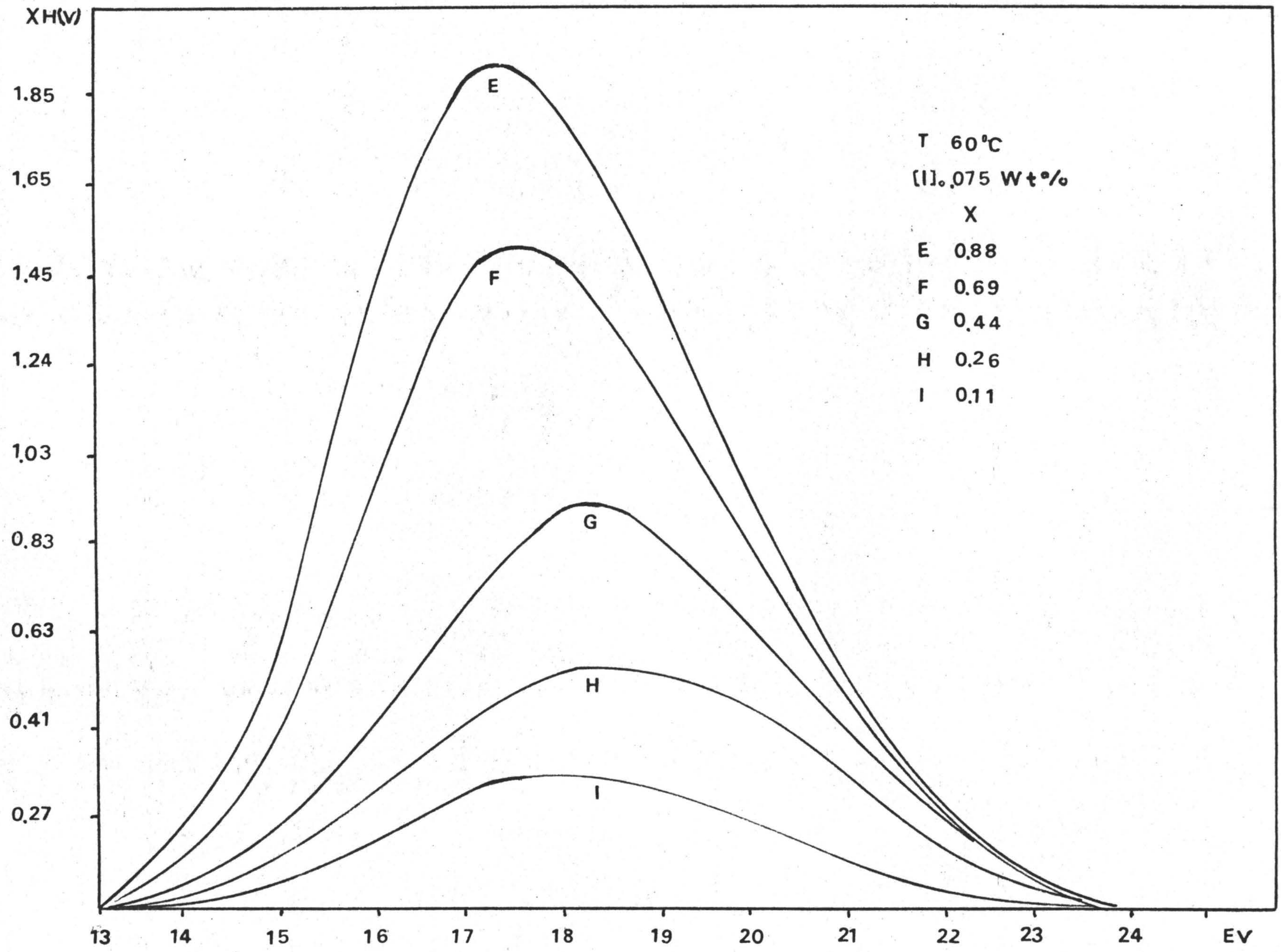

Fig. 4-28: Cumulative Chromatograms.

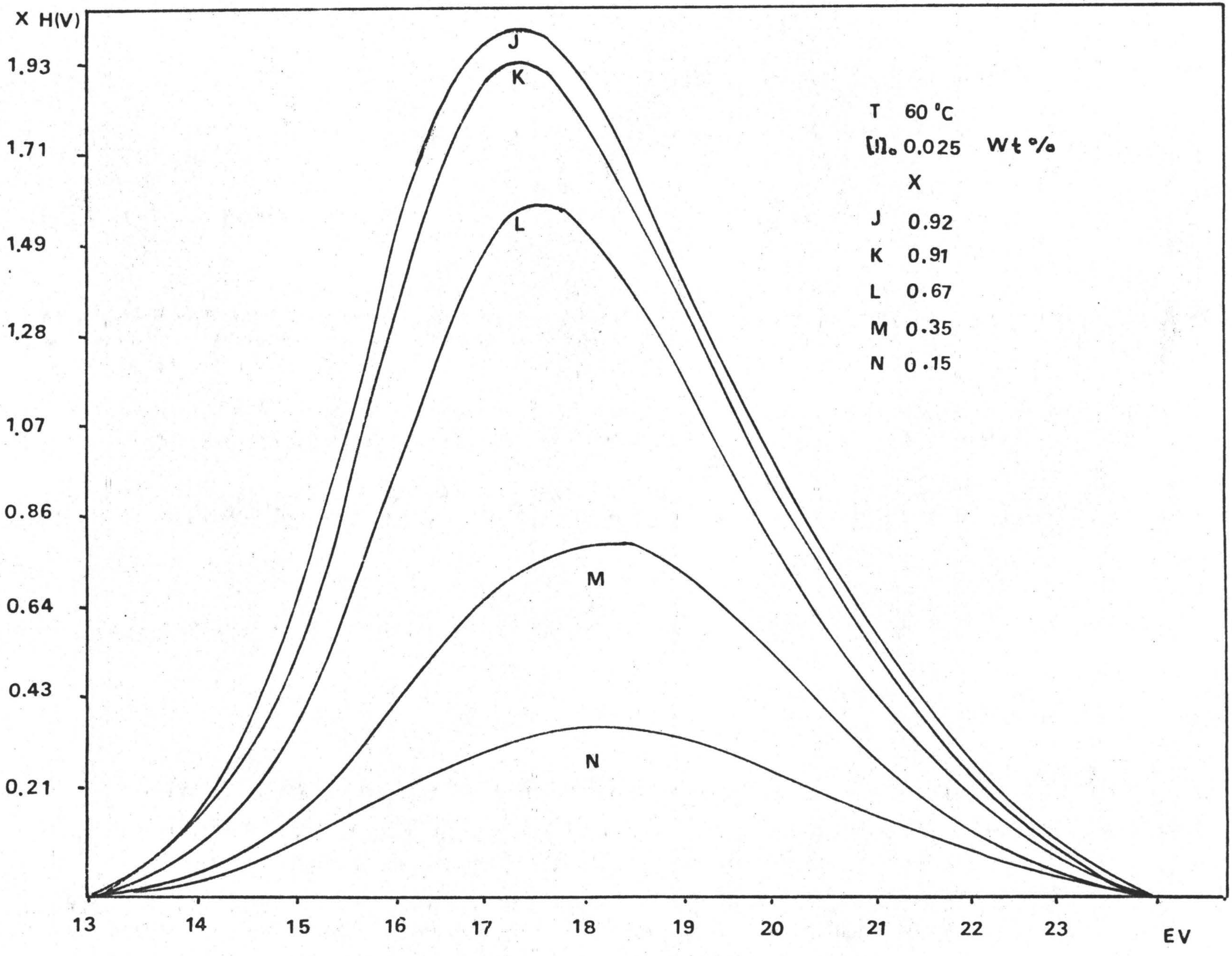

Fig. 4-29: Cumulative Chromatograms.

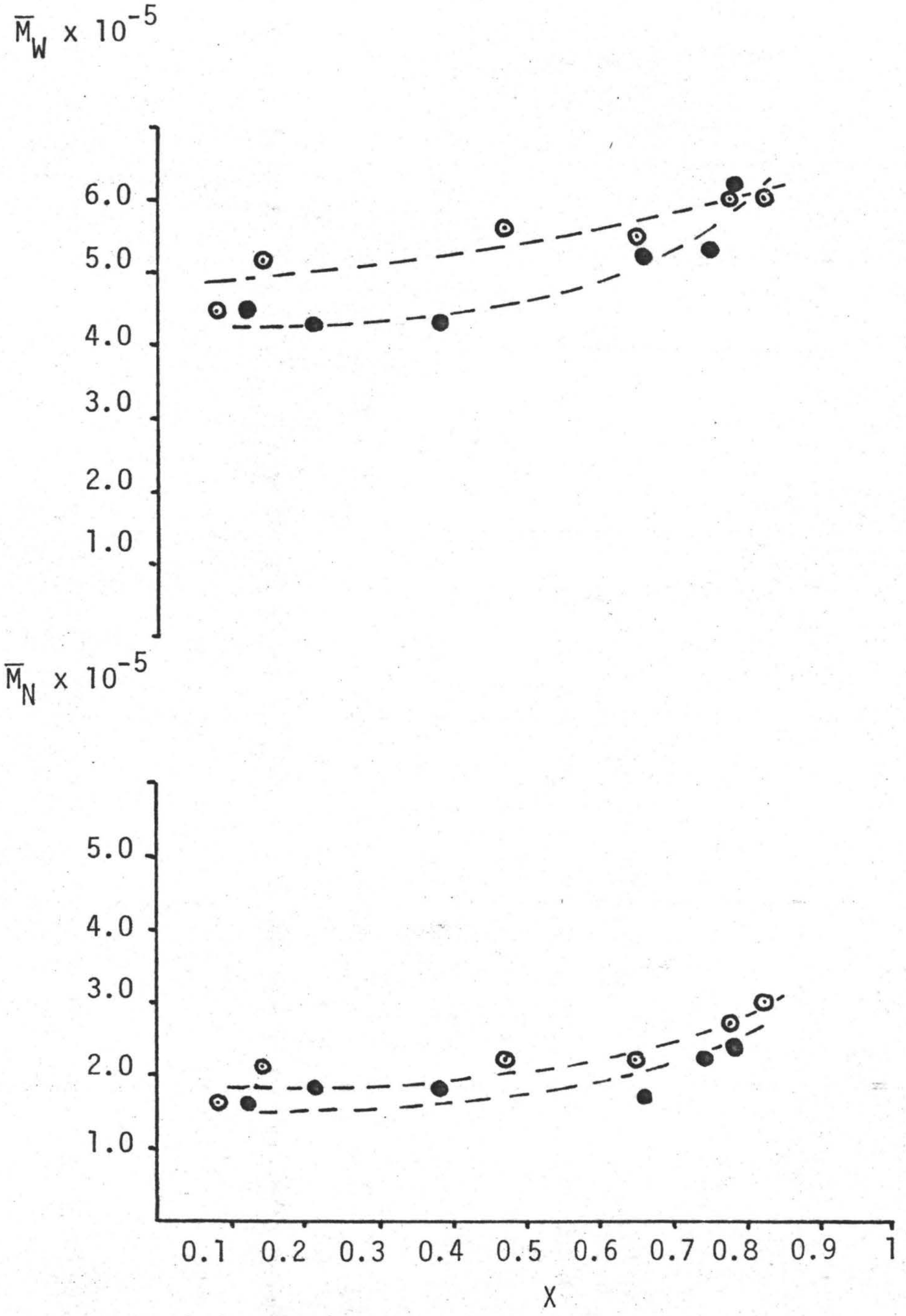

Fig. 4-30: Molecular weight averages versus conversion at 40°C ● $[I]_0$ = 2.0 wt% ⊙ $[I]_0$ = 0.05 wt%.

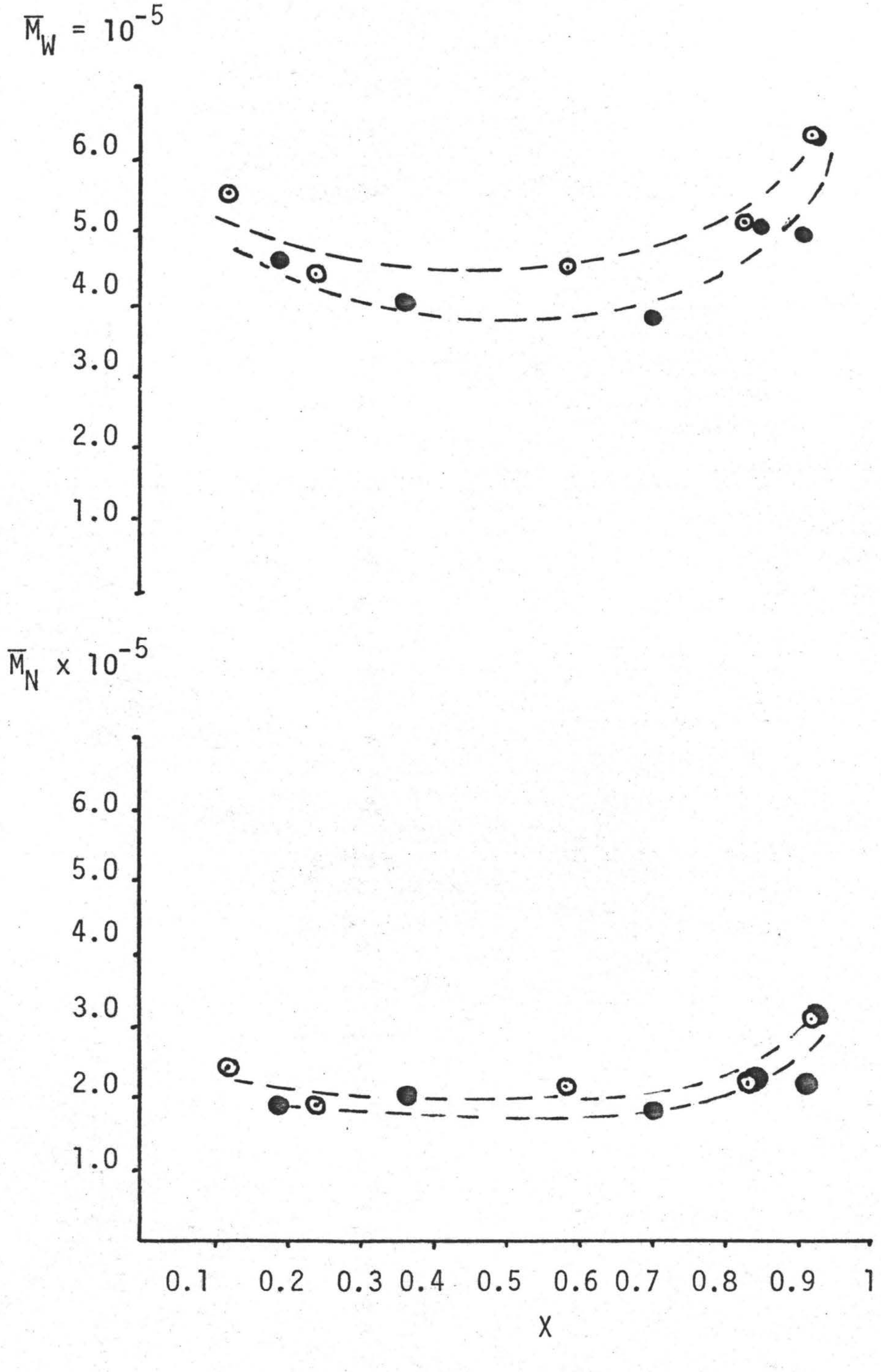

Fig. 4-31: Molecular weight averages versus conversion at 60°C ● $[I]_0$ = 0.2 wt% ⊙ $[I]_0$ = 0.025 wt%.

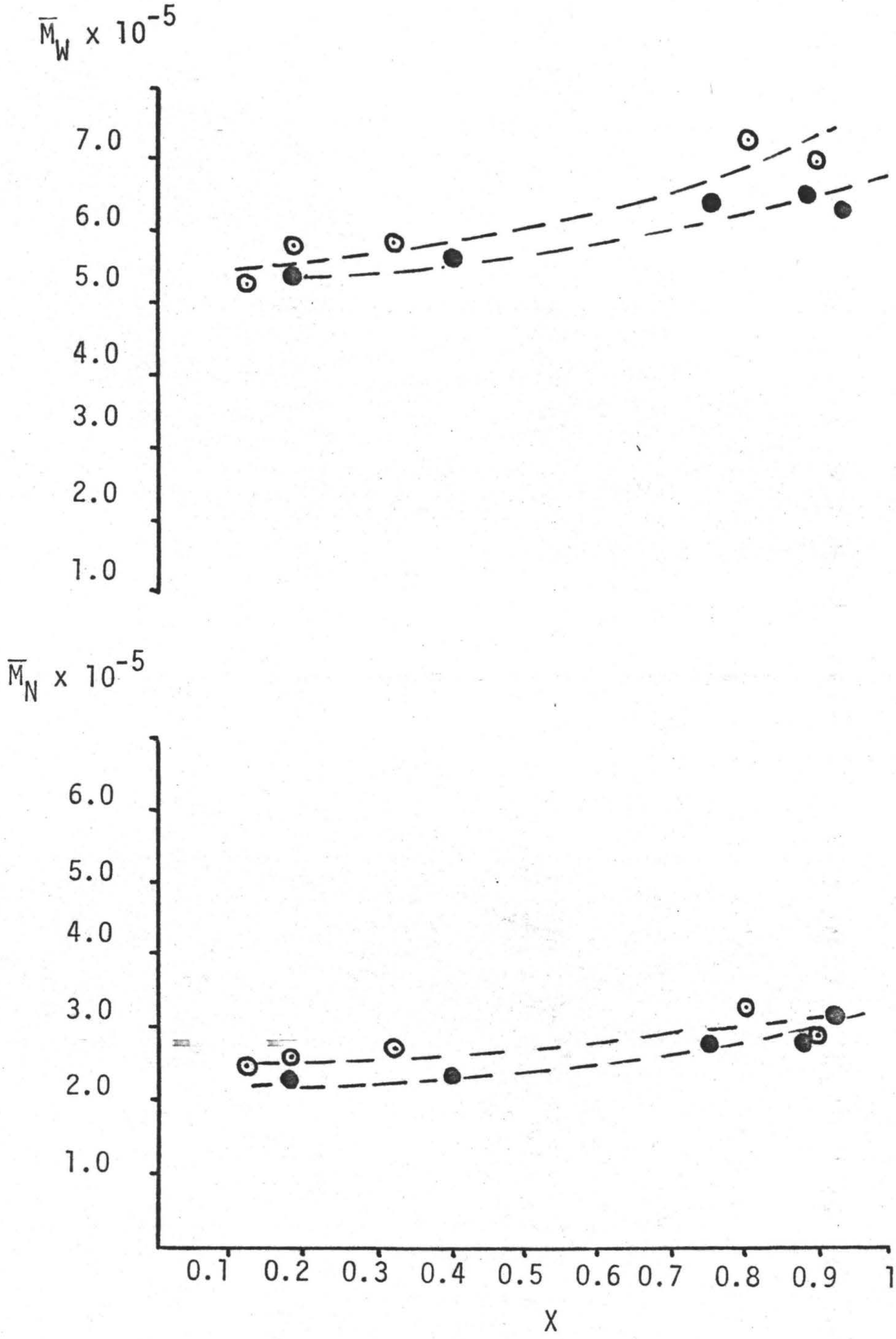

Fig. 4-32: Molecular weight averages versus conversion at 80°C ● $[I]_0 = 0.05$ ⊙ $[I]_0 = 0.025$.

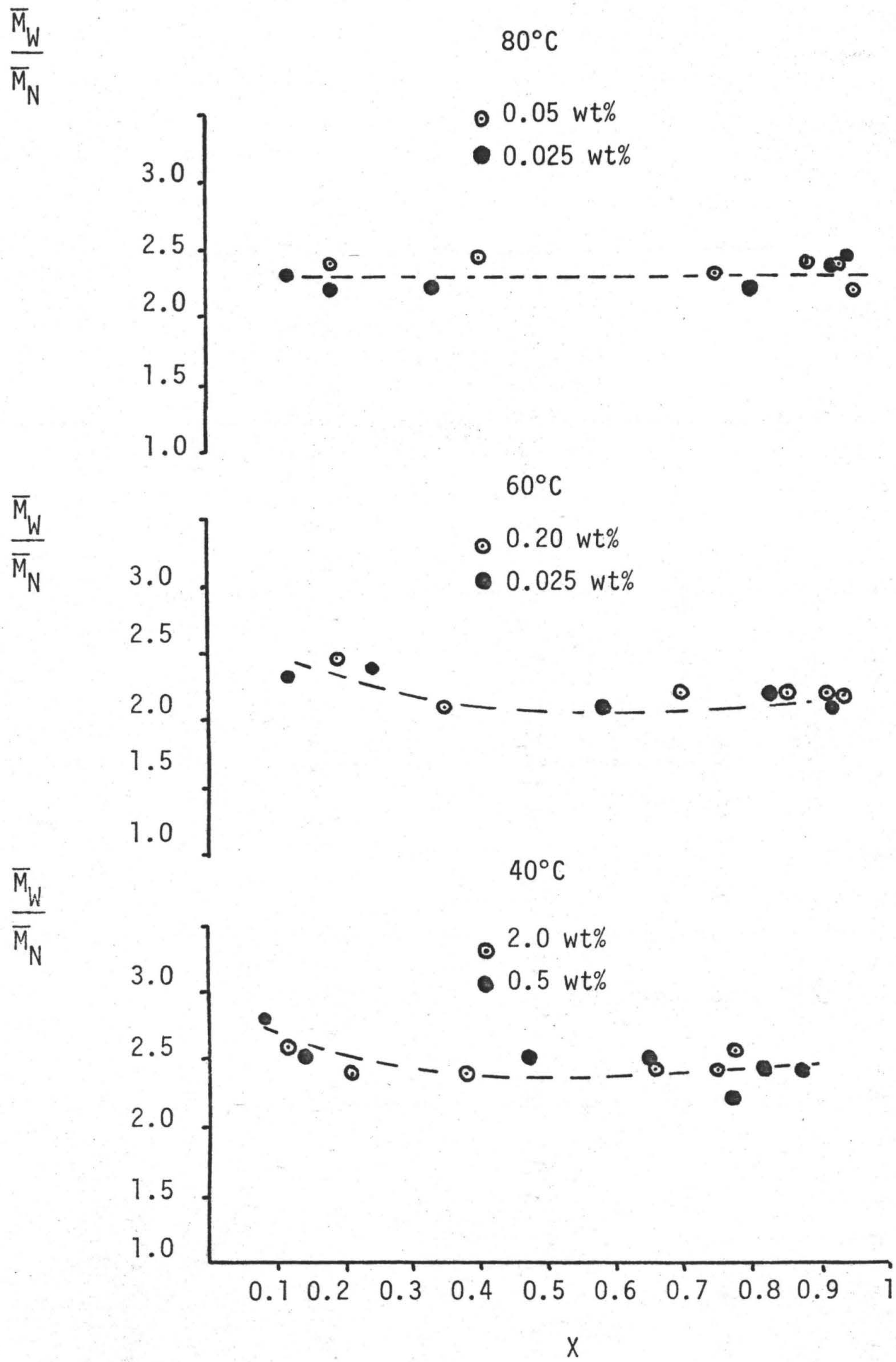

Fig. 4-33: Polydispersity ratios versus conversion.

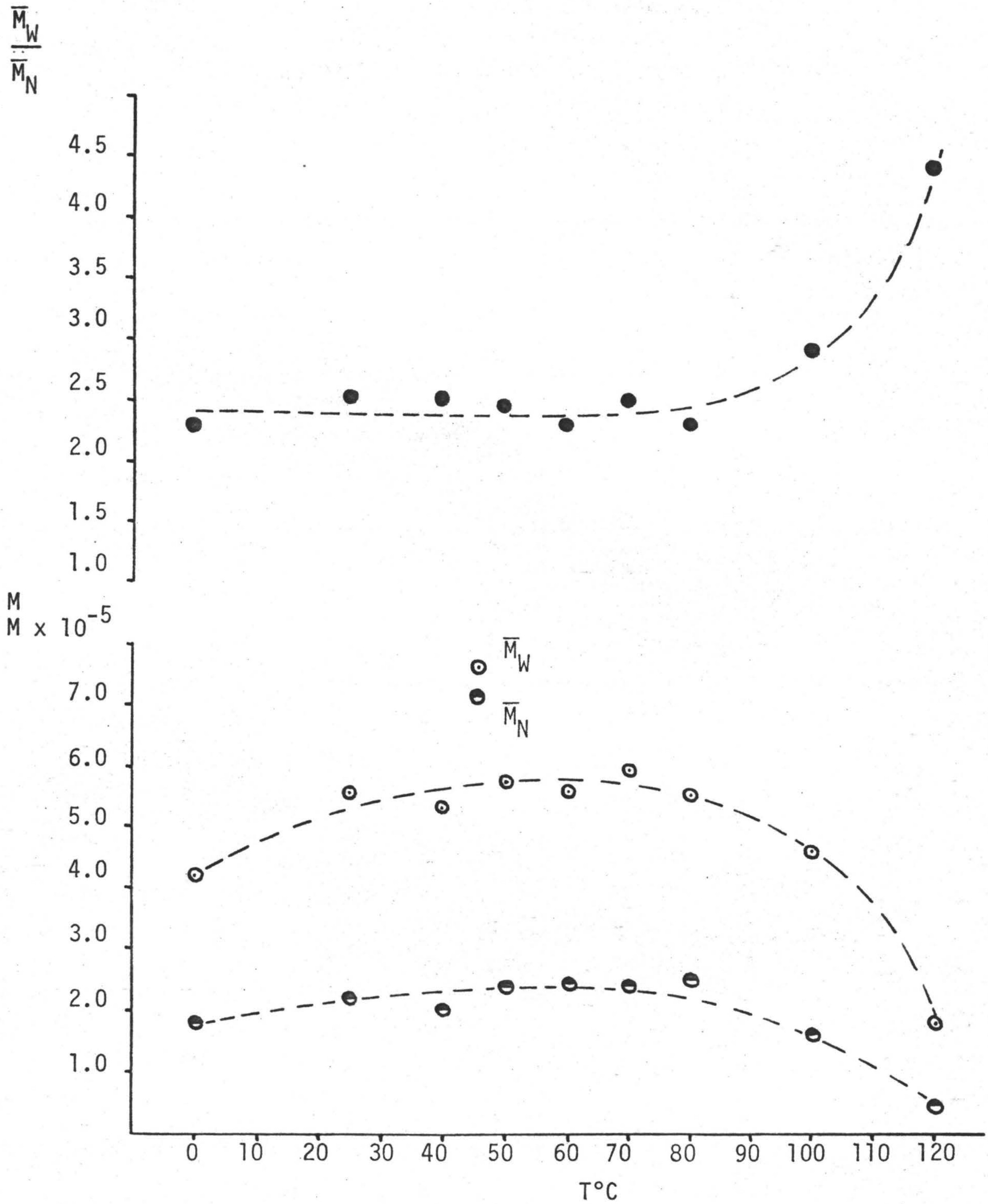

Fig. 4-34: Molecular weight averages and polydispersity ratios versus temperature.

CHAPTER 5

MODEL DEVELOPMENT

The experimental information obtained in this work and reported in the literature permits a systematic study of the kinetic behaviour of AN bulk polymerization. The models proposed and the assumptions on which they are based can be tested over the whole conversion and MWD range and at several temperatures. In this chapter, the bulk polymerization kinetics of AN are discussed in terms of a two-phase model.

5.1 Literature Review

The survey presented here is divided into two sections: the models and mechanisms proposed for AN bulk polymerization and the models and mechanisms proposed for vinyl chloride bulk polymerization that have been generalized for "precipitation polymerizations".

First detailed studies on the bulk polymerization of AN appeared in the 1940's, notably those of Kern and Fernow (40) and Koningsberger and Solomon. (44) Extensive work was done on AN polymerization in the 1950's. A very good review paper on the kinetic aspects of AN polymerization processes covering the literature up to 1960 is given by Thomas. (68) More recent publications are somewhat scarce. The most relevant papers follow:

Bamford et al. (8,9,10)

The kinetics of AN bulk polymerization were discussed in a series of papers. The following reaction scheme was proposed.

$$
\begin{aligned}
I &\longrightarrow 2R_i \\
R_r^{\cdot} + M &\longrightarrow R_{r+1}^{\cdot} \\
R_r^{\cdot} + M &\longrightarrow R_i^{\cdot} + P_r \\
R_m^{\cdot} + R_r &\longrightarrow P_{m+r}
\end{aligned}
$$

The assumptions made were that the reaction takes place only in the monomer phase. The acceleration observed is due to increasing initiator concentration in the monomer phase. Termination is by combination and transfer to monomer controls the molecular weights. The molecular weights are independent of conversion and a maximum is observed in the temperature range 50° - 60°C. The equations proposed are:

$$-\frac{dM}{dt} = k\, I^{1/2} M^{1/2}\, \rho^{1/2}$$

$$x = 1 - (At - 1)^2$$

$$A = \frac{1}{2}\,\frac{kI^{1/2}}{\rho^{1/2}}$$

where k is a constant, ρ is the density of the monomer, I is the mass of initiator and M is the mass of monomer. This model fits the data reasonably well but it does not predict the MWD. The main drawbacks of this model are that it does not predict the rate acceleration period and fails to explain the drop in rate at different initiator concentrations which does not have a square root dependence.

Thomas and Pellon (69)

These workers explained their experimental data in terms of two distinct termination steps. One of these was considered to be the normal bimolecular termination, and the other was regarded as a unimolecular process in which the growing chain becomes buried and is shielded from further growth. The liquid phase enriches in initiator concentration as the polymerization proceeds. The model proposed:

$$-\frac{d[R^{\cdot}]}{dt} = k_t[R^{\cdot}]^2 + k_b[R^{\cdot}]$$

$$k_d[I] = k_t[R^{\cdot}]^2 + k_b[R^{\cdot}]$$

$$[R^{\cdot}] = -\frac{k_b}{2k_t} + [k_b^2 + k_t k_d I]^{1/2}$$

$$R_P = \frac{k_p}{2k_t}[(k_b^2 + 4k_t k_d I)^{1/2} - k_b]$$

$$R_P = (A^2 + BI)^{1/2} - A$$

where

$$A = \frac{k_b k_P}{2k_t} \quad ; \quad B = \frac{k_d k_P^2}{k_t}$$

The molecular weights are predicted with the equation:

$$\bar{r}_N = k_P[R^{\cdot}]/(k_t[R^{\cdot}]^2 + k_b[R^{\cdot}])$$

Although the model predicts their data reasonably well, there are several objections to it: the number of radicals occlusion has been proved to be very small,(48,68) and therefore, the effect of occlusion is negligible. The polymerization rate was assumed constant and transfer to monomer neglected.

In a subsequent paper, Thomas (69) emphasised the possibility of the reaction taking place both in the monomer and in the polymer phase, and the similarities of this system with the emulsion system, at least during the early polymerization stages.

In the review presented by Thomas, three sources of uncertainty are evident. The rate dependency with respect to the initiator concentration exponent (the values reported are in the range 0.5 - 0.9), the extent and influence of the acceleration period and the termination reactions.

Lewis and King (48)

These workers studied the bulk polymerization of AN at 50°C using AIBN as initiator. The number of occluded radicals were measured as well as the number of particles and the surface area. The concentration of trapped radicals proved to be too small to have any effect on the kinetics. The specific area decreased with conversion and appears to be independent of initiator concentration. An acceleration followed by a constant rate period was observed. At low initiator concentrations, the rate is reported to vary as $I^{0.89}$ whereas at high concentrations, it varies as $I^{0.33}$. From microscopic observations and an estimated monomer concentration in the polymer phase of about 5%, the contribution of the polymer phase was neglected.

The following assumptions were reported. The surface of the polymer particles is the only locus of polymerization which needs to be considered. The propagation and termination rate constants are affected by the presence of the solid surface and therefore different from those in homogeneous conditions. The steady state approximation was assumed to hold.

The following reactions summarize the scheme:

$$\begin{array}{ll}
I \longrightarrow 2R_c^{\cdot} & \frac{dR^{\cdot}}{dt} = 2fk_dI \\
R_c^{\cdot} + M \xrightarrow{k_i} R_i^{\cdot} & -\frac{dR^{\cdot}}{dt} = \frac{dR_1}{dt} = k_iMR^{\cdot} \\
R_n^{\cdot} + M \xrightarrow{k_p} R_{n+1}^{\cdot} & -\frac{dM}{dt} = R_p = k_pMR^{\cdot} \\
R_n^{\cdot} + R_m^{\cdot} \xrightarrow{k_t} P_{n+m} & -\frac{dR^{\cdot}}{dt} = 2k_tR^{\cdot 2} + 2\frac{R^{\cdot}}{\tau} \\
R_n^{\cdot} + R_c^{\cdot} \longrightarrow P_n & -\frac{dR^{\cdot}}{dt} = -\frac{dR_i}{dt} = k'_tR^{\cdot}R_c \\
2R_c^{\cdot} \longrightarrow \text{products} & -\frac{dR_c}{dt} = 2k''_tR_c^{\cdot 2}
\end{array}$$

assuming steady state, the following equations were obtained

$$\beta_4 \frac{(1 - 4\beta_3)}{M^3} R_p^4 + \frac{(1 - 8\beta_3)}{M^2} R_p^3 -$$

$$\left(\frac{4\beta_3}{M\beta_4} + \frac{M\beta_4}{\beta_1^2} - \frac{k_dI}{M\beta_2}\right)R_p^2 -$$

$$(\frac{M^2}{\beta_1} + \frac{2Mk_dI}{\beta_1\beta_2})\ R_p + \frac{M^3k_dI}{\beta_1\beta_2} = 0$$

where

$$\beta_1 = \frac{k'_t}{k_ik}$$

$$\beta_2 = \frac{1}{f\tau k}$$

$$\beta_3 = \frac{k_tk_t}{k'^2_t}$$

$$\beta_4 = \frac{k_t\tau}{k}$$

This four parameter model is reported to fit the data very well and the constants estimated from it appear to be in agreement with values reported elsewhere. There are several objections to this model. Transfer to monomer is neglected, the change in initiator concentration due to monomer depletion has been neglected, a constant rate period is assumed after the initial acceleration region, and it has been proved that this is not always present. It does not predict the MWD and there is experimental evidence showing that the assumption that the polymerization takes place only on the surface of the polymer particles is a dubious one. (56, 68, 74)

Amdur (3)

Amdur studied the bulk polymerization of AN using $FeCl_3$ as terminator. The autoacceleration period was reported nonexistent. The following assumptions were made: the polymerization is governed by a steady state concentration of growing radical chains. Polymerization occurs at the surface of the aggregates; k_p and k_t are affected by the presence of the polymer phase. The scheme proposed:

$$[I] \xrightarrow{k_d} 2R^{\cdot}$$

$$R_n^{\cdot} + M \xrightarrow{k_p} R_{n+1}^{\cdot}$$

$$R_n^{\cdot} + F \xrightarrow{k_i} FeCl_2 + P_n$$

$$R_n^{\cdot} + R_m^{\cdot} \longrightarrow P_{n+m}$$

Applying the steady state kinetics, the following expression was obtained.

$$R_p = k_t \frac{- k_t'[F] + (k_t'^{2} [I]^2 + 8k_t k_d [I])^{1/2}}{2k_t} [M]$$

The model predicts the data very well in the experimental range (up to 3% conversion) and the rate constants were evaluated. If the terms containing $FeCl_3$ are neglected, the equation remaining is the normal rate expression for vinyl polymerization with square root initiator dependency. No change in volume is considered nor the effect of the water solution in the polymer formed during the reaction.

Marquardt and Mehnert (49)

These workers developed a dilatometric technique for measuring conversion. Two temperature levels were reported (50° and 60°C). A two parameter equation was derived using a Taylor series expansion to describe the time dependence of the monomer concentration:

$$\frac{x}{t} = A - \frac{n}{2} A^2 t$$

The following mechanism was proposed.

$$I \xrightarrow{fk_d} 2R_i + N_2$$

$$R_{\dot{n}}(\mathrm{hom}) + M \xrightarrow{k_p(\mathrm{hom})} R_{r+1}(\mathrm{hom})$$

$$R_{\dot{r}}(\mathrm{hom}) + R_{\dot{r}}'(\mathrm{hom}) \xrightarrow{k_t} P_{r+r'}, \mathrm{resp}\ P_r + P_r'$$

$$R_{\dot{r}}(\mathrm{hom}) \longrightarrow R_{\dot{r}}(\mathrm{het})$$

$$R_{\dot{r}}(\mathrm{het}) + M \xrightarrow{k_t(\mathrm{het})} R_{\dot{r}+1}(\mathrm{het})$$

For this scheme, the assumptions made are: no initiation takes place in the polymer phase, the radicals propagate in the polymer and monomer phase, no termination occurs in the polymer phase. Steady state is assumed in the monomer phase. The radical concentration in the monomer phase:

$$R_{\dot{M}} = \left(\frac{v_o}{k_t}\right)^{1/2} (1 - \xi)^{1/2} e^{-k_d t/2}$$

$$R_{\dot{P}} = \frac{v_o}{k_d} \xi (1 - e^{-k_d t})$$

where

$$v_o = 2fk_d[I_o]$$

$$\xi = (\frac{dR_P}{d_t})/(v_o\ e^{-k_d t})$$

$$R_{PM} = k_{PM}[M]R_{\dot{M}}$$

$$R_{PP} = k_{PP}[M]R_{\dot{P}}$$

$$-\frac{d[M]}{d_t} = \frac{k-1}{k} R_P$$

where k is a proportionality constant obtained from the dilatometric measurements and accounts for the change in volume:

$$-\frac{d[M]}{d_t} = \frac{k-1}{k}(k_{PM}[M]R_{\dot{M}} + k_{PP}[M]R_{\dot{P}}$$

and

$$\frac{dx}{dt} = \frac{k-1}{k}(k_P(1-x)(\frac{v_o}{k_P})^{1/2}(1-\xi)^{1/2}\ e^{-k_d t/2} + k_{PP}(1-x)$$

$$(\frac{v_o}{k_t})\ \xi(1 - e^{k_d t}))$$

which integrated:

$$\frac{\ln(1-x)}{(\exp -\frac{k_d t}{2} - 1)} = (\frac{k-1}{k})(\frac{k_{PM}}{k_t^{1/2}}\ \frac{(8f(1-\xi)^{1/2}}{k_d^{1/2}}\ [I_o]^{1/2} + k_{PM}2f\ [I_o]t)$$

The induction period was defined by $\frac{d^2[M]}{dt^2} = 0$ and the expression given:

$$t_{ip} = (2fk_d(1 - \quad)[I]_o k_t)^{-1/2}\ \text{arcsinh}(\frac{k}{k-1}\ \frac{k_t}{k_{PM}})^{0.5}$$

This model fits the data at low conversions, ignores transfer to monomer and neglects termination reaction in the polymer phase. This would cause a high concentration of radicals which has not been detected. No expression for the MWD was given.

5.2 The Two-Phase Model

5.2.1 Justification of the Two-Phase Model Approach for AN

Three different approaches have been proposed to describe the precipitation polymerization systems in general and AN in particular. Namely, the emulsion polymerization approach. Polymerization taking place at the polymer-monomer interphase, and the two-phase theory approach. In precipitation polymerization systems, the particles are not stabilized and it is therefore difficult to describe the system in terms of the number of particles. An additional difficulty is present for AN since after about 50% conversion, the polymer forms a coarse mass in which the particles are undetectable. The low solubility of the monomer in the polymer and the estimation that the average life time of a radical in the monomer phase is sufficient only to add ten monomer units before it collides with a polymer particle (48) led to the assumption that propagation and termination can be neglected in the monomer phase and therefore, the polymer-monomer interphase can be considered the only locus of polymerization. (3,48) The main features of AN bulk polymerization could be explained in terms of the surface area, but there is experimental evidence that invalidates the assumptions made for this approach and support the two-phase theory. This experimental evidence comes mainly from stirring studies and studies on precipitation polymerization processes in reaction medium where the monomer is insoluble. This evidence follows.

In general, if the polymerization rate is a function of the area available, one would expect it to increase with increasing initiator concentration and with agitation. This does not seem to occur. The area has been reported independent of initiator concentration. (48) No parallel correlation between the increasing rate of particle diameter and polymer rate at a given speed has been reported. Yamasaki et al. (74) in a recent electronic microscopy study on the effect of stirring speed observed that the particles grow not only by themselves but also by adhering secondary fine particles generated elsewhere on the surface of the polymer particles. The rate has been reported to decrease with agitation (56,74) and for polymerizations carried out in a centrifugal field. (57) This also supports the two-phase approach since agitation increases the monomer concentration in the polymer phase diminishing the diffusional resistance with agitation and in a centrifugation field, the monomer is completely depleted from the polymer particles. Addition of a swelling agent such as DMF to the reaction mixture in concentrations as low as 10 mol% reduces the rate by a factor of 15 (68), indicating that the diffusional resistance is lowered and therefore the rate decreases. Accordingly, the assumption that the polymerization proceeds only on the surface of the polymer particles is in doubt and it is evident that the polymerization takes place in both the monomer and the polymer phase.

The most recent models for precipitation polymerization systems have been developed for PVC and are based on the mechanism reported by Talamini. (66) The general theory for these models follows.

5.2.2 The Two-Phase Model Theory

The most successful model for PVC bulk polymerization was developed by Abdel-Alim and Hamielec (2) and recently generalized by Friis and Hamielec. (30) The model in its general form involves the following theoretical assumptions.

(a) Polymerization takes place in the monomer and in the polymer phase.

(b) The two-phases are in equilibrium, that is, have constant composition through all the two-phase region period.

A mass balance under these conditions will give the overall polymerization rate as the sum of the polymerization rates in each phase.

Monomer Consumption Rate

$$R_P = R_{PM} + R_{PP} \qquad 5\text{-}1$$

$$R_{PM} = k_{PM}[M]_M[R^{\cdot}]_M\phi_M \qquad 5\text{-}2$$

$$R_{PP} = k_{PP}[M]_P[R^{\cdot}]_P\phi_P \qquad 5\text{-}3$$

$$\phi_M = (1 - \phi_P) \qquad 5\text{-}4$$

where ϕ_M is the volume fraction of the monomer phase and ϕ_P is the volume fraction of the polymer phase. The overall monomer concentration:

$$[M] = [M]_P \phi_P + [M]_M (1 - \phi_P) \qquad 5\text{-}5$$

and introducing the monomer partition coefficient

$$k_M = \frac{[M]_P}{[M]_M} \qquad 5\text{-}6$$

in Equations 5-2 and 5-3 together with Eq. 5-5

$$R_{PP} = \frac{k_{PP}[M]\phi_P}{\phi_P + k_M(1 - \phi_P)}[R^{\cdot}]_P \qquad 5\text{-}7$$

$$R_{pM} = \frac{k_M kp_M [M](1 - \phi_p)}{\phi_P + k_M(1 - \phi_P)}[R^{\cdot}]_M \qquad 5\text{-}8$$

Equations 5-7 and 5-8 are completely general. The use of these equations requires expressions for the free radical concentrations. If it is assumed that each phase behaves like an homogeneous system (see Appendix 9-5),the following expressions are obtained:

$$[R^{\cdot}]_M = \left(\frac{2f_M kd_M [I]_M}{k_{tM}}\right)^{1/2} \qquad 5\text{-}9$$

$$[R^{\cdot}]_P = \left(\frac{2f\ k_{dP}[I]_P}{k_{tP}}\right)^{1/2} \qquad 5\text{-}10$$

The initiator in both phases is related to the overall initiator concentration.

$$[I] = [I]_P \phi_P + [I]_M (1 - \phi_P)$$

by introducing the partition coefficient in Equations 5-9 and 5-10

$$K_I = \frac{[I]_P}{[I]_M} \qquad 5\text{-}11$$

$$R_{PP} = \frac{k_{PP}[M]\phi_P}{\phi_P + K_M(1 - \phi_P)}\left(\frac{2f_P k_{dP}}{k_{tP}}\right)^{1/2}\left(\frac{[I]}{\phi_P + K_I(1 - \phi_P)}\right)^{1/2} \qquad 5\text{-}12$$

$$R_{PM} = \frac{k_{PM}[M](1 - \phi_P)}{\phi_P + k_P(1 - \phi_P)}\left(\frac{2f_M k_{dM}}{k_{tM}}\right)^{1/2}\left(\frac{K_I[I]}{\phi_P + K_I(1 - \phi_P)}\right)^{1/2} \qquad 5\text{-}13$$

It has been proved a valid assumption to consider two phases from the beginning of the reaction (1,30), therefore, the concentration in each phase is given by:

$$[M]_M = \frac{\rho_M}{\tilde{M}} \qquad 5\text{-}14$$

$$[M]_P = \frac{(1 - X_c)\rho_M}{(1 - X_c + X_c \frac{\rho_M}{\rho_P})\tilde{M}} \qquad 5\text{-}15$$

Substituting Equations 5-14 and 5-15 into 5-6

$$K_M = \frac{1 - X_c + X_c \frac{\rho_M}{\rho_P}}{1 - X_c} \qquad 5\text{-}16$$

A balance for the total system gives ϕ_P:

$$\phi_P = \frac{XX_c\rho_M + X(1 - X_c)\rho_P}{XX_c\rho_M + X_c(1 - X)\rho_P} \qquad 5\text{-}17$$

Since the composition of phases remains constant, the rate constants in the two phases assume a constant ratio P greater than unity:

$$\left(\frac{2f_P k_{dP}}{k_{tP}}\right)^{1/2} = p\left(\frac{2f_M k_{dM}}{k_{tM}}\right)^{1/2} \qquad 5\text{-}18$$

The initiator concentration can be expressed as:

$$[I] = \frac{[I]_o}{(1 - BX)} \exp(- k_d t) \qquad 5\text{-}19$$

where (1 - BX) corrects for the change in volume with conversion. B is defined as:

$$B = \frac{\rho_P - \rho_M}{\rho_M} \qquad 5\text{-}20$$

Combination of Equations 5-16 to 5-19 with 5-12 and 5-13 gives:

$$R_{PM} = k_{PM}[M]\left(\frac{[I]_o}{(1 - BX)}\right)^{1/2}\left(\frac{2f_M k_{dM}}{k_{tM}}\right)^{1/2}\left(\frac{X_c - X}{X_c(1 - X)}\right)\exp\left(- \frac{k_{dM}t}{2}\right) \qquad 5\text{-}21$$

$$R_{PP} = k_{PP}[M]\left(\frac{[I]_o}{(1 - BX)}\right)^{1/2}\left(\frac{2f_M k_{dM}}{k_{tM}}\right)^{1/2}\left(\frac{PX(1 - X_c)}{X_c(1 - X)}\right)\exp\left(- \frac{k_{dM}t}{2}\right) \qquad 5\text{-}22$$

and

$$R_P = \left(\frac{[I]_o}{1 - BX}\right)^{1/2}[M]\left(\frac{2f_M k_{dM}}{k_{tM}}\right)^{1/2}\exp\left(- \frac{k_{dm}t}{2}\right)\left\{k_{PM}\,\frac{(X_c - X) + k_{PP}X(1-X_c)P}{X_c(1 - X)}\right\} \qquad 5\text{-}23$$

Finally, using the definition of conversion, Eq. 5-23 can be transformed into

$$\frac{dX}{dt} = \left(\frac{2f_M k_{dM}}{k_{tM}}\right)^{1/2} \left(\frac{[I]_o}{1 - BX}\right)^{1/2} (k_{PM} + QX)\exp\left(- \frac{k_{dM}t}{2}\right) \qquad 5\text{-}24$$

where

$$Q = \frac{Pk_{PP}(1 - X_c) - k_{PM}}{X_c} \qquad 5\text{-}25$$

Equation 5-24 describes the polymerization course in the heterogeneous region, i.e., in the conversion interval $0 \leqslant X \leqslant X_c$. In the conversion interval $X_c \leqslant X \leqslant 1$, the system is homogeneous and the appropriate rate expression can be obtained directly from homogeneous kinetics. However, as the system approaches high conversions, all reactions become diffusion controlled, and to correct for this, Abdel-Alim and Hamielec suggested the use of the empirical correction factor, $(1 - X)/(1 - X_c)$. Using this together with the rate expression for homogeneous polymerization, the following expression was obtained for the conversion range, $X_c \leqslant X \leqslant 1$.

$$\frac{dX}{dt} = k_{PP}\left(\frac{2f_M k_{dM}}{k_{tM}}\right)^{1/2} P \, \frac{(1 - X)^2}{(1 - X_c)} \left(\frac{[I]_o}{1 - BX}\right)^{1/2} \exp\left(- \frac{k_d t}{2}\right) \qquad 5\text{-}25$$

Polymer Quality Equations

The instantaneous MWD and averages are generally different in the two phase because concentrations in each phase are different. The overall instantaneous and cumlative MWD's must therefore be calculated from the MWD in each phase. The overall weight fraction of polymer with chain length r is obtained as:

$$W(r) = \frac{R_{PP}}{R_{PP} + R_{PM}} W(r)_M + \frac{R_{PP}}{R_{PP} + R_{PM}} W(r)_P \qquad 5\text{-}26$$

and by integration of Equation 5-26, the overall cumulative MWD follows:

$$\text{cum}W(r) = \frac{1}{X} \int_0^X \left(\frac{R_{PM}}{R_{PM} + R_{PP}} w(r)_M + \frac{R_{PP}}{R_{PM} + R_{PP}} W(r)_P\right) dx \qquad 5\text{-}27$$

From Equations 5-26 and 5-27, it is possible to derive the following expressions for the overall instantaneous and cumulative number and weight average chain lengths.

$$\overline{r}_N = \frac{1}{\dfrac{R_{PM}}{R_{PP} + R_{PM}} \dfrac{1}{r_{NM}} + \dfrac{R_{PP}}{R_{PP} + R_{PM}} \dfrac{1}{r_{NP}}} \qquad 5\text{-}28$$

$$\overline{r}_W = \frac{R_{PM}}{R_{PP} + R_{PM}} \overline{r}_{WM} + \frac{R_{PM}}{R_{PP} + R_{PM}} \overline{r}_{WP} \qquad 5\text{-}29$$

and the cumulative averages:

$$\text{cum}\overline{r}_N = \frac{X}{\displaystyle\int_0^X \left(\frac{R_{PM}}{R_{PP} + R_{PM}} \frac{1}{\overline{r}_{NM}} + \frac{R_{PP}}{R_{PP} + R_{PM}} \frac{1}{\overline{r}_{NP}}\right) dx} \qquad 5\text{-}30$$

$$\text{cum}\overline{r}_W = \frac{1}{X} \int_0^X \left(\frac{R_{PM}}{R_{PP} + R_{PM}} \overline{r}_{WM} + \frac{R_{PP}}{R_{PP} + R_{PM}} \overline{r}_{WP}\right) dx \qquad 5\text{-}31$$

The validity of Equations 5-24, 5-25, 5-30 and 5-31 has been tested for bulk and suspension polymerization of vinyl chloride. (1,2)

Recently (47,62) this model has been criticized as being a simplification of the actual polymerization process. A number of variables not easily measurable have been proposed to complete the basic two-phase model. Until now, the "two-phase model" is the only one that gives a complete description of the precipitation polymerization process and has been tested at least for vinyl chloride over a wide range of conditions. It stands therefore as a first alternative in approaching the bulk polymerization of AN.

5.3 Model Fitting

Prior to the application of the "two-phase model", it is convenient to analyse the similarities and differences of the vinyl chloride and acrylonitrile systems. The first difference appears to be the initiator concentration dependency of the polymerization rate. It has been shown that the square root initiator concentration dependency holds for vinyl chloride.(1) A plot of the same type for AN shows that the overall rate does not appear to follow the square root initiator dependency. (48,68,69) (Fig. 5-1) neither the first order in the initiator exponent which has also been reported (67) (Figs. 5-2-5-4). An intermediate value of approximately 0.8 appears as the most reliable. (48,68).

This abnormal dependency has been accounted for by the change of the initiator concentration in the monomer phase and a decrease in the termination rate constant in the polymer phase which would give an intermediate value between 0.5 and 1. (8,68) Transfer reactions are

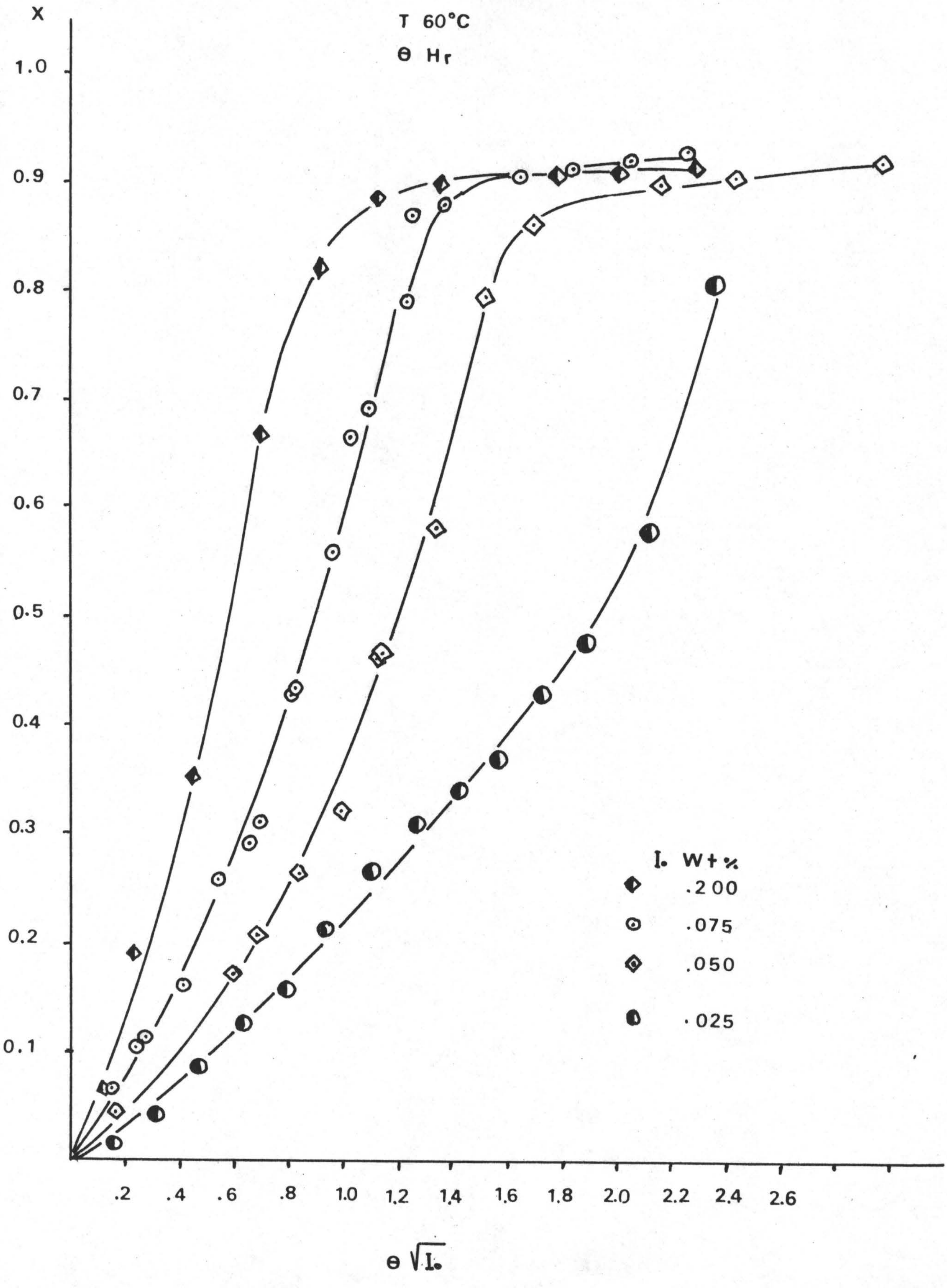
X
T 60°C
θ Hr
1.0
0.9
0.8
0.7
0.6
0.5
0.4
0.3
0.2
0.1
.2
.4
.6
.8
1.0
1.2
1.4
1.6
1.8
2.0
2.2
2.4
2.6
θ √I₀
I₀ Wt %
.200
.075
.050
.025

Fig. 5-1

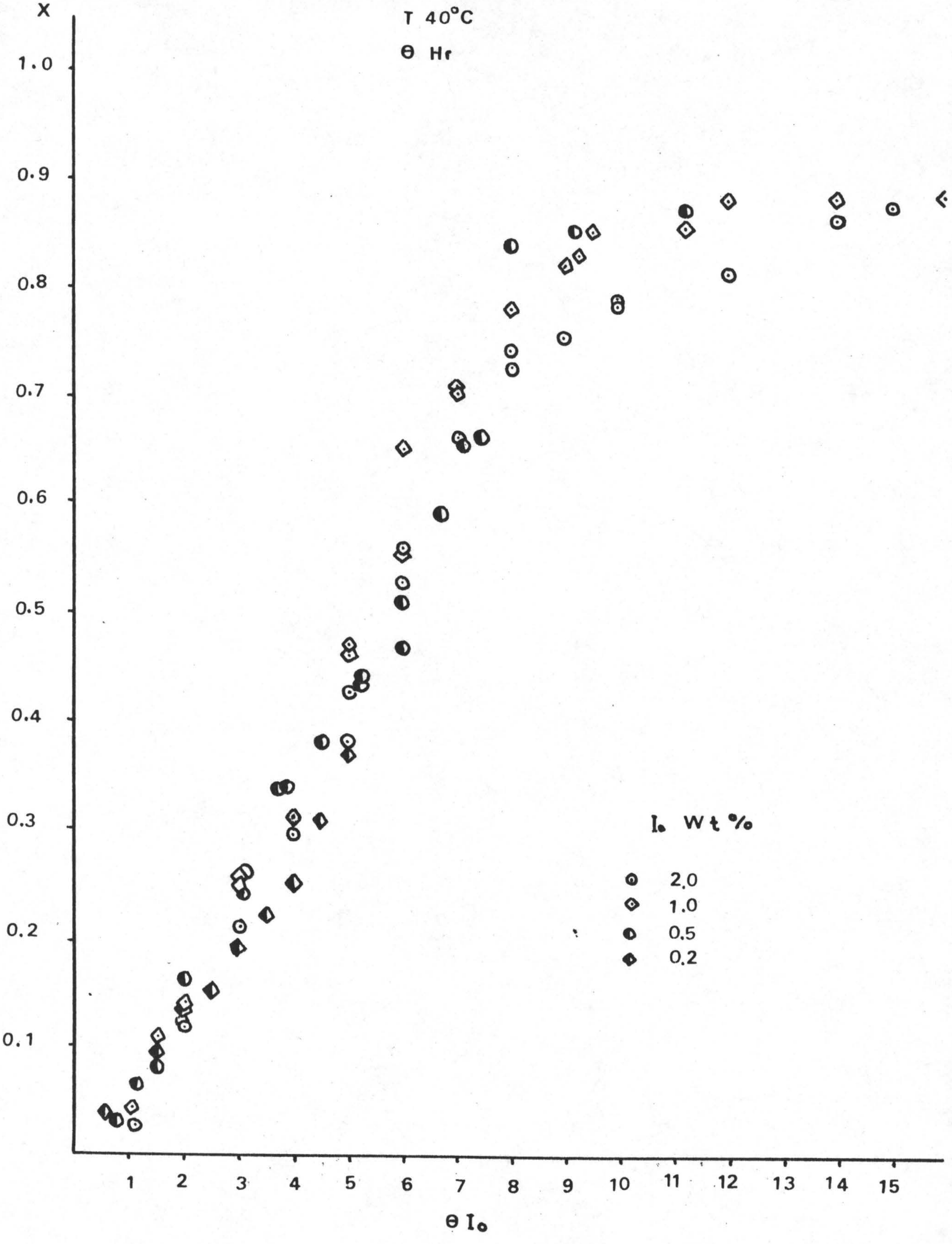
X
T 40°C
θ Hr
1.0
0.9
0.8
0.7
0.6
0.5
0.4
0.3
0.2
0.1
I₀ Wt %
2.0
1.0
0.5
0.2
1
2
3
4
5
6
7
8
9
10
11
12
13
14
15
θ I₀

Fig. 5-2

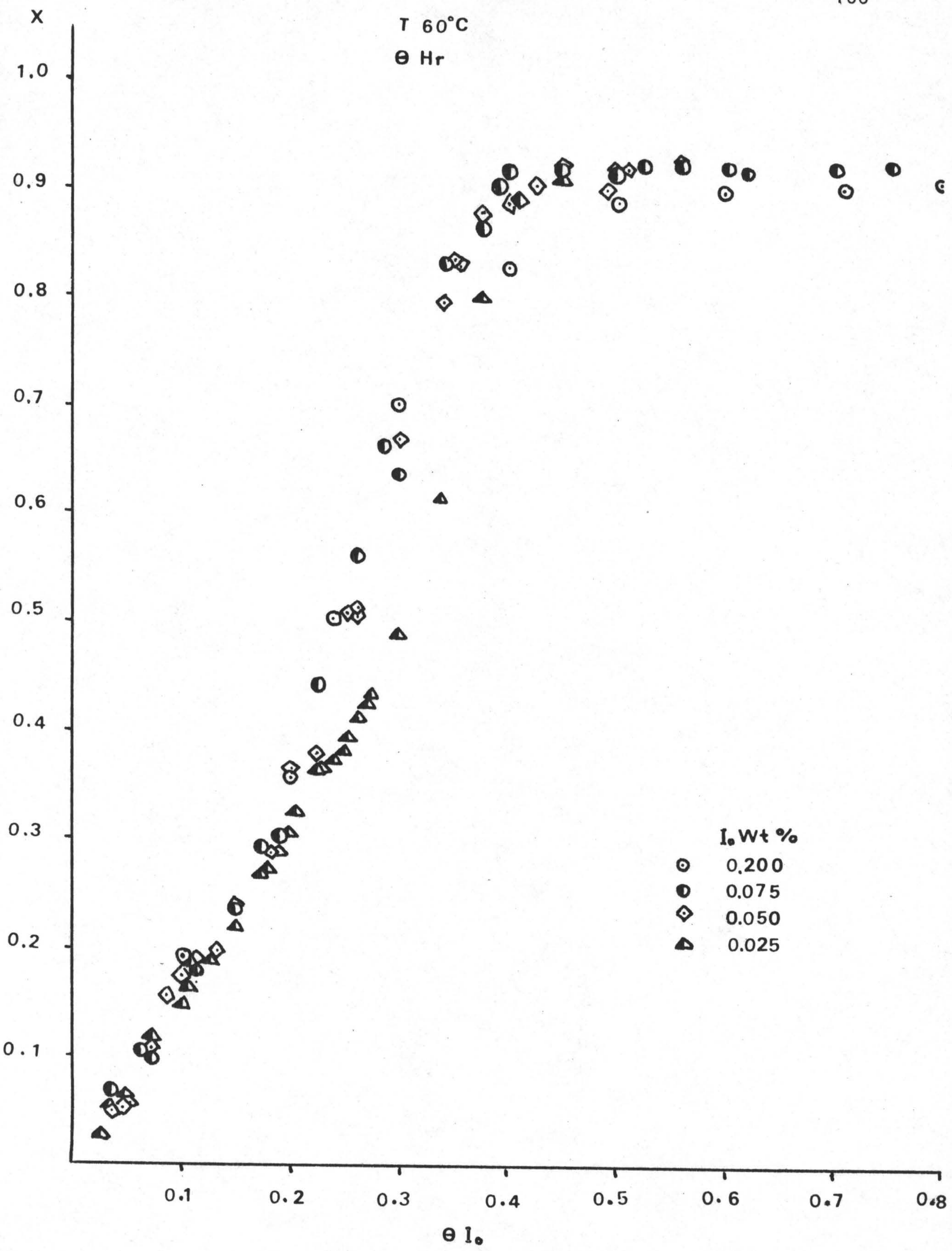
X
T 60°C
θ Hr
1.0
0.9
0.8
0.7
0.6
0.5
0.4
0.3
0.2
0.1
0.1
0.2
0.3
0.4
0.5
0.6
0.7
0.8
θ I₀
I₀ Wt %
0.200
0.075
0.050
0.025

Fig. 5-3

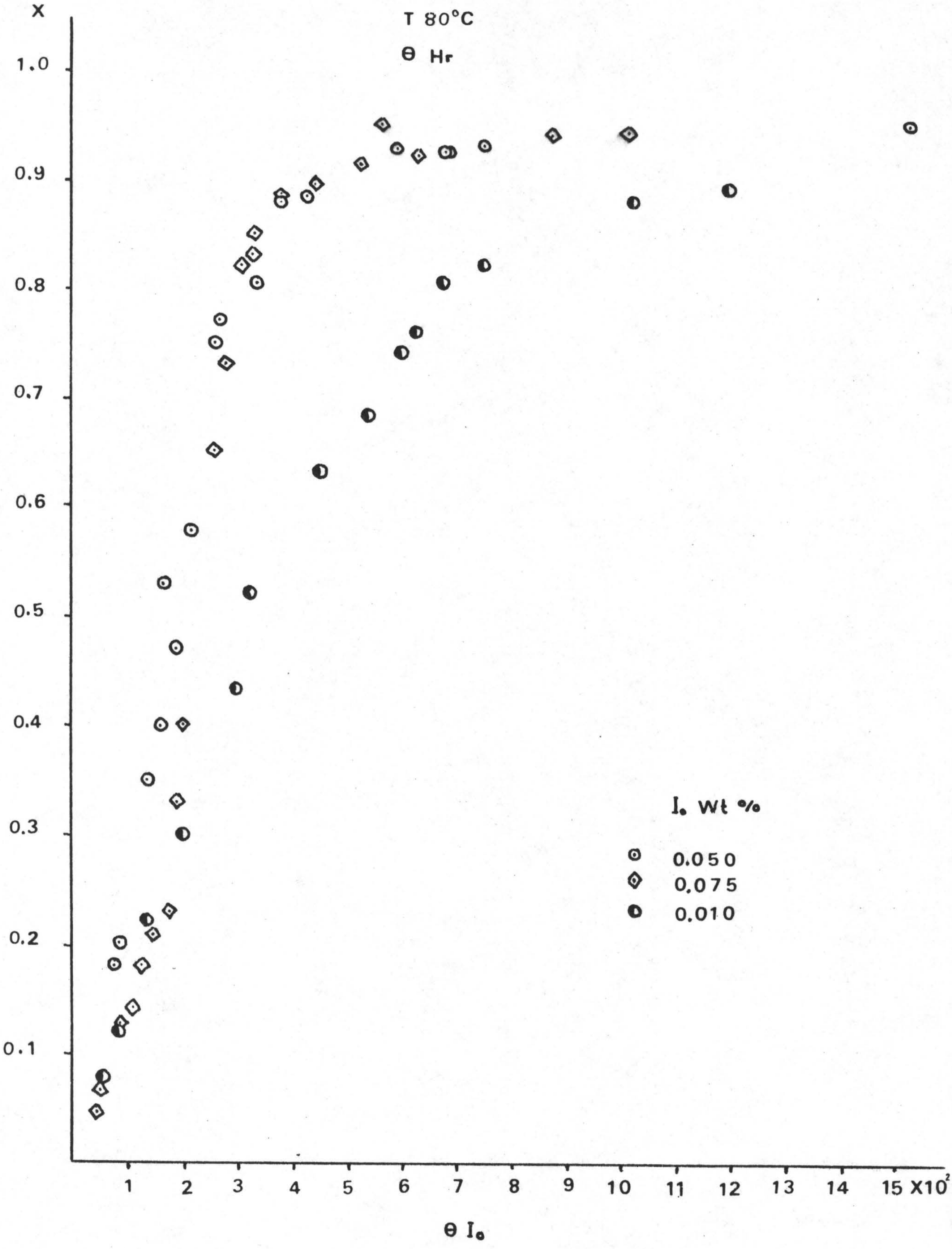
X
T 80°C
θ Hr
1.0
0.9
0.8
0.7
0.6
0.5
0.4
0.3
0.2
0.1
1
2
3
4
5
6
7
8
9
10
11
12
13
14
15 X10²
θ I₀
I₀ Wt %
0.050
0.075
0.010

Fig. 5-4

important in both VC and AN systems and they appear to control the MWD, although in AN, bimolecular termination seems to have more influence than in VC. Termination in VC is by disproportionation (6) and in AN is considered to be mainly by combination. (9) The MWD and averages do not provide additional information for the predominant termination mechanism in this case and the traditional method based upon the difference of the free energies of the two transition states, one leading to combination and the other leading to disproportionation is by no means certain. (53) AN and VC up to this point appear to be very similar with all the differences mentioned so far being accounted for with the two phase model. The most striking difference between the two systems is in the polymerization rate.

As mentioned earlier, the conversion histories for PVC and PAN show the following features: there is an acceleration period early in the reaction, followed by a constant rate region, then the rate increases up to a maximum and drops to zero as the limiting conversion is reached. A typical VC rate curve is shown in Fig. 5-5.

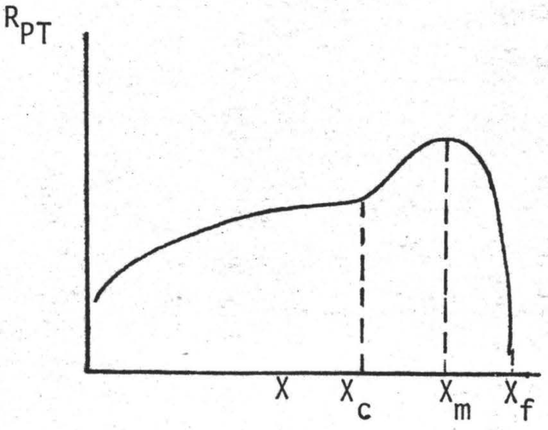

Fig. 5-5: Typical Vinyl Chloride Rate Curve.

At X_c conversion equals the mass fraction of polymer in the polymer phase at the polymerization temperature and the rate increase is due to the gel effect. X_m is the conversion at which the rate is maximum and X_f is the limiting conversion. These values are only function of the polymerization temperature. For AN, the acceleration period has been reported and studied extensively. (68) Variations in the acceleration period extent have also been reported. (8) A period of constant rate has been assumed by several authors (3,49,68) although it is evident from their data that the rate varies with conversion. It must be mentioned that in most cases, the data reported were obtained at low and intermediate conversion, therefore, the averages taken did not affect considerably the results when the models were fitted. In order to obtain more information about the rates, an empirical model was fitted to the conversion versus time data.

5.3.1 Empirical Model

The conversion histories reported here are complex functions and it is difficult to find a simple mathematical expression that gives the best fit over the whole range. Some rather involved mathematical techniques have to be used. In order to select the appropriate technique, the following premises were set:

i) The function is to be continuous, for conversion is a continuous function of time.

ii) The first derivative has to be continuous at least up to X_c where a phase inversion occurs.

iii) Oscillations in the functions are to be kept at the minimum possible, for the data does not show oscillatory behaviour.

iv) As a first approach, the derivative is to be analysed in one dimension, with respect to time.

From these and the alternatives proposed by Anderssen and Bloomfield (5) and Wold (72), the most convenient functions appear to be "the Spline functions".

Spline functions are defined as piecewise polynomials of degree n. The pieces join in the so called knots and fulfill the continuity conditions for the function and the first n-1 derivatives. (72) The general theory for splines and details of the fitting procedure are shown in Appendix 9-2.

Third order degree splines with four knots were fitted using a routine available from McMaster Computer Library. The parameters and the fit obtained were considered adequate (see Appendix 9-2). The least squares error for almost every case was less than 2%. The rates obtained are shown in Figs. 5-6 to 5-9 and are discussed below.

The initial rates estimated are slightly greater than those reported at low conversions, this is not unexpected since the data obtained is not very accurate at low conversions.

The instantaneous rates obtained show different behaviour at different initiator concentrations and are dissimilar to those reported for VC. Strong differences are now evident between AN and VC if Fig. 5-5 is compared with Figs. 5-7 to 5-9:

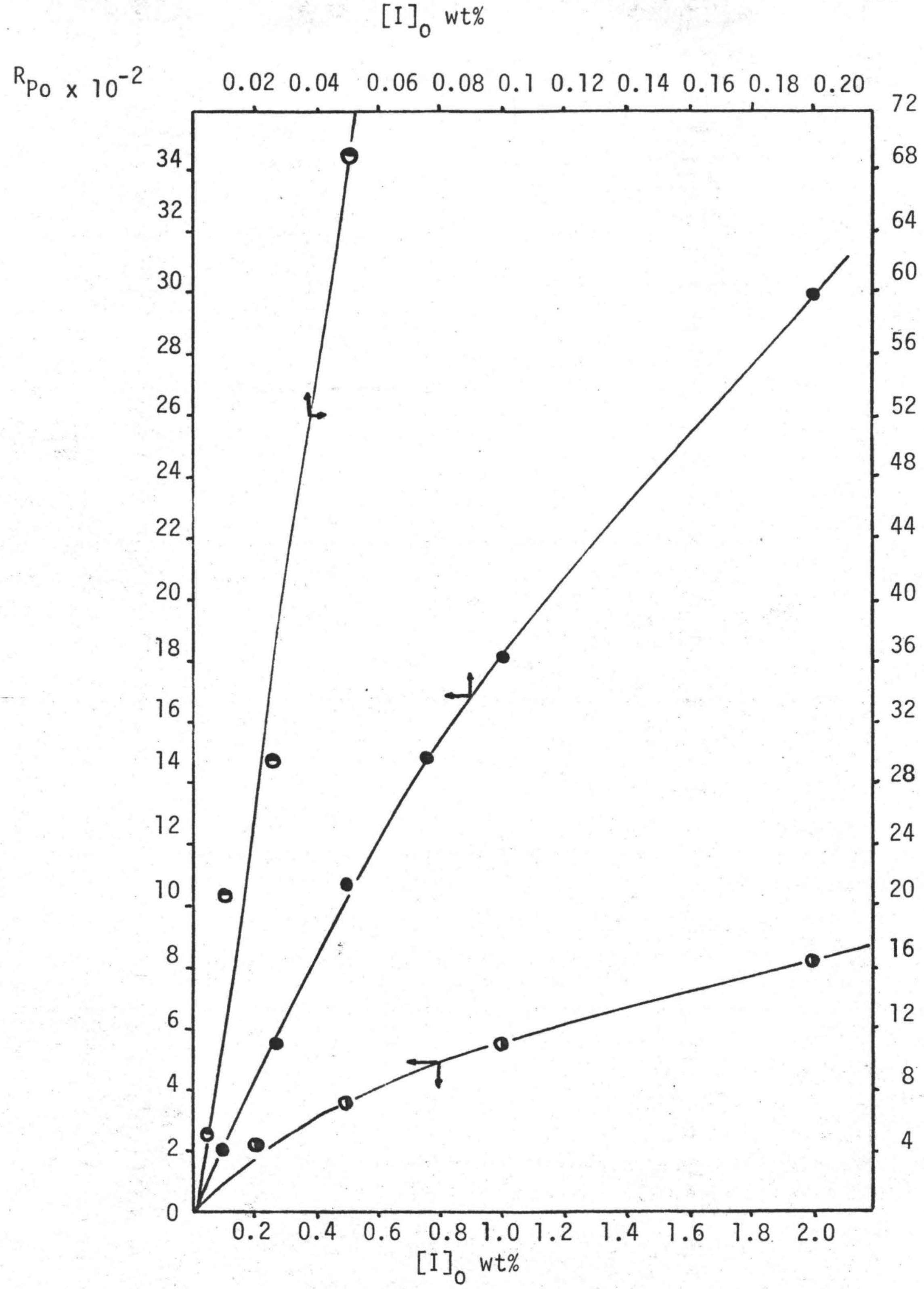

Fig. 5-6 Estimated polymerization rates at ◐ 40°C

● 60°C ⊖ 80°C.

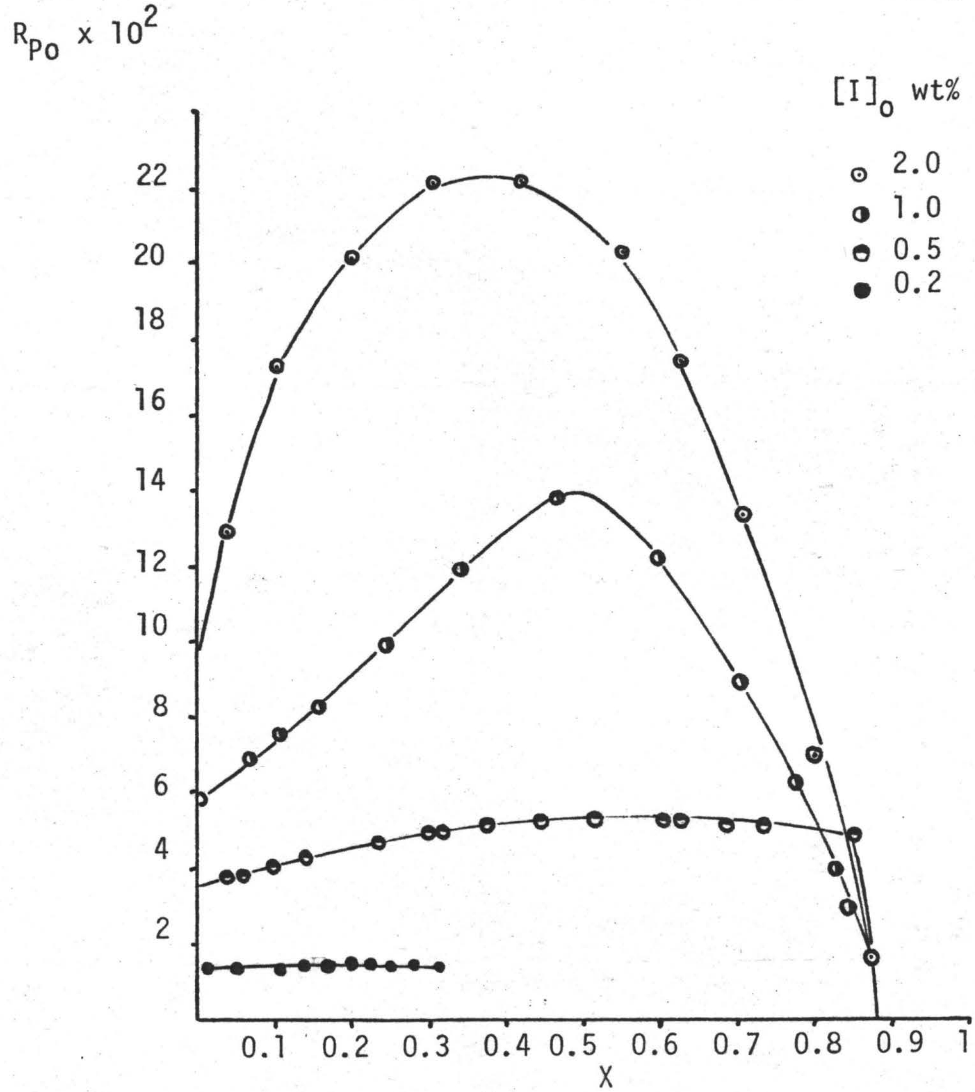

Fig. 5-7: Polymerization rate at 40°C

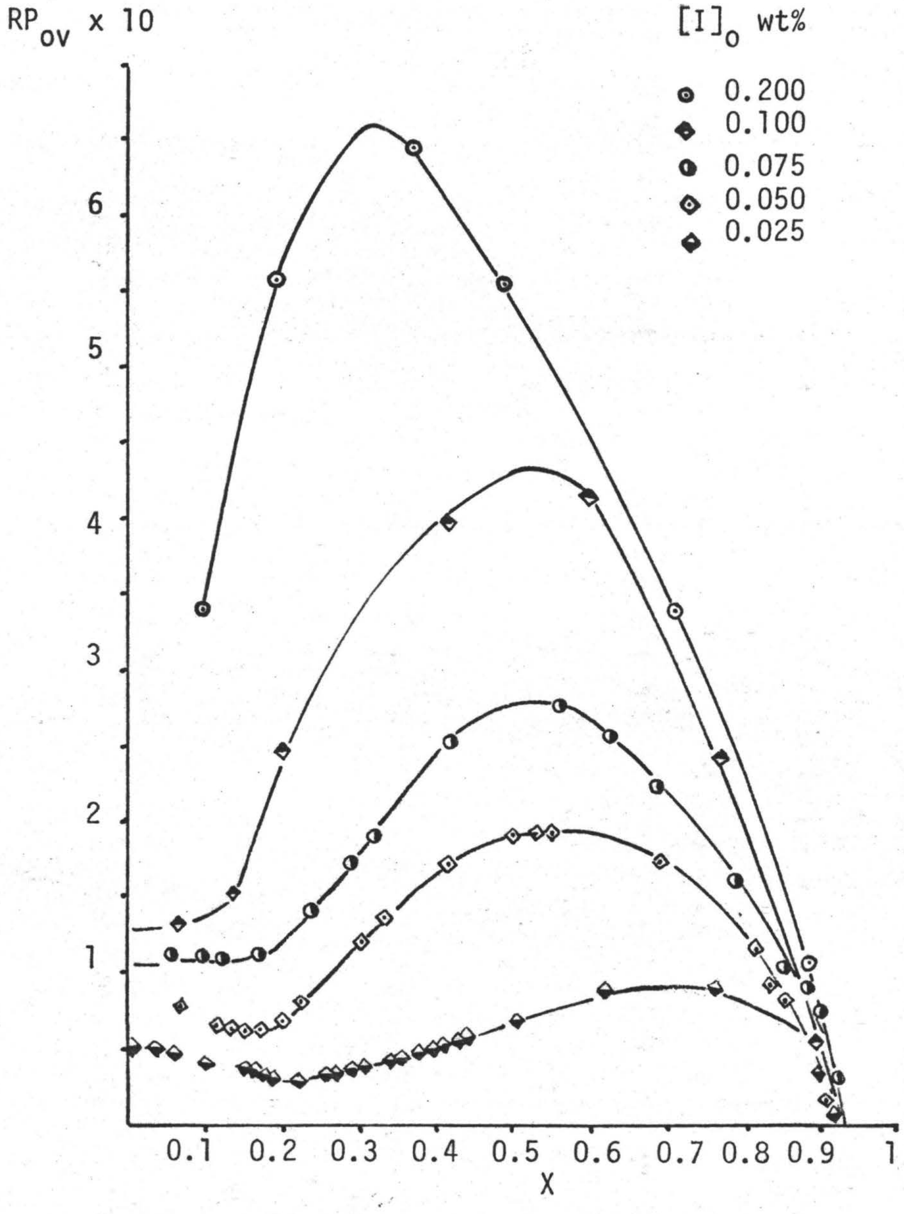

Fig. 5-8: Polymerization rate at 60°C.

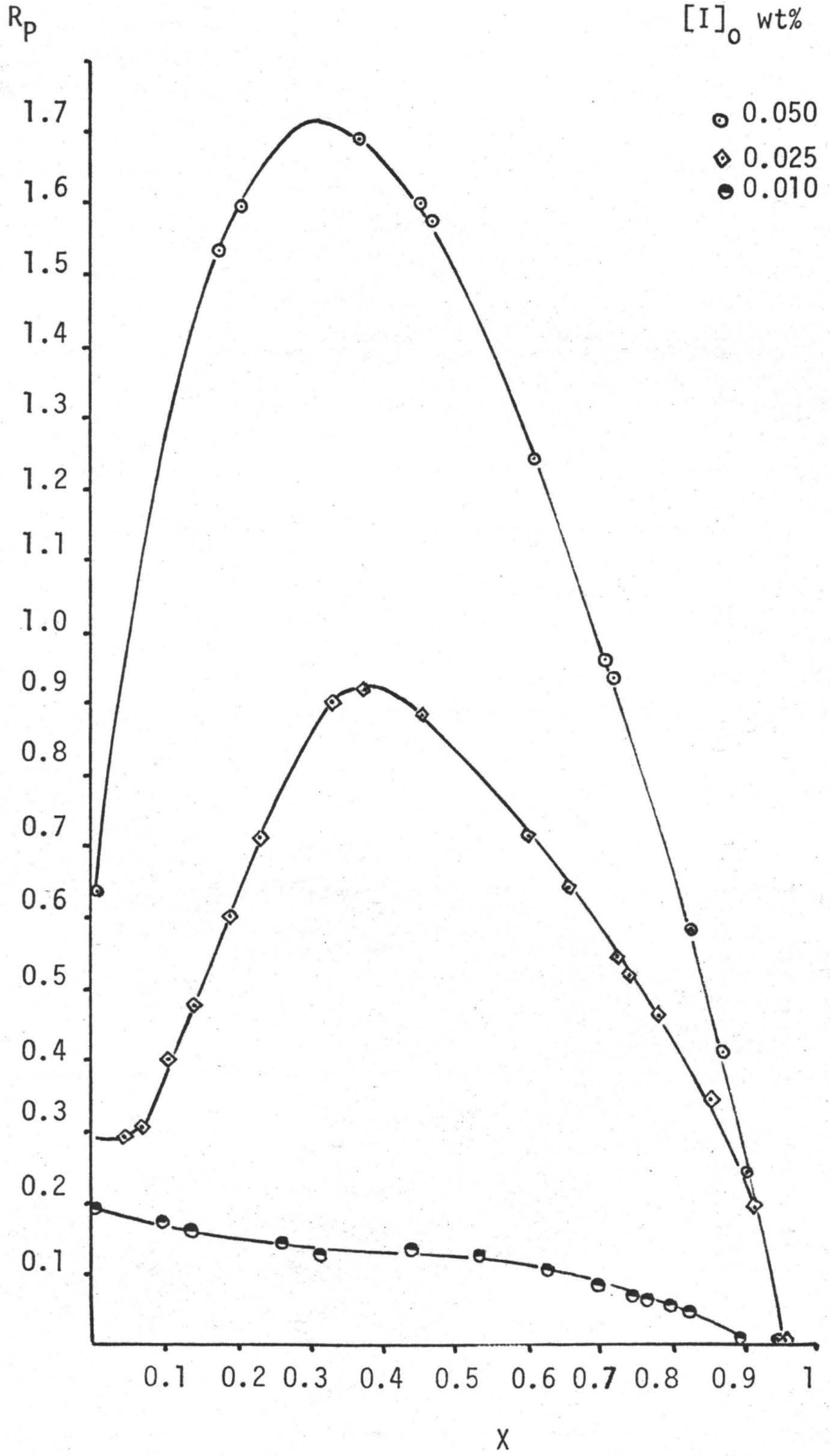

Fig. 5-9: Polymerization rates at 80°C.

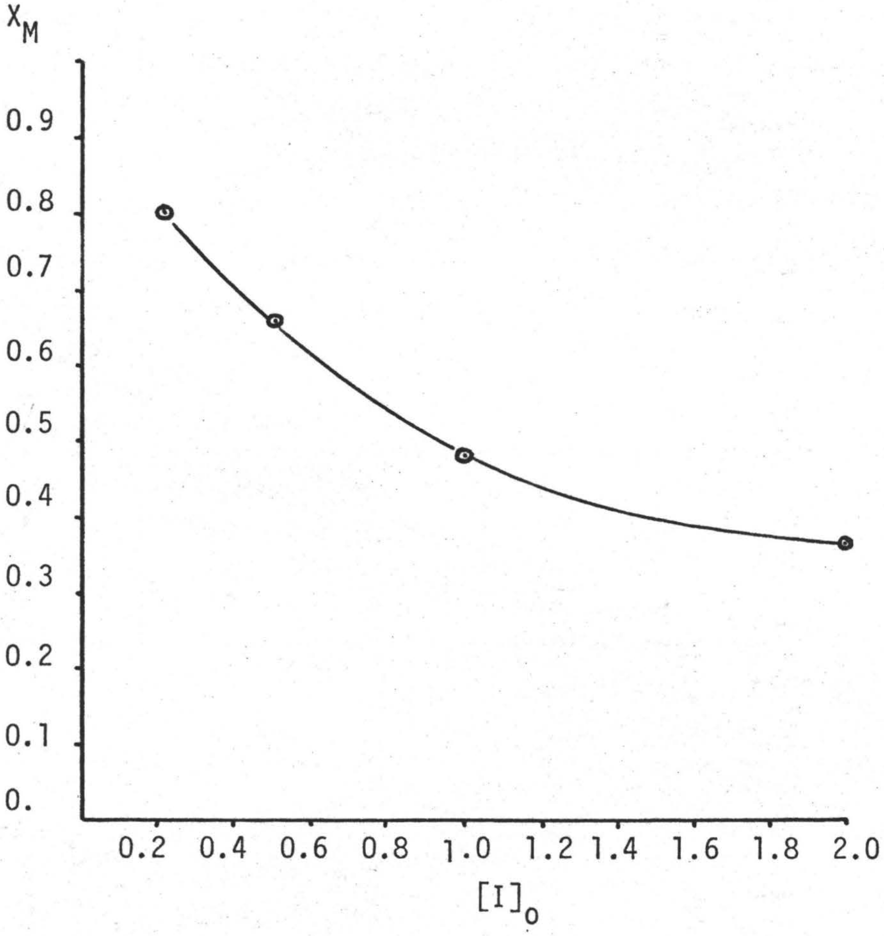

Fig. 5-10: X_M vs. $[I]_o$ at 40°C, $[I]_o$ in wt%.

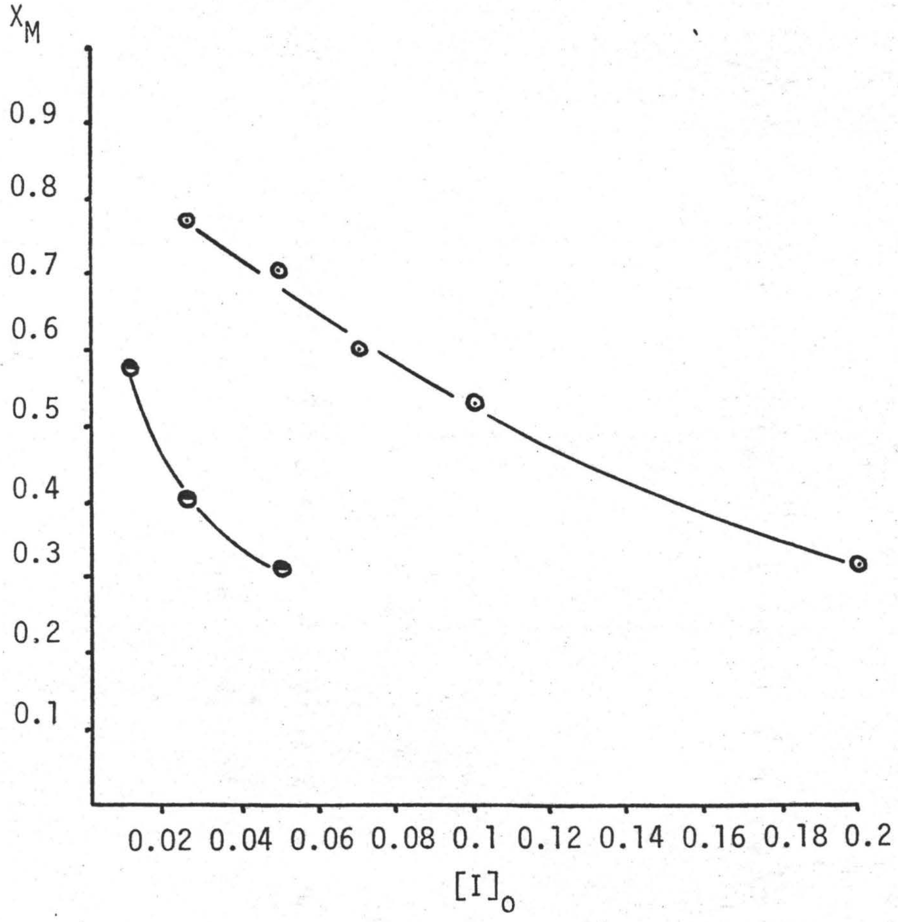

Fig. 5-11: X_M vs. $[I]_o$ in weight% at 60° and 80°C

⊙ 60°C ⊖ 80°C.

i) The acceleration period is a strong function of initiator concentration.

ii) The constant rate region is present only at certain initiator concentrations.

iii) The solubility value for the monomer-polymer system can not be considered as the onset of pronounced gel effect when the phase inversion occurs, since no increase in rate around the estimated solubility value is observed.

iv) A distinct maximum is observed as function of the initiator concentration and polymerization temperature

The variations of X_m with initiator concentration at the three polymerization temperatures are shown in Figs. 5-10 and 5-11. With the information available at this point, the validity of the two-phase model was tested.

5.3.2 The Two-Phase Model Test

This model is based, as mentioned before, on the assumption of the polymerization taking place in two phases which are in equilibrium. The composition of these two phases remains constant through all the heterogeneous region, that is, until X_c is reached. It is evident from Figs. 5-7 to 5-9 that this does not apply to AN since the rate reaches a maximum at a conversion (X_M) smaller than the experimental estimated X_c. This does not contradict the assumptions of the two-phase model, at least up to the point where the rate starts decreasing. It has been reported before (8,68) and now appears evident that the rates depend on the physical state of the polymer produced at given conditions and this state depends on the temperature, the initiator concentration and conversion.

In an attempt to fit the model to the first section of the rate curves, two alternative expressions were used for which the basic assumptions of the two-phase model were assumed to hold:

$$R_P = R_{PM}(1 - \phi_P) + R_{PP}\phi_P \qquad 5\text{-}32$$

$$\xi = \frac{R_{PP}}{R_{PM}} \qquad 5\text{-}33$$

Combining Eq. 5-32 with Eq. 5-33

$$R_P = \xi R_{PM}\phi_P + R_{PM}(1 - \phi_P) \qquad 5\text{-}34$$

$$R_P = R_{PM}(1 + \phi_P(\xi - 1)) \qquad 5\text{-}35$$

The volume fraction of the polymer phase ϕ_P is defined by Eq. 5-17. Equation 5-33 is a nonlinear two parameter model from which cases A and B were run. From the results obtained with this model (see next section), it was assumed that the rates are proportional to the square root of the initiator mass. Therefore,

$$R_P = \frac{R_{PM}(1 - \phi_P)}{V_M^{1/2}} + \frac{R_{PP}\phi_P}{V_P^{1/2}} \qquad 5\text{-}36$$

Combining Eqs. 5-33 and 5-36

$$R_P = \frac{R_{PM}}{(V_P V_M)^{1/2}} (V_P{}^{1/2} + \phi_P(\xi V_M{}^{1/2} - V_P{}^{1/2})) \qquad 5\text{-}37$$

The volume of the monomer phase and polymer phase at a given conversion X are defined by Eqs. 5-38 and 5-39

$$V_M = \frac{1 - X}{\rho_M} - \frac{(1 - X_c)X}{X_c \rho_M} \qquad 5\text{-}38$$

$$V_P = \frac{X}{\rho_P} + \frac{(1 - X_c)X}{X_c \rho_M} \qquad 5\text{-}39$$

Equation 5-37 is a non linear two parameter model from which cases C and D were run.

Equations 5-35 and 5-37 were fitted to the rate curves obtained from the splines by using a non linear least squares regression routine. R_{PM} and ξ were the parameters evaluated. Since this is considered a first attempt, no statistical analysis is reported. The results follow.

5.4 Results and Discussion

The results obtained from the two models are shown in Figs. 5-12 to 5-14.

The cases A and C were run with $X_c = X_M$ to verify whether the value obtained experimentally for X_c was reliable. The B and D cases were run with $X_c = 0.88$ for all the temperatures. As it was expected, the response obtained for low X_c values is lower, and the effect is more pronounced at high rates. The first model is completely inadequate. The second model gives a better fit and this can be improved as shown in Fig. 5-12. Two important assumptions appear to be valid at least in the first stage of the rate curve: the two-phase model assumptions hold and the square root dependency with respect to the initiator concentration (corrected by the change in volume) seems to be valid. Table 5-1 shows the absolute rates obtained with the best fit at 60°C for several initiator concentrations.

Table 5-1

Estimated Absolute Rates at 60°

I_o wt%	$R_{PM}\ \frac{\text{mol}}{\text{hr}}$	$R_{PP}\ \frac{\text{mol}}{\text{hr}}$	ξ
0.20	0.279×10^{-2}	0.639×10^{-1}	22.9
0.10	0.197×10^{-2}	0.264×10^{-1}	13.4
0.075	0.171×10^{-2}	0.091×10^{-1}	5.3
0.050	0.149×10^{-2}	0.056×10^{-1}	3.8

It can be seen that although the figures in Table 5-1 are rough estimates) at least at high initiator concentrations, the polymerization rate in the monomer phase follows $\sqrt{I_o}$ dependency, indicating therefore, that normal homogeneous kinetics may be applicable to the monomer phase.

If the homogeneous kinetics are applicable in each phase. The value of ξ would be defined as:

$$\xi = \frac{k_{PP}(2_{fP}k_{dP}/k_{tP})^{1/2}}{k_{PM}k_M(2_{fM}k_{dM}/k_{tM})^{1/2}k_I^{\ 1/2}} \qquad 5\text{-}40$$

ξ is only a function of temperature and therefore constant at a given polymerization temperature in the region where the reactions are not diffusion controlled. For AN, ξ appears to increase with increasing initiator concentration indicating therefore, that the characteristics of the polymer phase are strongly influenced by the initiator concentration. The main difficulty in describing the AN bulk is the initiator concentration effect on the polymerization rate behaviour for which the following explanation is proposed.

The solubility of the monomer in the polymer is very low and therefore the polymer phase is close to its glass transition point. If the initiation rate is high, the particles formed will aggregate rapidly and will be closely packed increasing the resistance to diffusion. This will increase the rate to the point where diffusion is so slow that the rate will start decreasing. As the initiation rate is diminished, the particles are less closely packed and the maximum in the rate will appear later in the polymerization process. The fact that the rate drops substantially when a swelling agent is added to the reaction mixture supports this scheme. For the rate would not drop if the reactions were not diffusion controlled. Electron micrographs and more information concerning the effect of the swelling agents would be convenient at this point to elucidate the actual reaction mechanism.

The mathematical description of such polymerization system is difficult and extensive work is required. In addition, no independent estimation of the rate parameters at this point seems to be possible which indicates that the system has to be treated as a multiresponse system where conversion and rate data together with molecular weight averages are used to estimate simultaneously all the parameters involved.

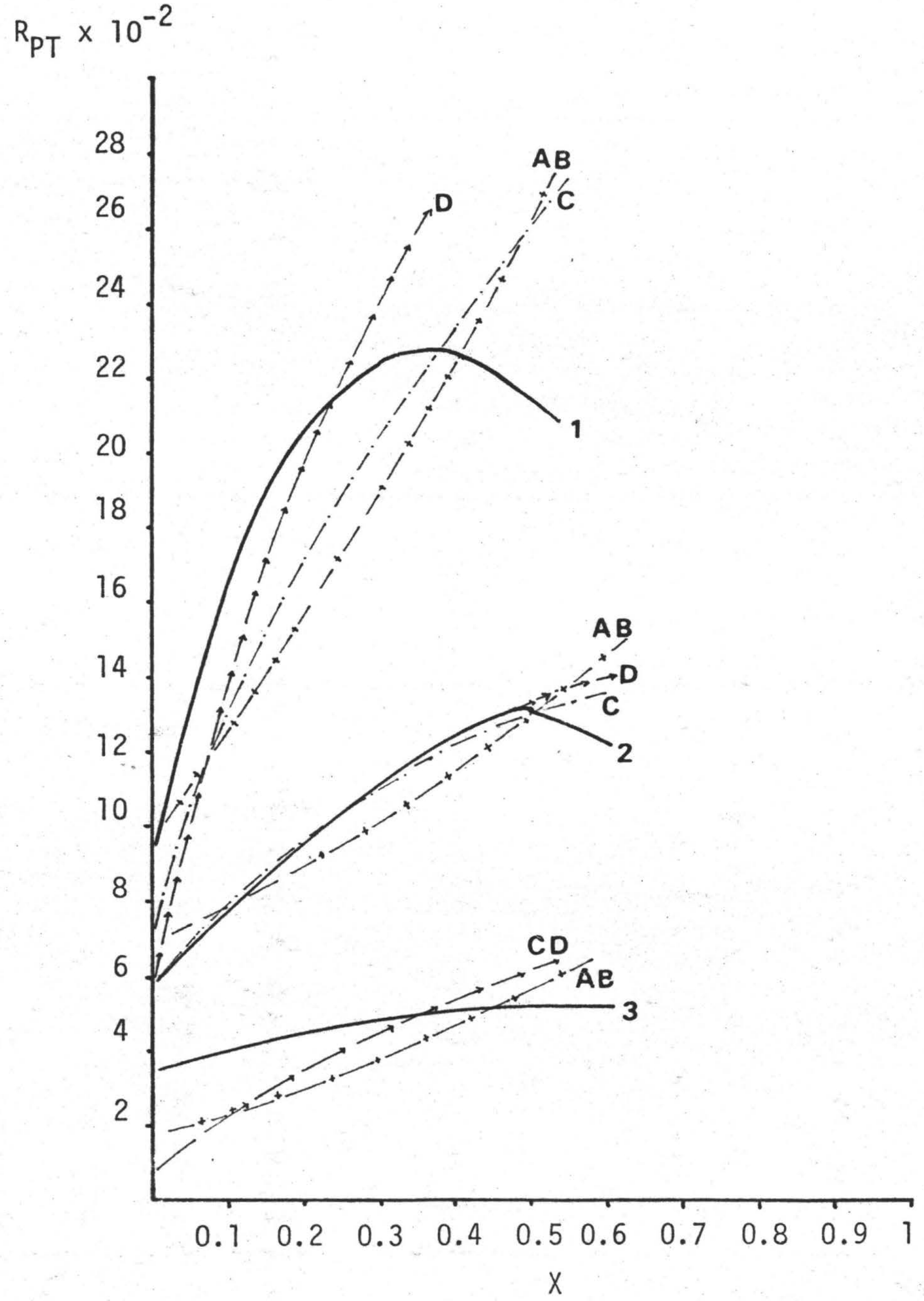

Fig. 5-12: Model fitting to rate data at 40°C (1) $[I]_0$ = 2 wt% (2) $[I]_0$ = 1 wt% (3) $[I]_0$ = 0.5 wt% - actual rate Model 1: _+_ cases A,B, Model 2: _.__. case C, →→ Case D.

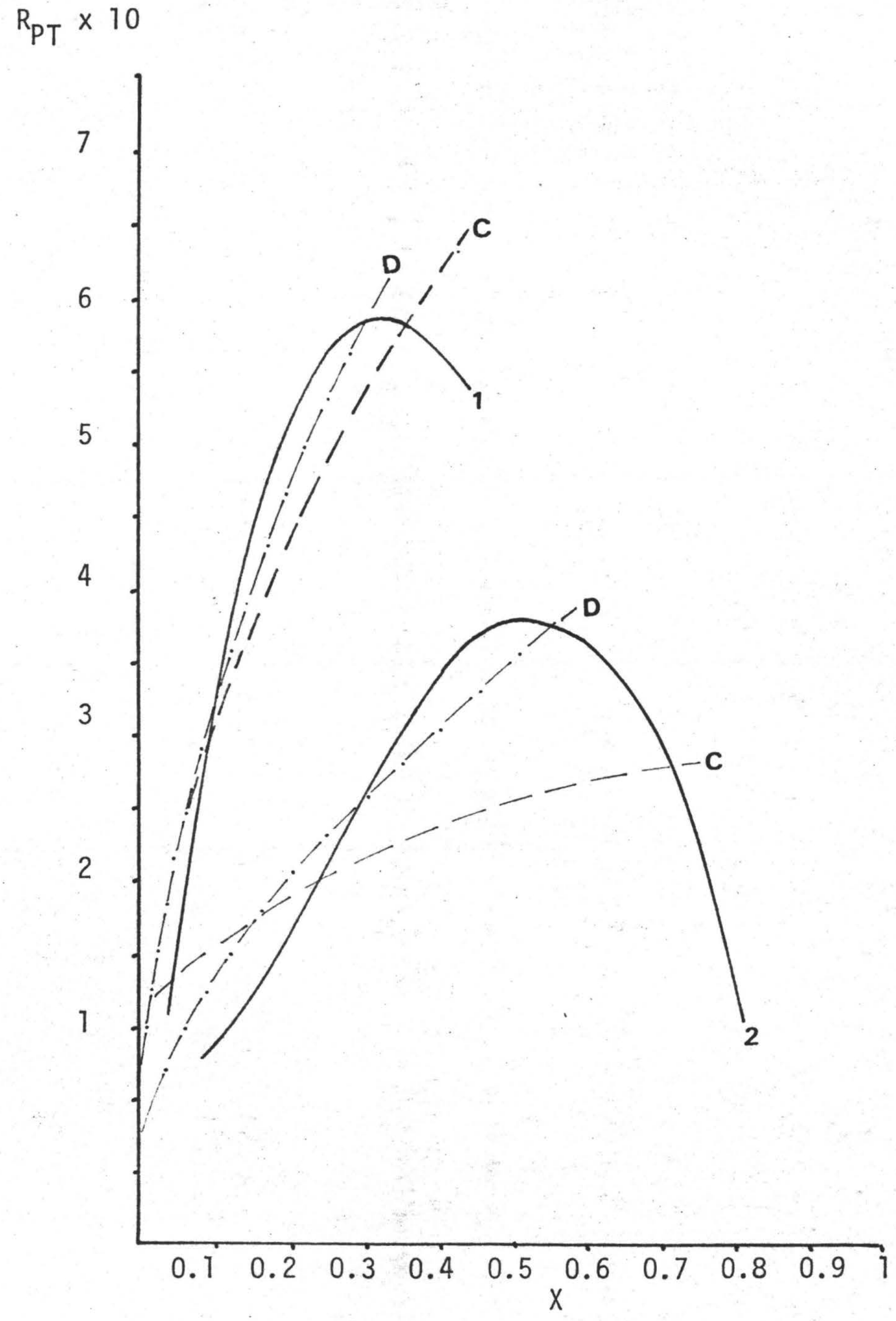

Fig. 5-13: Model fitting to rate data at 60° (1) $[I]_o$ = 0.2 wt% (2) $[I]_o$ = 0.1 wt% Model 2: —·—. Case C, —+— Case D.

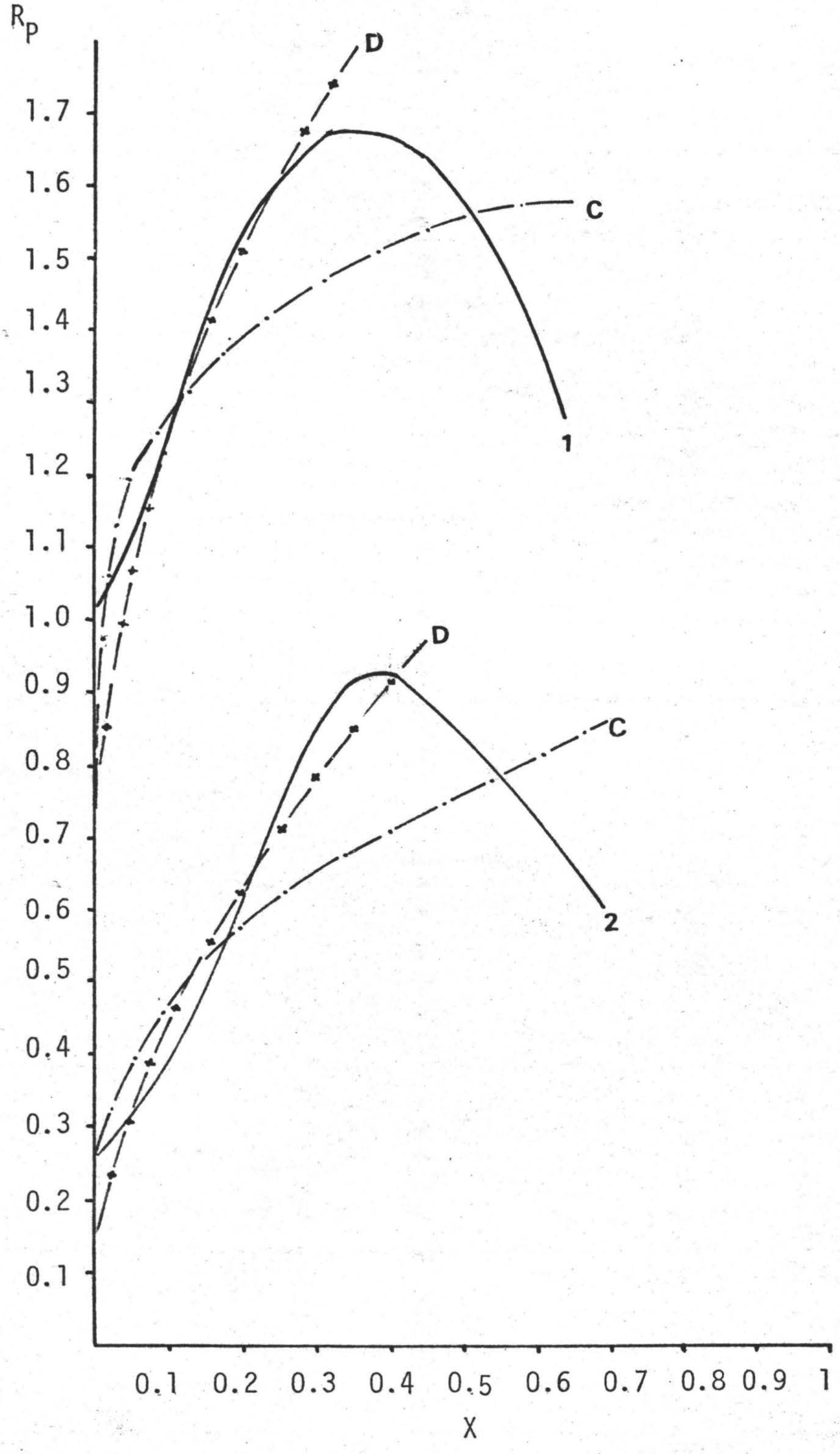

Fig. 5-14: Model fitting to rate data at 80°C. (1) $[I]_o$ = 0.05 wt% (2) $[I]_o$ = 0.025 wt%. Model 2 —·— Case C, —+— Case D.

CHAPTER 6

SUMMARY OF THE RESULTS, CONCLUSIONS AND RECOMMENDATIONS

The results obtained here give for the first time, a complete description of AN bulk polymerization process using AIBN as initiator in the temperature range 40°C - 80°C. Additional properties of the polymer such as the solubility of the monomer in the polymer and the glass transition temperature were estimated. The values obtained are in agreement with those reported in the literature. It has been suggested that the polymerization depends on the past history of the system, meaning the characteristics of the polymer phase. It has been shown here, by analysing the rate data over a wide range of temperatures and initiator concentrations that the physical characteristics of the polymer phase are a strong function of the temperature, the initiator concentration and conversion. The kinetic behaviour of AN has been compared with the well known vinyl chloride system, concluding that the mechanism through which they polymerize is similar.

As an integral part of the kinetic study on the bulk polymerization of AN, the molecular weight development was followed by gel permeation chromatography over the temperature range 0°C - 120°C. The results obtained provide for the first time, an overall picture of the molecular weight development for the bulk process. the MWD and averages appear to be fairly constant over the temperature range 20°C - 90°C. They increase slightly with conversion and decrease with increasing initiator concentration. By analysing the polydispersity ratios, it appears that branching is unimportant and that transfer to monomer plays a major role in controlling the MWD. The intrinsic viscosities obtained were compared with values reported for polymers produced under the same conditions. Agreement was satisfactory. The hydrodynamic theory was proved to be valid, provided that an electrolyte is added to the carrier solvent and the adequate Mark-Howink constants were used. The literature was reviewed exhaustively and agreement was found with the Mark-Howink constants reported by Fujisaki and Kobayashi.

The models proposed to date to describe the bulk polymerization kinetics of AN have been reviewed and discussed extensively. From the results obtained and experimental evidence found in the literature, it was concluded that polymerization takes place in both the monomer and the polymer phase; therefore, the two-phase model theory was reviewed. A two parameter semi-empirical model derived from the two-phase theory was used as a first attempt to describe the process. It is evident from the results obtained that the two-phase model as it stands is not entirely valid for the bulk polymerization of AN. Nevertheless it appears promising for describing the process up to the conversion where the rate is maximum.

The mathematical description of AN bulk polymerization process appears to be very complicated. In order to obtain a useful model, two alternatives are proposed: the first one implies the improvement of a semi-empirical model of the same form as the one used here for which the polymerization rates have to be correlated at different temperatures and initiator concentrations. The MWD and averages can be obtained on the same grounds from the two-phase theory. Such a model will be able to predict MWD and conversion histories for isothermal and nonisothermal conditions. The second alternative, a more lengthy one, is the improvement of the basic two-phase model. This can be done by finding the appropriate expressions basically for the propogation and termination rate parameters in terms of temperature initiator concentration and conversion. It is worthwhile to note here that the first alternative is a natural step for the improvement of both the semi-empirical and the theoretical models. In either case, additional experimentation is required. Particularly, studies on the effect of agitation on the polymerization rate are recommended, since this information will make the models more realistic for industrial applications. It is expected that with adequate agitation, the two-phase model will be applicable. Experimentation on the effect of a swelling agent appears also interesting, particularly for the improvement of the two-phase model, since it would be possible to estimate the rate parameters by extrapolating to zero concentration of swelling agent.

7

NOMENCLATURE

a = constant in the Mark-Howink equation

B = parameter defined in Eq. 5-20

D_1 = constant in the linear effective calibration curve

D_2 = constant in the linear effective calibration curve

$[I]$ = initiator concentration

$[I]_o$ = initial initiator concentration

k_d = initiator decomposition rate constant

k_{fM} = rate constant for transfer to monomer

k_{fP} = rate constant for transfer to polymer

k_{PM} = propagation rate constant in the monomer phase

k_{PP} = propagation rate constant in the polymer phase

k_{tP} = termination rate constant in the polymer phase

k_{tM} = termination rate constant in the monomer phase

K = constant in the Mark-Howink equation

K_I = initiator partition coefficient

K_M = monomer partition coefficient

M = molecular weight of single species

$\tilde{M}$ = molecular weight of monomer

$\overline{M}$ = mean of molecular weight distribution

$\overline{M}_N$ = number average molecular weight

$\overline{M}_W$ = weight average molecular weight

$[M]_o$ = molar concentration of pure monomer

$[M]_M$ = monomer concentration in the monomer phase

$[M]_P$ = monomer concentration in the polymer phase

P = parameter defined in Eq. 5-18

Q = parameter defined in Eq. 5-25

$\overline{r}_N$ = instantaneous number average chain length

$\overline{r}_W$ = instantaneous weight average chain length

$\mathrm{cum}\overline{r}_N$ = cumulative number average chain length

$\mathrm{cum}\overline{r}_W$ = cumulative weight average chain length

R_I = rate of initiation

R_P = total polymerization rate

R_{PM} = polymerization rate in the monomer phase

R_{PP} = polymerization rate in the polymer phase

$[R^{\cdot}]$ = radical concentration

t = reaction time

T = temperature

Tg = glass transition temperature

V_M = volume of the monomer phase

V_P = volume of the polymer phase

X = fractional conversion

X_c = mass fraction of the polymer

= conversion at which the separate monomer phase disappears

X_f = limiting conversion

X_M = conversion of which the rate is maximum

Greek Letter Symbols

α = kinetic parameter

β = kinetic parameter

$[\eta]$ = limiting viscosity number

ξ = parameter defined in Eq. 5-33

ρ_M = density of the monomer

ρ_P = density of the polymer

σ^2 = variance

τ = kinetic parameter

ϕ = kinetic parameter

ϕ_M = volume fraction of the monomer phase

ϕ_P = volume fraction of the polymer phase

8. REFERENCES

1. Abdel Alim, Polymerization Kinetics and Properties of Vinyl Polymers, Ph.D. Thesis, McMaster University (1973).
2. Abdel Alim and Hamielec, A., J. App. Polym. Sc. 16, 783 (1972).
3. Amdur, S., J. Polym. Sci. A-1 9, 175-181 (1971).
4. American Cyanamid Co., The Chemistry of Acrylonitrile, New York.
5. Anderssen, R.S., 8 Bloomfield P. Numer. Math 22, 157 (1974).
6. Andrews, R.D. and Kimmel, R.M., J. Polym. Sc. B 3, 171 (1975).
7. Bamford, C.H. and Eastmond, G.C., Encyclopedia of Polymer Science and Technology, Vol.I (1974), Ed. by H.F. Mark, N.G. Gaylard, N.M. Bikales, Interscience, N.Y.
8. Bamford, C.H. and Jenkins, Proc. Roy. Soc. A 216, 515-539 (1953).
9. Bamford, C.H., Jenkins, A.D. and Johnston, R., Trans Farady Soc. 55, 1777 (1959).
10. Bamford et al., Trans Faraday Soc. 55,179 (1959).
11. Beevers, R.B., Polymer London 8, 419 (1967).
12. Beevers, R.B. and White E.F., J. Polym. Sc. B 1, 171 (1963).
13. Beevers, R.B. and White, E.F., Trans Faraday Soc. 56, 303 (1961).
14. Beevers, R.B., Polymer London 8, 463 (1967).
15. Beevers, R.B., Polymer London 9, 535 (1968).
16. Beevers, R.B., Polymer London 10, 791 (1969).
17. Beevers, R.B., J. Polymer Sc. A2, 52-57 (1964).
18. Beevers, R.B., Macromolecular Review 3, (1968).
19. Bell F.A., Lehrle, R.S. and Robb, J.C., Polymer London 12, 9 (1971)

20. Bengounough, W.I., Proc. Roy. Soc. London A 260, 205 (1965).

21. Bevington, J.C. and Eaves, D.E., Initiation in the Polymerization of Acrylonitrile, Trans Faraday Soc. 42, 1777-1782 (1959).

22. Bisschops, J., Journal of Polym. Sci. 17, 89-88 and 89-98 (1955)

23. Bohen, C.R., Schaefgen, Jr. and Statton, W.O., J. Polym. Sci. 55, 531 (1961).

24. Brandrup, J. and Emmergut, E.H., Polymer Handbook, Interscience, New York (1975).

25. Cha, C.Y., J. Polym. B 7, 343 (1969).

26. Chiang, R. and Stauffer, J.C., J. Polymer Sc. A2 5, 101-112 (1967).

27. Cleland and Stockmayer, J. Polym. Sci. 17, 476 (1955).

28. Dalin, M.A. "Acrylonitrile" Technomic (1971).

29. Fordyce, R.G. and Chapin, E.C., J. Am. Chem. Soc. 69, 581 (1947).

30. Friis, N.and Hamielec, A.E., Private communication.

31. Friis, N. and Hamielec, A.E., ACS Symposium Series 24, American Chemical Soc. (1975).

32. Fujisaki, Y. and Kobayashi, H., J. Polym. S. B 15-17 (1963).

33. Howard, J. App. Polym. Sc. 5, 303 (1961).

34. Inagaki, H., Hayashi, K. and Matsuo, T., Makromol Chem. 84, 80 (1965).

35. Jenkins, A.D. and Johnstone, Termination Reaction in the Polymerization of Acrylonitrile, Trans Faraday Soc. 55, 179-184 (1959).

36. Jenkins, A.D. and North, A.M., Reactivity Mechanism and Structure in the Polymer Chemistry, Wiley (1974).

37. Jenkins, A.D., Kinetics and Mechanisms of Polymerization, Vol. I, Part 1, ed., G. Ham, Marcel Rekker (1967).

38. Kenyon, A.S. and Mottus A.E., Applied Polym. Symp. 25, 52-67 (1974).

39. Kenyon, A.S., Private Communication, January (1976).

40. Kern W. and Fernow, H., J. Prakt. Chem. 160, 281, 295 (1942).

41. Kobayashi, H., J. Polym. Sci. 39, 369 (1959).

42. Kobayashi, H., J. Polym. Sci. B 299 (1963).

43. Kogura, S. and Kawamura, S., Macromolecules 4, 79 (1975).

44. Koningsberger, C., and Salomon, G., J. Polym. Sci. 1, 200 (1942).

45. Krigbaum, W.R. and Kotliar, A.M., J. Polym. Sci. B 323 (1958).

46. Krigbaum, W.R. and Tokita, N., J. Polym.Sci. 43, 467 (1960).

47. Kuchanov, S.I. and Bort, D.M., Vysokomol Soyed, A15 10, 2393 (1973).

48. Lewis, O.G. and King, R.M., Addition and Condensation Polymerization Processes. Advances in Chemistry, Series 91, Cm. Chem. Soc. (1969).

49. Marquardt, K. and Mehnert, P., Angew Makromal Chem. 28, 177 (1974).

50. Mencick, Z., J. Polym. Sci. 17, 147 (1955).

51. Moreau, A., Chem. Phys. [7] 2, 186 (1893).

52. North, A.M. and Postlethwaite, D., The Termination Mechanism in Radical Polymerization in Structure and Mechanism in Vinyl Polymerization, ed., T. Tsuruta and K.F. O'Driscoll, Marcell Dekker (1967).

53. North, A.M., The Influence of Chain Structures on the Free-Radical Termination Reaction in Reactivity Mechanism and Structure in Polymer Chemistry, ed., A.D. Jenkins and A. Ledwith, Wiely (1974).

54. Onyon, P.F., J. Polym. Sci. 22, 13 (1956).

55. Onyon, P.F., J. Polym. Sci. 22, 19 (1956).

56. Palit, S.R. and Guha, T., J. Polym. Sci. 34, 243 (1959).

57. Parts, A.G. and Elbing, E., Emulsion Polymerization, A.C.S. Symposium Series 24 (1975).

58. Peebles, L.H., Jr., J. Am. Chem. Soc. 80, 5603 (1958).

59. Peebles, L.H., Jr., J. Polym. Sci. A3, 361 (1965).

60. Peebles, L.H., Jr., J. Polym. Sci. 17, 113 (1973).

61. Pellon, J. and Smith, J., J. App. Polym. Sci. 10, 429 (1969).

62. Ray, W.H. and Jain, S.K., J. App. Polym. Sci. 19, 1297 (1975).

63. Saito, S. and Nakajima, T., J. App. Polym. Sci. 2, 93 (1959).

64. Soum, A.M., J. Polym. Sci. 42, 57 (1960).

65. Statton, W.O., Ann. N.Y. Ac. Sci. 83, 27 (1959).

66. Talamini, G. and Peggion, E., in Vinyl Polymerization, Vol. I, G. Ham, Marcel Dekker (1967).

67. Taninaka, T. and Minoura, Y., J. Polym. Sci. 13, 2335 (1975).

68. Thomas, W.M., Adv. Polymer Sci. 2, 401 (1961).

69. Thomas, W.M. and Pellon J.J., J. Polym. Sci. 13, 329 (1954).

70. Vidotto, G., Grosato-Arnaldi, A. and Talamini, G., Makrome Chem. 122, 91 (1969).

71. Vollmert Bruno, Polymer Chemistry, Springer-Verlag, N.Y. (1973).

72. Wold, S., Technometrics 16, 1 (1974).

73. Yamadera, R. and Murano, M., J. Polym. Sci. 5, 333 (1967).

74. Yamasahi, S., Fukuda, M. and Namashima, M., Kobushi Kagaku 27, 459 (1970).

General References

75. Draper N. and Smith, H., Applied Regression Analyses, Wiley (1966).

76. Flory, M., Principles of Polymer Chemistry, Cornell University Press (1969).

77. Himmelblau, D., Process Analysis by Statistical Methods, Wiley (1968).

9. APPENDICES

9.1 Statistical Analysis of the Data

As mentioned in Chapter 4, in order to ensure isothermal conditions at the two conversion ranges considered, (0 - 50%, 50% - X_f) ampoules of different surface to volume ratio were used. To analyse the effect of the ampoule size at different conversions and initiator levels, replicates were taken randomly along the conversion-time curves at 60°C for three different initiator concentration levels (0.075, 0.05, 0.025 wt%). The main number of replicates were taken at 0.05 wt% $[I]_0$. The individual variances for the replicates at given conversions were tested using the Bartlett's test. There is no evidence showing that these variances are different, therefore, it was concluded that the ampoule size appears to have no effect on the conversion measurements. The pooled variance is considered representative for the whole curve. The same procedure was followed for the two remaining initiator concentrations and the same results were observed. The pooled variance of each curve was compared with that of 0.05 wt% $[I]_0$ to analyse whether the ampoule size had any effect on the rate data at different initial rates. No evidence of such effect was encountered. Additional replicates were taken at all the polymerization temperatures and the pooled variance from each curve was compared with that from 60°C and 0.05 wt% $[I]_0$ by means of an F test. No evidence that the variances were different was found. Similar analysis was performed for the molecular weight distributions.

From the previous analysis, it was concluded that: the ampoule size had no effect on the conversion histories and MWD and averages with in the experimental conditions reported here. The variance can be assumed constant along the conversion-time curves and molecular weight averages-conversion curves. The pooled variance gives the best estimate of the variance of the system.

The 95% C.I. for the conversion histories and molecular weight averages is given by:

$$\frac{S^2{}_x \nu}{\chi^2{}_{r\frac{\alpha}{2}}} \leqslant \sigma^2 < \frac{S^2{}_x \nu}{\chi^2{}_{\frac{\alpha}{2}}} \tag{9.1.1}$$

which gives

$$0.0004 \leqslant \sigma_X{}^2 < 0.0016$$

$$0.145 \times 10^{13} \leqslant \sigma\,\frac{2}{M_W} < 6.49 \times 10^{13}$$

$$0.5 \times 10^{9} \leqslant \sigma\,\frac{2}{M_N} < 2.16 \times 10^{9}$$

The statistical tests applied follow.

Bartlett's Test

A commonly used test to detect differences among two or more variances is Bartlett's Test. M.S. Bartlett devised a test to determine the homogeneity of two or more variances by comparing the logarithm of the average variance with the sum of the logarithms of the separate variances. The formulas necessary for the use of this test are based on the hypothesis: $H_0 : \sigma_1^2 = \sigma_1^2 = \ldots\sigma_n^2 = \sigma^2$ and the presumption that the variables measured are normally distributed. If the test is correct, a pooled S^2 has an χ^2 distribution with a mean of σ^2 and ν degrees of freedom, where $\nu = \sum_{i=1}^{n} \nu_i$

$$S^2 = \frac{\sum_{i=1}^{k} \nu_i S_i^2}{\sum_{i=1}^{k} \nu_i} = \frac{1}{\left(\sum_{i=1}^{n} P_i - n\right)} \sum_{i=1}^{n} (P_i - 1) S_i^2 \qquad 9.1.2$$

Bartlett showed that

$$\Lambda = -\frac{1}{c} \sum_{i=1}^{n} P_i \ln\left(\frac{S_i^2}{S^2}\right) \qquad 9.1.3$$

where

$$c = 1 + \frac{1}{3(n - 1)}\left(\sum_{i=1}^{n} \frac{1}{P_i} - \frac{1}{\sum_{i=1}^{k} P_i}\right) \qquad 9.1.4$$

has an approximate χ^2 distribution with $(n - 1)$ degrees of freedom. For large values of P_i, $c \simeq 1$. If the value calculated by Eq. 9.1.3 exceeds the value of $\chi^2_{1-\alpha}$ for $(k - 1)$ degrees of freedom, the test hypothesis that $\sigma_1^2 = \sigma_2^2 = \ldots$ is rejected.

F- Test

For two products or variables designated A and B, it is possible to test whether the variance of A differs from that of B with the aid of the variance ratio (F) distribution. The test is based upon the assumption that the observations are taken randomly of a normal random variable (77). The hypothesis H_0 is: $\sigma_A^2 = \sigma_B^2$, i.e., $(\sigma_A^2/\sigma_B^2) = 1$, and the sample variance ratio is used to test if σ_A^2/σ_B^2 is greater than or less than unity. If the hypothesis is true, then the region of acceptance for equal tail areas is defined through the probability statement:

$$P\{F_{\frac{\alpha}{2}}(\nu_A,\nu_B) \leqslant \frac{S_A^2}{S_B^2} \leqslant F_{1-\frac{\alpha}{2}}(\nu_A,\nu_B)\} \qquad 9.1.5$$

Because $F_{\frac{\alpha}{2}}(\nu_A,\nu_B) = 1/(F_{1-\frac{\alpha}{2}}(\nu_A,\nu_B)) < 1$, always the left hand side of the probability statement is always satisfied and it is only needed to determine if $S_A^2/S_B^2 \leqslant F_{1-\frac{\alpha}{2}}$.

For the runs at 50°C and $[I]_0 = 0.05$ wt%:

$$S_P^2 = \frac{\sum_i \nu_i S_i^2}{\sum_i \nu_i} = \frac{0.0214}{31} = 0.0007$$

$$n = 17$$

$$\sum_{i=1}^{n} P_i = 48$$

$$\sum_{i=1}^{n} \frac{1}{P_i} = 6.833$$

$$c = 1 + \frac{1}{16}(6.833 - \frac{1}{48}) = 1.4258$$

$$\sum_{i=1}^{n} P_i \ln(S_i^2/S_P^2) = -\ 27.9393$$

$$\Lambda = -\ \frac{1}{c}\sum_{i=1}^{n} P_i \ln\left(\frac{S_i^2}{S_P^2}\right) = 19.5955$$

$$\nu = n - 1 = 16$$

$$\chi^2_{0.95}(16) = 36.296$$

Therefore H_o: $\sigma_1^2 = \sigma_2^2 = \ldots = \sigma_n^2 = \sigma_n^2$ is accepted if
$\sigma_B^2 = S_P^2(60°C,\ [I]_o = 0.05\ \text{wt\%})\nu = 31$

T°C	$[I]_o$wt%	σ_A^2	ν_A	σ_A^2/σ_B^2	$F_{1-\frac{\alpha}{2}}(\nu_A,\nu_B)$	H_o
40	av	7.7×10^{-4}	6	1.00	2.8667	✓
60	0.200	19×10^{-4}	2	2.71	4.1821	✓
60	0.075	8.6×10^{-4}	17	1.23	2.3072	✓
60	0.050	7.0×10^{-4}	31	1.00	2.0739	✓
60	0.025	2.4×10^{-4}	21	0.34	2.1952	✓
60	0.010	10×10^{-3}	10	34.29	2.5112	X
80	0.025	6.0×10^{-4}	2	0.86	4.1821	✓

The only set of data for which the test did not hold is 60°C $[I]_o$ = 0.01 wt%. This is not unexpected, since for this run, low conversions were obtained and several solutions were prepared for it. The results should be looked upon carefully.

Tables 9-1 to 9-7 show the conversion measured at the experimental conditions including the replicates. Tables 9-8 to 9-11 show the molecular weight averages including replicates as measured for the GPC.

9.2 Spline Functions

A spline function is defined as a piecewise polynomial of the degree n. The polynomials join in the so called knots (ξ_i ; j = 1,2,3...m) obeying the continuity conditions for the function itself and its first n - 1 derivatives. Most commonly n equals three; a cubic spline function is defined as:

$$y = S(x) = P_j(x) = a_j + b_jX + c_jX^2 + d_jX^3$$

$$\xi_{J-1} \leqslant X \leqslant \xi_j \ ; \ (\xi_o = -\infty \ ; \ \xi_{m+1} = \infty) \qquad 9.2.1$$

$$P_j^k(\xi_j) = P_{J+1}^k(\xi_j) \ ; \ k = 0,1,2 \ ; \ j = 1,2,\ldots m$$

where P_j^k denotes the kth derivative of the jth polynomial piece. The parameters at the user's disposal are:

i) The degree of the spline function, n.

ii) The number of knots, m.

iii) The position of the knots, ξ_j ; j = 1,2,...,m.

iv) The free coefficients of the spline function, m+n+1 in number.

(Each polynomial piece has n+1 coefficients, and the continuity conditions introduce n bands per knot (72) leaving (m+1)(n+1) - mn = m+n+1 free coefficients.

The definition of the splines in terms of polynomials is convenient once the polynomial coefficients are known. In the computational process of least squares curve fitting, however, it is simpler to define the spline in terms of the β-splines.(72) For cubic splines

$$y = S(x) = \sum_{t=-1}^{m+2} \lambda_t \beta_t(x) \qquad 9.2.2$$

The β-splines are defined by means of divided differences

$$\beta_t(x) = \sum_{k=t-2}^{t+2} (x - \xi_k)^3 + / \prod_{\substack{s=t-2 \\ s \neq k}}^{t+2} (\xi_k - \xi_s) \qquad 9.2.3$$

where the additional knots are defined by

$$\xi_k \quad \begin{array}{ll} \xi_1 - (1 - k)(\xi_1 - X_{min}) & k \leqslant 0 \\ \\ \xi_m + (k - m)(X_{max} - \xi_m) & k \geqslant m+1 \end{array} \qquad 9.2.4$$

X_{min} and X_{max} are the smallest and largest X values in the data respectively. The notation $(X - \xi_k)_t$ has the meaning of $(X - \xi_k)$ where $X > \xi_k$ and zero otherwise. Due to their definition (Eqs. 9.2.2 - 9.2.4) the β splines satisfy the property:

$$\beta_t(x) = 0 \quad \begin{array}{l} X > \xi_{t+2} \\ \\ X < \xi_{t-2} \end{array} \qquad 9.2.5$$

This definition (9.2.2 - 9.2.4) has the advantage that the number of unknown parameters (λ_t) is the same as the number of free parameters in the spline function. Therefore, the fitting of a spline function defined by Eq. 9.2.2 is a linear problem, once the positions of the knots are specified. Moreover, the property 9.2.5 makes the moment matrix (X'X) in least squares fittings heptadiagonal, which is advantageous when the number of knots is large. (72)

The computation of the polynomial coefficients in Eq. 9.2.1 from the β-spline coefficients in Eq. 9.2.2 is easily made by identification of the function and its derivative values in the knots; the following equation system is solved recursively by d_j, c_j, b_j and a_j:

$$S''(\xi_j) = 6d_j = \sum \lambda_t \beta''_t(\xi_j)$$

$$S''(\xi_j) = 2c_j + 6d_j\xi_j = \sum \lambda_t \beta''_t(\xi_j)$$

$$S'(\xi_j) = b_j + 2c_j\xi_j + 3d_j\xi_j^2 = \sum \lambda_t \beta'_t(\xi_j)$$

$$S(\xi_j) = a_j + b_j\xi_j + c_j\xi_j^2 + d_j\xi_j^3 = \sum \lambda_t \beta_t(\xi_j)$$

$$j = 1,2,\ldots m+1 \qquad 9.2.6$$

The choice and the positions of the knots are regarded as important problems. There exist strategies for the optimal selection of the number and positions of the knots. These strategies are reported efficient when the number of points is large. For few points, Wold (72) has suggested the following rules:

i) Have as few knots as possible ensuring that there are at least 4 or 5 points per interval. This rule corresponds to the usual striving to keep the number of parameters as small as possible. With spline functions, extra caution is necessary in this respect, since the great flexibility of the splines can make overfitting a problem.

ii) Have no more than one extremum point (maximum or minimum) and one inflection point per interval. This is because a cubic polynomial is not capable of approximating more variations.

iii) Have extremum points centered in the intervals.

iv) Have inflection points close to knots.

Polynomial spline functions are naturally best suited to describe a polynomial like behaviour of the data. If the data behave otherwise, a transformation of the data may be required prior to the fitting of the spline function. These transformations and further details on the spline function are analysed in a recent publication by Wold. (72)

To fit the splines to the conversion data, a McMaster Library routine was used. This routine computes a least squares approximation to a given set of points by cubic splines. The optimal knot locations are determined so as to minimize the least squares error. The adequacy of every curve was verified. Tables 9-12 to 9-14 show the analysis of variance for the splines.

Table 9-1: Conversion Data at 40°C

I_0 = 2 wt%		I_o = 1.0 wt%		I_o = 0.5 wt%		I_o = 0.2 wt%	
Time hr	X	Time hr	X	Time hr	X	Time hr	X
0.57	0.029	1.0	0.046	1.5	0.033	2.0	0.042
1.	0.117	1.5	0.105	2.0	0.068	6.1	0.099
1.5	0.210	2.0	0.140	3.0	0.0810	8.1	0.132
2.	0.297	3.1	0.251	4.1	0.163	10.1	0.150
2.5	0.380	4.0	0.311	6.1	0.246	12.0	0.187
3.1	0.528	5.0	0.472	7.5	0.343	14.0	0.224
3.5	0.660	6.0	0.650	7.8	0.345	16.0	0.240
4.0	0.720	7.0	0.700	9.0	0.380	18.0	0.281
4.5	0.749	8.0	0.780	10.5	0.441	20.0	0.307
5.0	0.780	9.0	0.820	12.0	0.516		
6.0	0.861	9.25	0.830	13.5	0.593		
7.0	0.869	9.5	0.855	14.0	0.650		
7.5	0.875	11.25	0.856	15.1	0.671		
		12.0	0.888	16.0	0.749		
		14.02	0.882	18.5	0.856		
		16.00	0.882	22.5	0.880		

Replicates

2.5	0.427	3.1	0.259	6.1	0.266		
3.1	0.56	5.0	0.465	10.5	0.437		
		6.0	0.555	12.0	0.506		
		7.0	0.707				

$S_p^2 = 0.0007$

$S_p = 0.027$

Table 9-2: Conversion Data at 60°C

$[I]_o$ = 0.2 wt%		$[I_o]$ = 0.1 wt%	
Time	X	Time	X
0.51	0.192		
1.00	0.356	0.50	0.061
1.20	0.502	1.00	0.155
1.70	0.697	1.53	0.225
2.03	0.824	2.03	0.420
2.50	0.885	2.50	0.576
3.01	0.894	3.00	0.800
3.56	0.895	3.50	0.833
4.01	0.901	4.00	0.874
4.50	0.906	4.53	0.894
5.00	0.906	5.0	0.933

Replicates	
1.20	0.503
3.01	0.906
5.00	0.914

$$S_P{}^2 = \frac{\sum \nu_i S_i^2}{\sum \nu_i} = 0.0019$$

$$SP = 0.044$$

Table 9-3: Conversion Data at T = 60°C

$[I_o]$ = 0.075 wt%								
Time	A-4 X	A-5 X	A-9 X	A-14 X	$\sum X_i$	$\overline{X}$	S_2	$S/\overline{X}$
0.50	-	-	0.066	-	0.066	0.066	-	-
0.83	-	-	-	0.103	0.103	0.103	-	-
1.00	0.103	0.088	0.107	-	0.298	0.099	6.69×10^{-5}	0.083
1.50	-	-	0.176	-	0.176	0.176	-	-
2.00	0.250	0.175	0.259	-	0.648	0.228	1.0×10^{-3}	0.163
2.37	-	-	-	0.292	0.292	0.292	-	-
2.50	-	-	0.312	-	0.312	0.312	-	-
3.00	0.394	0.505	0.437	0.436	1.772	0.443	2.0×10^{-3}	0.090
3.50	-	-	0.561	-	0.561	0.561	-	-
3.75	-	-	-	0.637	0.637	0.637	-	-
4.00	0.633	0.592	0.689	-	1.914	0.638	2.0×10^{-3}	0.062
4.50	-	-	0.790	0.870	1.660	0.830	2.0×10^{-3}	0.048
5.00	0.843	-	0.877	-	1.720	0.860	3.0×10^{-4}	0.020
5.20	-	0.909	-	-	0.909	0.909	-	-
5.37	-	-	-	0.919	0.919	0.919	-	-
6.00	0.916	0.924	-	0.906	2.746	0.915	5.4×10^{-5}	0.008
6.75	-	-	-	0.910	0.910	0.910	-	-
7.00	0.922	0.926	-	-	1.848	0.924	4.0×10^{-6}	0.002
7.50	-	-	-	0.920	0.920	0.920	-	-
8.00	0.923	0.924	-	-	1.847	0.924	$1. \times 10^{-6}$	0.001
8.25	-	-	-	0.921	0.931	0.931	-	-
9.30	0.925	0.924	-	-	1.849	0.925	$1. \times 10^{-6}$	0.001
10.12	0.927	0.928	-	-	1.855	0.928	$1. \times 10^{-6}$	0.001

$$S_P^2 = \frac{\sum \nu_i S^2_i}{\sum \nu_i} = \frac{.01455}{17} = 0.86 \times 10^{-3}$$

S_P = 0.029

Table 9-4: Conversion Data at 60°C

$$S_P^2 = \frac{\sum \nu_i S_i^2}{\sum \nu_i} = \frac{0.0214}{31} = 0.0007$$

$[I]_o$ = 0.05 wt%

Time Hr	A-3	A-6	-10	A-15	A-19	A-23	A-24	$\sum X_i$	$\overline{X}$	S^2	$S/\overline{X}$
0.75	-	-	-	0.048	-	-	-	0.048	0.048	-	-
0.80	-	-	-	-	0.058	-	-	0.058	0.058	-	-
1.00	0.085	0.053	0.057	-	-	-	-	0.195	0.065	$2. \times 10^{-4}$	0.219
1.53	-	-	-	-	0.121	-	0.098	0.219	0.110	$1.3 \times 10^{-}$	0.105
1.65	-	-	-	0.154	-	-	-	0.154	0.154	-	-
2.00	0.196	0.179	0.148	-	-	-	-	0.523	0.174	3.9×10^{-4}	0.114
2.25	-	-	-	-	0.183	-	-	0.183	0.183	-	-
2.65	-	-	-	0.192	-	-	-	0.192	0.192	-	-
3.00	0.284	0.216	0.249	0.208	0.242	-	0.2107	0.410	0.235	1.0×10^{-3}	0.114
3.75	-	-	-	0.324	0.289	-	-	0.613	0.307	3×10^{-4}	0.057
4.00	0.369	0.281	0.354	-	-	-	-	1.104	0.368	1.2×10^{-4}	0.030
4.53	-	-	-	0.421	0.423	-	0.390	1.234	0.411	2.8×10^{-4}	0.015
5.00	0.524	-	0.537	0.469	-	-	-	1.530	0.510	1.0×10^{-3}	0.058
5.16	-	0.514	-	-	-	-	-	0.514	0.514	-	-
5.25	-	-	-	-	0.495	0.527	-	1.022	0.511	2.6×10^{-4}	0.031
6.00	0.713	0.635	0.673	0.582	0.709	-	0.662	3.974	0.662	2.0×10^{-3}	0.068
6.76	-	-	-	0.795	-	-	-	0.795	0.795	-	-
7.00	0.850	-	0.810	-	-	-	-	1.160	0.830	$4. \times 10^{-4}$	0.024
6.16	-	0.800	-	-	0.857	-	-	1.657	0.829	$1. \times 10^{-3}$	0.034
7.60	-	-	-	0.864	-	-	0.878	1.742	0.871	$5. \times 10^{-5}$	0.008
8.00	-	0.880	0.880	-	-	-	-	1.760	0.880	0	0
8.52	0.914	-	-	-	0.887	-	-	1.801	0.901	1.8×10^{-4}	0.015
8.75	-	-	-	-	-	0.899	-	0.899	0.899	-	-
9.00	0.920	0.911	0.920	-	-	-	-	2.751	0.917	1.8×10^{-5}	0.005
10.00	-	-	0.920	-	-	-	-	0.920	0.920	-	-
10.16	0.925	0.925	-	-	-	-	-	1.950	0.925	0	0
11.00	0.934	-	-	-	-	-	-	0.934	0.934	-	-

Table 9-5: Conversion Data at T = 60°C

$[I_o]$ = 0.025 wt%

Time Hr	A-13 X	A-16 X	A-20 X	A-22 X	A-23 X	A-24 X	$\sum X_i$	$\overline{X}$	S_2	$S/\overline{X}$
1.00	0.016	0.024	0.033	-	-	-	0.073	0.024	4.8×10^{-5}	0.285
1.50	-	-	-	0.054	-	-	0.054	0.054	-	-
2.00	0.044	0.064	0.076	-	-	-	0.184	0.061	1.7×10^{-4}	0.215
3.00	0.086	0.142	0.116	0.122	-	-	0.466	0.117	$4. \times 10^{-4}$	0.172
4.00	0.129	-	0.165	-	-	-	0.249	0.147	3.2×10^{-4}	0.122
4.10	-	0.162	-	-	-	-	0.162	0.162	-	-
4.50	-	-	-	0.184	0.180	-	0.364	0.182	$4. \times 10^{-6}$	0.000
5.00	0.176	0.177	0.172	-	-	-	0.525	0.175	4.7×10^{-6}	0.012
6.00	0.212	0.200	0.220	0.243	-	-	0.875	0.219	2.5×10^{-4}	0.072
7.00	-	-	0.257	0.269	-	-	0.506	0.263	3.6×10^{-5}	0.023
7.10	-	0.271	-	-	-	-	0.271	0.271	-	-
7.50	0.290	-	-	-	-	-	0.290	0.290	-	-
8.00	-	-	0.307	-	-	-	0.307	0.307	-	-
8.23	-	0.326	-	-	-	-	0.326	0.326	-	-
9.00	0.339	-	0.372	-	0.372	-	1.083	0.361	2.4×10^{-4}	0.043
9.17	-	-	-	0.365	-	-	0.365	0.365	-	-
9.50	-	0.371	-	-	-	-	0.371	0.371	-	-
10.00	0.378	-	-	-	-	-	0.378	0.378	-	-
10.25	-	-	0.397	-	-	-	0.397	0.397	-	-
10.50	-	-	-	0.417	-	-	0.417	0.417	-	-
10.81	-	0.423	-	-	-	-	0.423	0.423	-	-
11.00	0.435	-	-	-	-	-	0.435	0.435	-	-
12.00	-	-	-	0.476	0.493	0.499	1.468	0.489	9.4×10^{-5}	0.020
13.50	-	-	-	0.579	-	0.644	1.223	0.612	1.0×10^{-3}	0.050
15.00	-	-	-	0.776	0.809	-	1.585	0.793	2.7×10^{-4}	0.021

......continued

Table 9-5: Conversion Data at T = 60°C(continued)

$[I_o]$ = 0.025 wt%										
Time Hr	A-13 X	A-16 X	A-20 X	A-22 X	A-23 X	A-24 X	$\sum X_i$	$\overline{X}$	S_2	$S/\overline{X}$
16.50	-	-	-	-	-	0.887	0.887	0.887	-	-
18.00	-	-	-	-	-	0.919	0.919	0.919	-	-

$$S_P^{\ 2} = \frac{\sum \nu_i S_i^{\ 2}}{\sum \nu_i} = \frac{0.005}{21} = 0.000236$$

Table 9-6: Conversion Data at T = 60°C

$[I]_o$ = 0.01 wt%

Time	A-11	A-12	A-17	$\sum X_i$	$\overline{X}$	S^2	$S/\overline{X}$
1.00	-	-	.014	0.014	0.014	-	-
1.50	0.023	0.013	-	0.036	0.018	2.5×10^{-5}	0.278
2.00	-	-	0.20	0.020	0.020	-	-
3.00	0.034	0.036	0.031	0.101	0.034	4.2×10^{-6}	0.061
4.10	-	-	0.040	0.040	0.040	-	-
4.50	0.073	0.053	-	0.126	0.063	1.0×10^{-4}	0.159
5.00	-	-	0.045	0.045	0.045	-	-
6.00	0.087	0.058	0.056	0.201	0.067	2×10^{-4}	0.211
7.10	-	-	0.070	0.070	0.070	-	-
7.50	0.132	0.075	-	0.207	0.104	1.6×10^{-3}	0.275
8.23	-	-	0.082	0.082	0.082	-	-
9.00	0.168	-	-	0.168	0.168	-	-
9.25	-	0.089	-	0.080	0.089	-	-
9.50	-	-	0.113	0.113	0.113	-	-
10.50	0.191	0.112	-	0.303	0.152	1.6×10^{-3}	0.261
10.85	-	-	0.144	0.144	0.144	-	-
12.00	0.217	0.154	-	0.371	0.186	2.0×10^{-3}	0.170
13.50	-	0.158	-	0.168	0.168	-	-
15.00	0.266	0.164	-	0.430	0.215	5.1×10^{-3}	0.237

$$S_p^2 = \frac{\sum \nu_i S_i^2}{\sum \nu_i} = \frac{0.010}{10} = 0.001$$

Table 9-7: Conversion Data at T = 80°C

$[I_o]$ = 0.05 wt%		$[I_o]$ = 0.025 wt%		$[I_o]$ = 0.01 wt%		$[I_o]$ = 0.005 wt%	
Time	X	Time	X	Time	X	Time	X
.15	.180	.17	0.048	.52	0.080	1.067	0.050
.17	.200	.23	0.068	.75	0.120	1.50	0.078
.27	.350	.35	0.128	1.25	0.220	2.00	0.130
.32	.400	.42	0.140	2.00	0.300	3.10	0.170
.33	.530	.51	0.180	3.05	0.436	4.05	0.195
.43	.580	.58	0.210	3.75	0.520	4.60	0.180
.52	.750	.70	0.230	4.60	0.636	5.05	0.180
.53	.770	.75	0.330	5.38	0.684	6.30	0.210
.67	.804	.84	0.40	6.00	0.740	8.32	0.230
.75	.880	1.02	0.650	6.26	0.760	9.00	0.220
.85	.882	1.10	0.730	6.78	0.804	10.60	0.210
1.18	.928	1.22	0.820	7.52	0.820	13.50	0.210
1.35	.924	1.25	0.830	10.23	0.880	14.60	0.200
1.50	.932	1.33	0.850	12.05	0.890	17.50	0.200
3.05	.949	1.50	0.886	16.85	0.900		
		1.75	0.894				
		2.08	0.915				
		2.25	0.950				
		2.50	0.928				
		3.5	0.941				
		4.05	0.940				

Replicates

		0.75	0.31			3.10	0.21
		1.5	0.908			6.30	0.19

$S^2_{P_{80°}} = 0.0006$

$S_{P_{80°}} = 0.0235$

Table 9-8: Molecular Weight Averages and Replicates

40°C

$[I_o]$ = 2.0 wt%				$[I_o]$ = 0.5 wt%			
X	$\overline{M}_n \times 10^{-5}$	$\overline{M}_W \times 10^{-5}$	$\frac{\overline{M}_W}{\overline{M}_n}$	X	$\overline{M}_n \times 10^{-5}$	$\overline{M}_W \times 10^{-5}$	$\frac{\overline{M}_W}{\overline{M}_n}$
.12	1.7	4.5	2.6	.08	1.6	4.5	2.8
.21	1.8	4.3	2.4	.14	2.1	2.3	2.5
.38	1.8	4.3	2.4	.47	2.2	5.6	2.5
.66	2.1	5.0	2.4	.65	2.2	5.5	2.5
.75	2.2	5.3	2.4	.78	2.7	6.0	2.2
.78	2.3	5.3	2.3	.82	2.3	5.7	2.5
.88	2.1	5.1	2.4	.87	2.0	4.8	2.4

Replicates

0.66	2.0	5.05	2.5	0.14	2.1	5.3	2.6
0.66	2.3	5.5	2.4	0.14	2.0	5.1	2.6
0.78	2.4	6.6	2.7	0.82	2.6	6.1	2.4
0.78	2.5	6.6	2.7	0.82	2.6	6.1	2.4
0.66	2.14	5.19	2.4	0.14	2.04	5.2	2.5
0.78	2.4	6.10	2.5	0.82	2.5	6.0	2.4

Table 9-9: Molecular Weight Averages and Replicates

60°C

I_o = 0.20 wt%				I_o = 0.025 wt%			
X	$\overline{M}_n \times 10^{-5}$	$\overline{M}_w \times 10^{-5}$	$\frac{\overline{M}_w}{\overline{M}_n}$	X	$\overline{M}_n \times 10^{-5}$	$\overline{M}_w \times 10^{-5}$	$\frac{\overline{M}_w}{\overline{M}_n}$
0.19	1.8	4.3	2.5	0.12	2.4	4.9	2.1
0.36	2.0	4.0	2.1	0.24	1.9	4.4	2.4
0.70	1.8	3.8	2.2	0.58	2.8	5.7	2.1
0.85	2.3	5.0	2.2	0.83	2.2	5.2	2.4
0.91	2.2	4.9	2.2	0.92	2.5	5.3	2.1
0.93	2.5	5.2	2.1				

Replicates

0.19	1.7	4.2	2.5	0.12	2.1	4.3	2.2
0.19	2.3	5.3	2.3	0.12	2.5	6.3	2.5
0.19	2.0	5.2	2.6	0.12	2.5	6.3	2.5
0.093	3.4	7.4	2.2	0.92	3.7	7.4	1.95
0.93	3.7	7.9	2.1	0.92	3.8	7.6	2.0
0.19	2.0	4.9	2.5	0.92	2.7	4.7	2.4
0.93	3.1	6.8	2.2	0.12	2.5	5.9	2.4
				0.92	3.2	6.7	2.1

Table 9-10: Molecular Weight Averages and Replicates

80°C

$[I_o]$ = .05 wt%				$[I_o]$ = .025 wt%			
X	$\overline{M}_n \times 10^{-5}$	$\overline{M}_w \times 10^{-5}$	$\frac{\overline{M}_w}{\overline{M}_n}$	X	$\overline{M}_n \times 10^{-5}$	$\overline{M}_w \times 10^{-5}$	$\frac{\overline{M}_w}{\overline{M}_n}$
.18	2.2	5.1	2.4	.12	2.5	5.3	2.1
.40	2.6	6.1	2.3	.18	2.6	5.8	2.2
.75	2.8	6.4	2.3	.33	3.1	6.6	2.2
.88	2.8	6.5	2.4	.80	3.3	7.3	2.2
.93	2.8	6.3	2.3	.92	3.0	7.1	2.4
.95	2.4	5.2	2.2	.94	3.0	7.1	2.4

Replicates							
0.4	2.1	5.1	2.5	0.33	2.6	5.7	2.2
0.4	2.0	5.0	2.5	0.33	2.3	5.2	2.3
0.93	2.8	6.3	2.3	0.92	2.5	6.2	2.5
0.93	2.3	5.7	2.5	0.92	3.0	6.5	2.2
0.18	2.4	5.7	2.4	0.94	2.0	5.1	2.5
0.93	2.8	6.5	2.4	0.33	2.6	5.9	2.3
0.4	2.6	6.1	2.4	0.92	2.8	6.6	2.4

Table 9-11: Molecular Weight Averages and Replicates versus Temperature

X	$\bar{M}_n \times 10^{-5}$	$\bar{M}_W \times 10^{-5}$	$\frac{\bar{M}_W}{\bar{M}_n}$	$[I_o]$ wt%	T°C	t(Hr)
.10	1.8	4.2	2.3	2.0	0	26
.05	2.2	5.5	2.7	2.0	25	3.33
.13	2.5	6.4	2.6	0.1	50	0.51
.15	2.4	6.1	2.5	0.1	70	0.33
.92	2.0	5.3	2.6	0.1	100	0.41
.35	0.41	1.8	4.4	0.1	120	0.1

			Replicates			
0.15	2.4	5.7	2.4	0.1	70	
0.13	2.2	5.1	2.3	0.1	50	
0.92	1.5	4.4	2.9	0.1	100	
0.92	1.5	4.4	2.9	0.1	100	
0.92	1.5	4.3	2.9	0.1	100	

Table 9-12: Anova Table for 40°C Polymerization

I° wt%	Source	Sum of squares SS	Degrees of freedom ν	Mean squares MS = SS/ν	$\frac{\text{(L.O.F.)MS}}{\text{(P.E.)MS}}$	$F_{0.95}$ $(\nu_{L.O.F.}, \nu_{P.E})$	Is the model adequate
	Residuals	5×10^{-3}	B	6.3×10^{-4}			
0.2	Pure error (P.E.)	1.4×10^{-3}	2	7×10^{-4}	0.857	19.32	Yes
	Lack of fit (L.O.F.)	3.6×10^{-3}	6	6×10^{-4}			
	Residuals	7.1×10^{-3}	13	5.5×10^{-4}			
1.0	Pure error (P.E.)	2.8×10^{-3}	4	7×10^{-4}	0.683	5.99	Yes
	Lack of fit (L.O.F.)	4.3×10^{-3}	9	4.8×10^{-4}			
	Residuals	2.2×10^{-3}	12	1.8×10^{-4}			
0.5	Pure error (P.E.)	2.1×10^{-3}	3	7×10^{-4}	0.016	8.81	
	Lack of fit (L.O.F.)	0.1×10^{-3}	9	0.1×10^{-4}			
	Residuals	0.2×10^{-3}	2	1×10^{-4}			
0.2	Pure error (P.E.)			7×10^{-4}	0.143	3.32	Yes
	Lack of fit (L.O.F.)	0.2×10^{-3}	2	1×10^{-4}			

Table 9-13: Anova Table for 60°C Polymerization

I wt%	Source	Sum of squares SS	Degrees of freedom ν	Mean squares MS = SS/ν	$\frac{\text{(L.O.F.)MS}}{\text{(P.E.)MS}}$	$F_{.95}$ $(\nu_{L.O.F.}, \nu_{P.E.})$	Is the model adequate
0.2	Residuals	2.7×10^{-3}	9	$3. \times 10^{-4}$	0.122	8.89	Yes
	Pure error (P.E.)	2.1×10^{-3}	3	$7. \times 10^{-4}$			
	Lack of fit (L.O.F.)	$6. \times 10^{-4}$	7	0.86×10^{-4}			
0.1	Residuals	2.7×10^{-3}	6	4.5×10^{-4}	0.286	9.28	Yes
	Pure error (P.E.)	2.1×10^{-3}	3	7×10^{-4}			
	Lack of fit (L.O.F.)	0.6×10^{-3}	3	$2. \times 10^{-4}$			
0.075	Residuals	36.4×10^{-3}	33	11.0×10^{-4}	2.1875	2.35	Yes
	Pure error (P.E.)	11.9×10^{-3}	17	$7. \times 10^{-4}$			
	Lack of fit (L.O.F.)	24.5×10^{-3}	16	$15. \times 10^{-4}$			
0.05	Residuals	48.6×10^{-3}	51	9.5×10^{-4}	1.92	1.93	Yes
	Pure error (P.E.)	21.7×10^{-3}	31	7.0×10^{-4}			
	Lack of fit (L.O.F.)	26.9×10^{-3}	20	13.5×10^{-4}			

....continued

Table 9-13: Anova Table for 60°C Polymerization (continued)

I wt%	Source	Sum of squares SS	Degrees of freedom ν	Mean squares MS = SS/ν	$\frac{\text{(L.O.F.)MS}}{\text{(P.E.)MS}}$	$F_{.95}$ $(\nu_{L.O.F.}, \nu_{P.E.})$	Is the model adequate
0.025	Residuals	15.1×10^{-3}	43	3.51×10^{-4}	.026	2.096	Yes
	Pure error (P.E.)	14.7×10^{-3}	21	7×10^{-4}			
	Lack of fit (L.O.F.)	$4. \times 10^{-4}$	22	1.8×10^{-5}			
0.01	Residuals	18.0×10^{-3}	22	8.18×10^{-4}	1.310	2.913	Yes
	Pure error (P.E.)	$7. \times 10^{-3}$	10	$7. \times 10^{-4}$			
	Lack of fit (L.O.F.)	$11. \times 10^{-2}$	12	9.7×10^{-4}			

Table 9-14: Anova Table for 80°C Polymerization

I wt%	Source	Sum of squares SS	Degrees of freedom ν	Mean squares MS = SS/ν	$\frac{\text{(L.O.F.)MS}}{\text{(P.E.)MS}}$	$F_{.95}$ $(\nu_{L.O.F.}, \nu_{P.E.})$	Is the model adequate
0.05	Residuals	12×10^{-3}	8	15×10^{-4}	2.143	2.266	Yes
	Pure error (P.E.)			7×10^{-4}			
	Lack of fit (L.O.F.)	12×10^{-3}	8	15×10^{-4}			
0.025	Residuals	62.43×10^{-3}	16	7.8×10^{-4}	6.27	19.429	Yes
	Pure error (P.E.)	1.4×10^{-3}	2	7×10^{-4}			
	Lack of fit (L.O.F.)	61.4×10^{-3}	14	43.9×10^{-4}			
0.010	Residuals	1.1×10^{-3}	8	1.4×10^{-4}	0.196	2.262	Yes
	Pure error (P.E.)			7×10^{-4}			
	Lack of fit (L.O.F.)	1.1×10^{-3}	8	1.4×10^{-4}			
0.005	Residuals	0.9×10^{-3}	9	1×10^{-4}	0.036	238.88	Yes
	Pure error (P.E.)	0.7×10^{-3}	1	7×10^{-4}			
	Lack of fit (L.O.F.)	0.2×10^{-3}	8	0.3×10^{-4}			

9.3 Qualitative Description of Polyacrylonitrile Degradation via GPC

As it was mentioned in Chapter 4, a drop in the molecular weight averages was observed when the ampoules remained for a long time in the bath after the limiting conversion was reached. This molecular weight drop was attributed to degradation. In order to verify this, solutions containing polymer produced at three different temperatures were heated for several periods of time, quenched and injected in the GPC at room temperature. The chromatograms were analysed and the following results obtained.

i) Polymers produced at high temperatures degrade more easily than those produced at low temperatures, indicating therefore, that the stereoregularity is strongly affected by the polymerization temperature.

ii) The degradation process is very slow compared to the reaction times, and therefore, can be neglected for the purposes of this study.

The GPC responses and the molecular weight averages for the polymers analysed are shown in Figs. 9-1 to 9-3.

9.4 Solubility of the Monomer in the Polymer

To obtain an estimate of the solubility of the monomer in the polymer over the temperature range, 0° - 80°C, the following technique was used.

Films were cast from concentrated solutions of PAN in DMF

(10 wt%). Also polymer rods were prepared polymerizing with low initiator concentrations for very long times. The conversions were measured carefully.

Films and rods were soaked in AN at the given temperature, normally for 24 hours. Once the equilibrium was reached, the films and rods were rapidly quenched at temperatures below 0°C, wiped and weighed. The samples were weighed at several time intervals and equilibrium was assumed when constant weights were obtained.

The films were assumed to be 100% polymer without pores and the rods were corrected for conversion. The equilibrium was reached only by heating the polymer-monomer mixture to a given temperature and therefore the thermodynamical equilibrium has not yet been proved.

The results are shown in Figs. 9-4 and 9-5. The actual values are shown in Table 9-15.

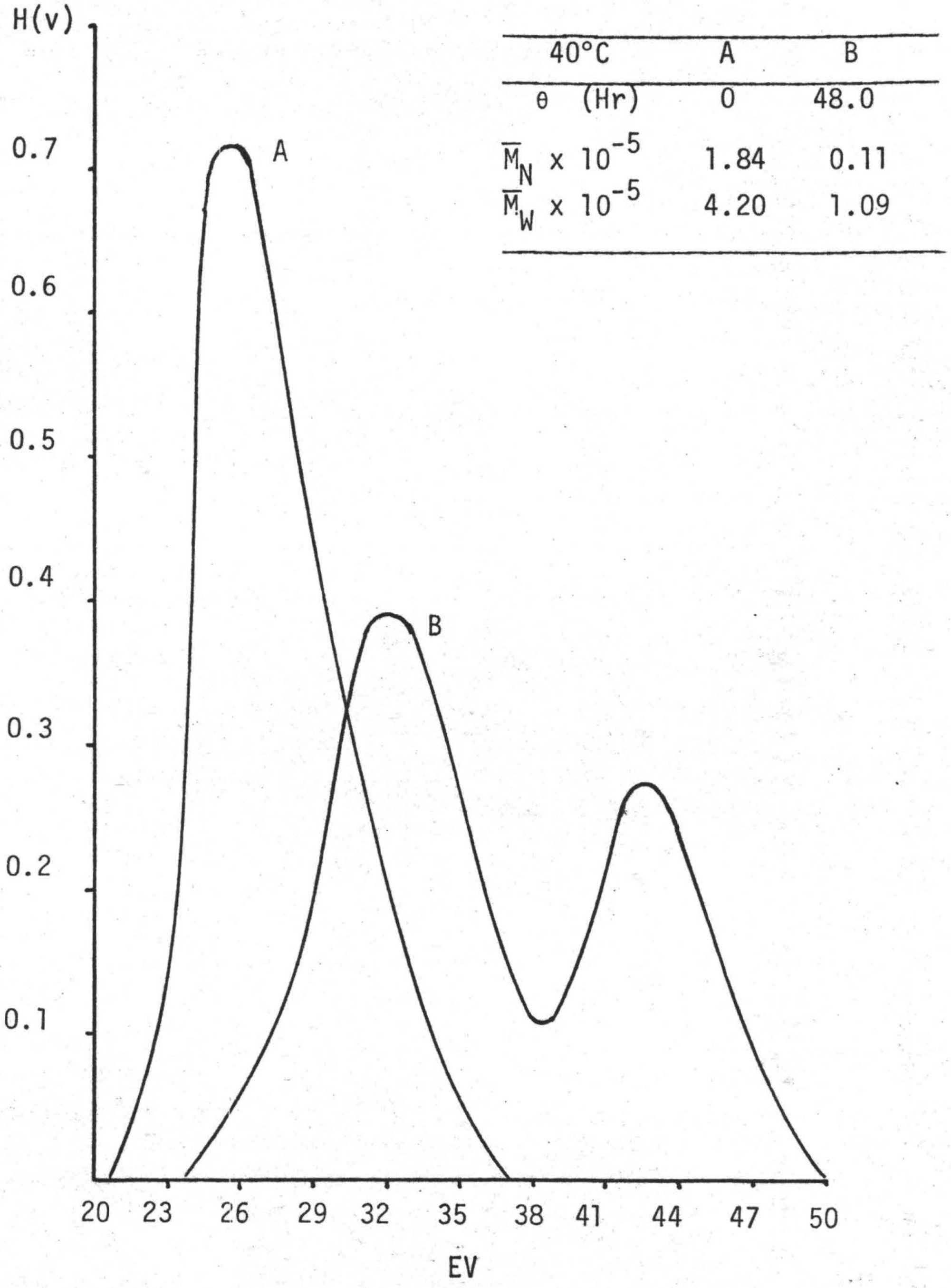

40°C	A	B
θ (Hr)	0	48.0
$\overline{M}_N \times 10^{-5}$	1.84	0.11
$\overline{M}_W \times 10^{-5}$	4.20	1.09

Fig. 9-1: GPC response for polyacrylonitrile thermal degradation at 120°C (polymer produced at 40°C).

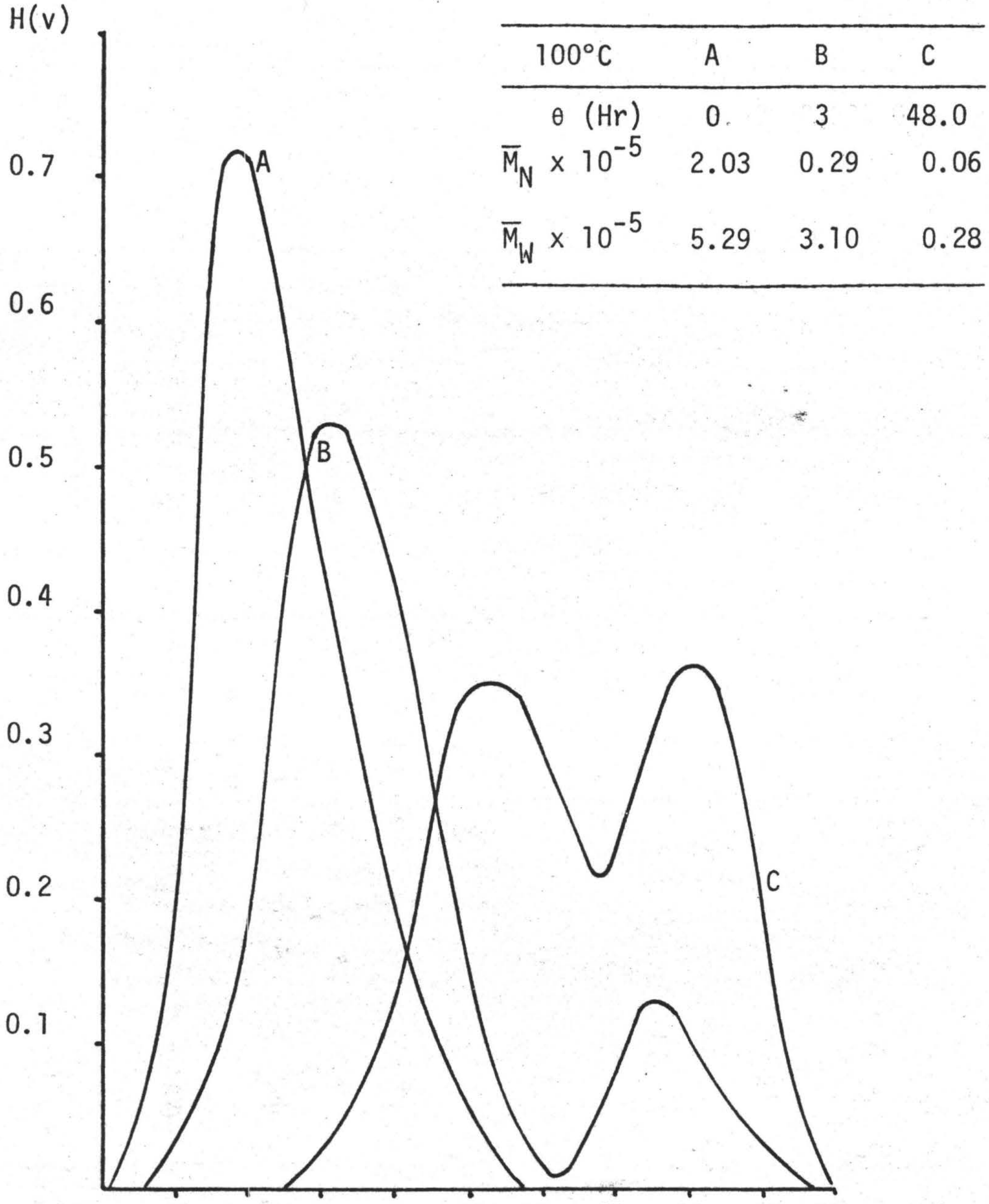

100°C	A	B	C
θ (Hr)	0	3	48.0
$\overline{M}_N \times 10^{-5}$	2.03	0.29	0.06
$\overline{M}_W \times 10^{-5}$	5.29	3.10	0.28

Fig. 9-2: GPC response for polyacrylonitrile thermal degradation at 120°C (polymer produced at 100°C).

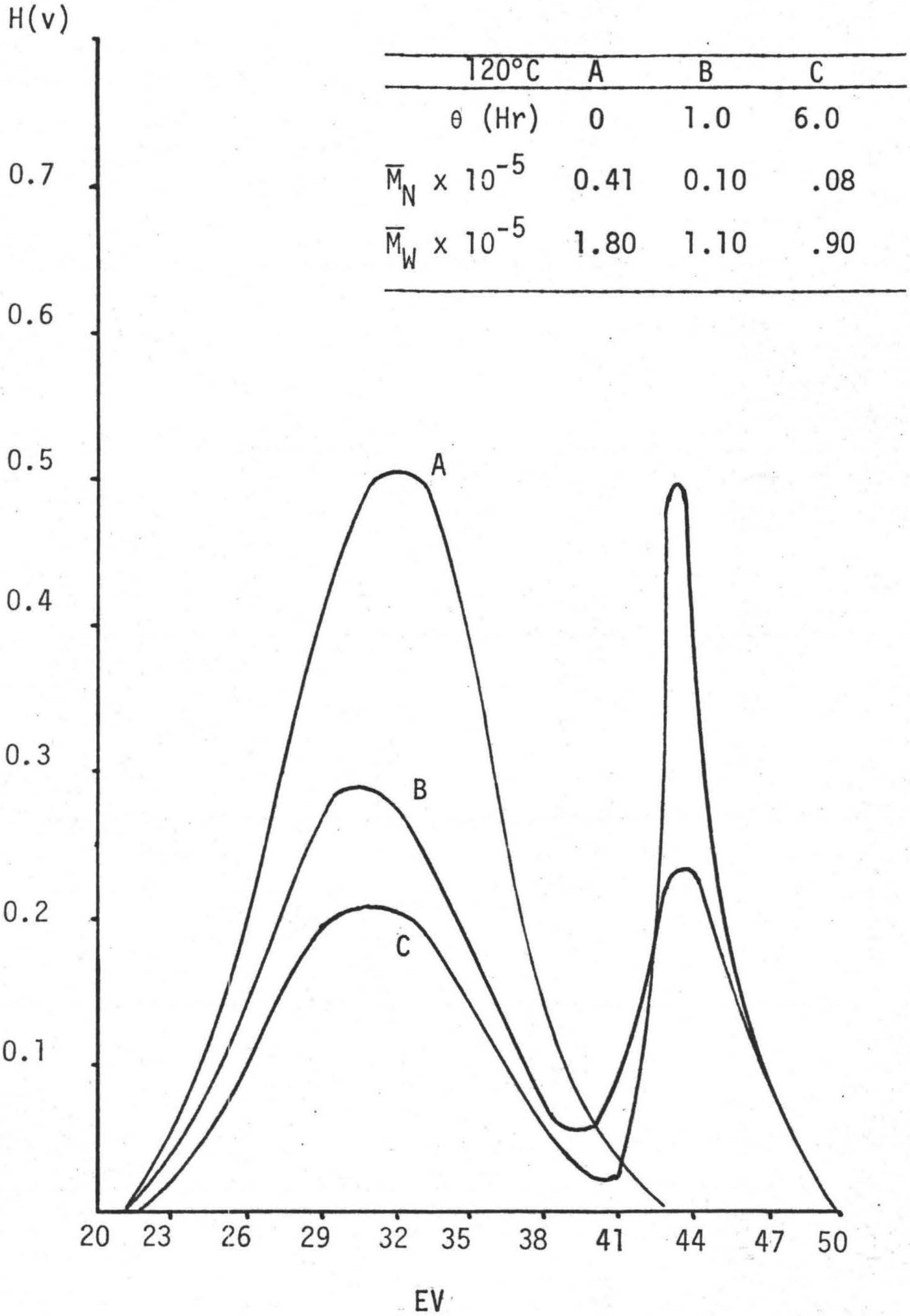

120°C	A	B	C
θ (Hr)	0	1.0	6.0
$\overline{M}_N \times 10^{-5}$	0.41	0.10	.08
$\overline{M}_W \times 10^{-5}$	1.80	1.10	.90

Fig. 9-3: GPC response for polyacrylonitrile thermal degradation (polymer produced at 120°C).

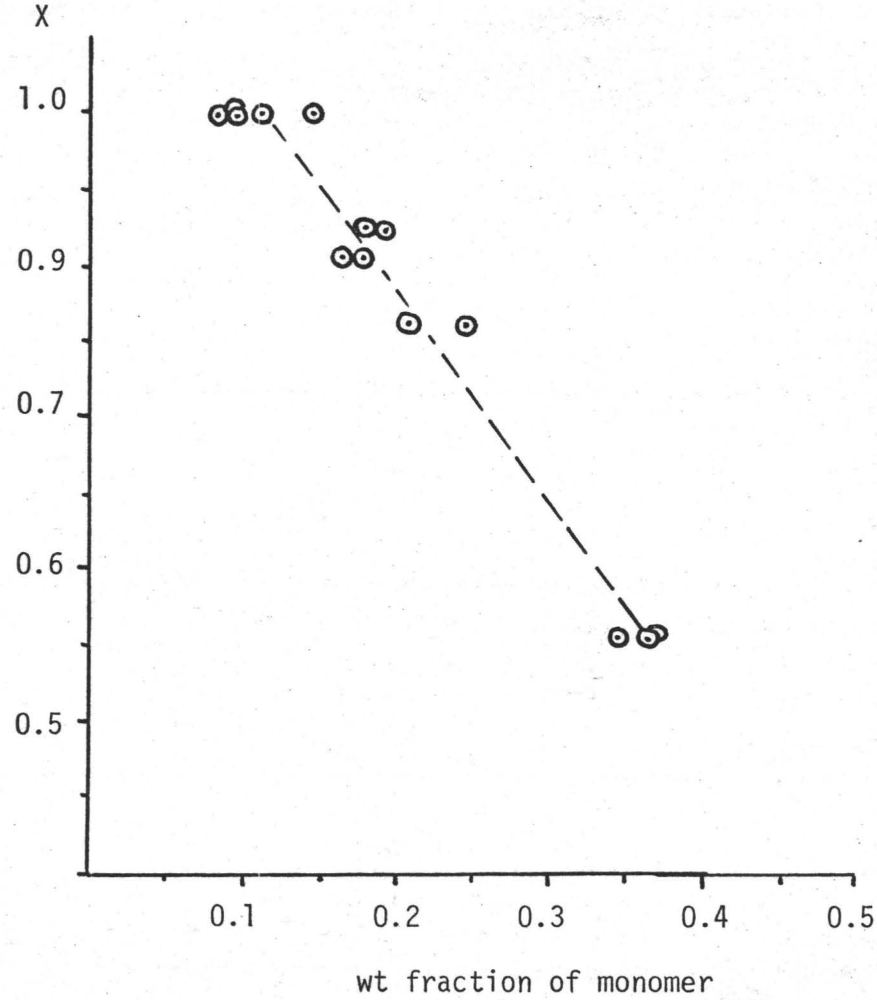

Fig. 9-3: Percentage of monomer in the polymer at 60°C

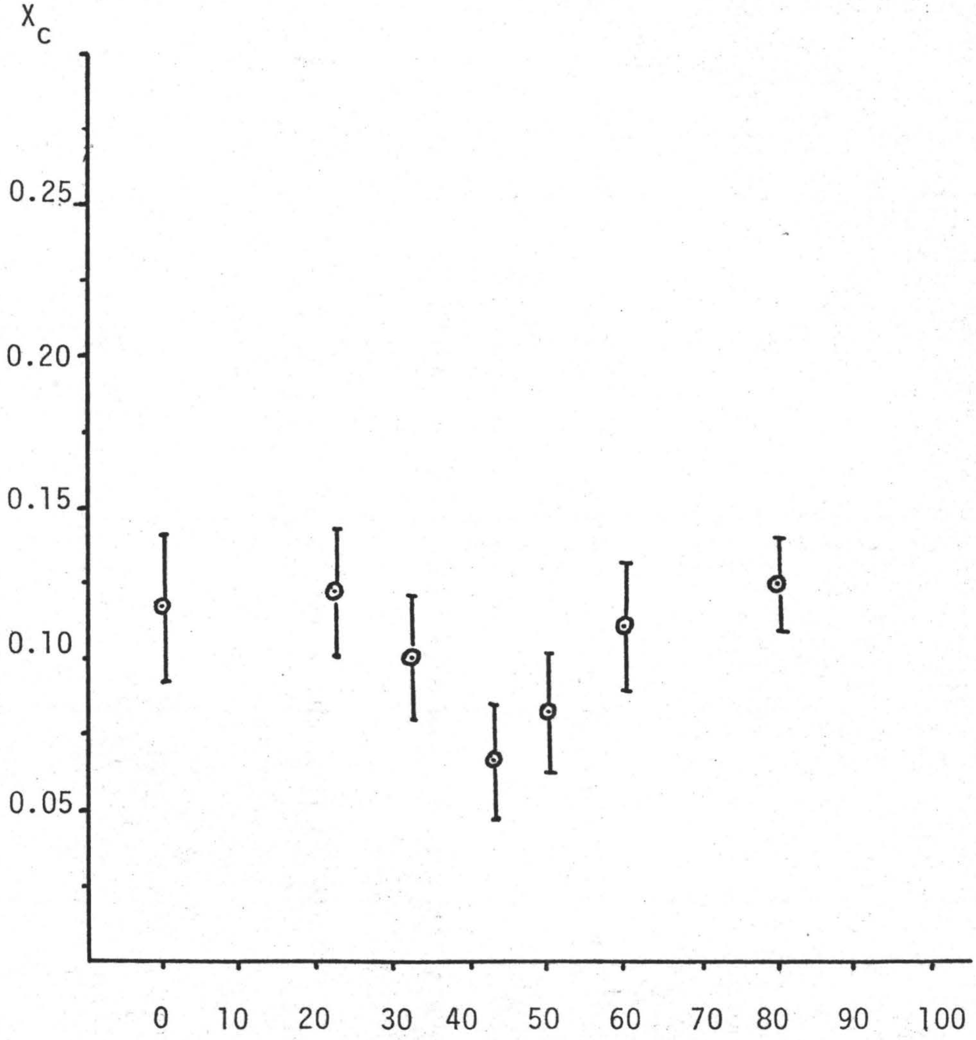

Fig. 9-4: Solubility of the monomer in the polymer.

Table 9-15: Monomer Weight Fraction in the Solution

°C Sample	0°C	23°C	30°C	43°C	50°C	60°C	80°C
1	0.103	0.108	0.142	0.060	0.086	0.133	0.131
2	0.151	0.132	0.122	0.054	0.067	0.085	0.117
3	0.148	0.135	0.105	0.053	0.047	0.100	0.120
4	0.089	0.138	0.095	0.064	0.083	0.149	0.146
5	0.126	0.121	0.105	0.097	0.102	0.117	0.112
6	0.076	0.112	0.094	0.072	0.106	0.091	0.127
7	0.119	0.159	0.075	0.042	0.080	0.104	
8	0.170	0.096	0.085	0.049		0.136	
9	0.118	0.089	0.080	0.046		0.092	
10	0.112	0.115	0.101	0.095		0.079	
11	0.110	0.140		0.077		0.108	
12	0.110			0.080		0.121	
13	0.110						
14	0.101						
$\sum X_i$	1.643	1.345	1.00	0.789	0.571	1.315	0.753
$\bar{X}$	0.117	0.122	0.100	0.066	0.082	0.110	0.126
S^2	0.0001	0.0004	0.0004	0.0003	0.0002	0.0005	0.0002
$S/\bar{X}$	0.213	0.170	0.211	0.282	0.248	0.200	0.097

9.5 Theory of Homogeneous Bulk Polymerization

It is well established that free radical homogeneous bulk polymerization involves the following reaction:

Reaction Step	Reaction	Rate Constant
Initiation: 9.5.1	$\text{Initiator} \longrightarrow 2I$	k_d
9.5.2	$I^{\cdot} + M \longrightarrow R_i$	
Propagation: 9.5.3	$R_i + M \longrightarrow R^{\cdot}_2$	k_p
	$R^{\cdot}_r + M \longrightarrow R^{\cdot}_{r+1}$	
Chain Transfer: 9.5.4	$R^{\cdot}_r + M \longrightarrow P_r + M^{\cdot}$	k_{fM}
9.5.5	$R^{\cdot}_r + I \longrightarrow P_r + I^{\cdot}$	k_{fI}
9.5.6	$R^{\cdot}_r + P_S \longrightarrow P_r + P^{\cdot}_S$	
Termination: 9.5.7	$R^{\cdot}_r + R^{\cdot}_S \longrightarrow P_{r+S}$	k_{tc}
9.5.8	$R^{\cdot}_r + R^{\cdot}_S \relbar\relbar P_r + P_S$	k_{td}

where $I^{\cdot}$ is an initiator fragment radical, M and I are monomer and initiator molecules respectively. $M^{\cdot}$ is monomer radical. $R^{\cdot}_r$ is a polymer radical containing r monomer units and P_r is a dead polymer molecule (usually called dead for irreversible polymerizations).

The initiation step is usually much more complex. For the present, it will be assumed to involve thermal decomposition of the initiator molecule into two radical fragments. These radicals initiate a polymer chain by reacting with monomer molecules. Some radicals may undergo side reactions. The initiator efficiency f is defined as the fraction of radicals which initiates polymer chains.

The chain transfer step involves transfer of the radical activity from an active to an inactive species. The total number of free radicals does not change by transfer reactions, but the molecular weight distribution is strongly affected by them.

Equation 9.5.7 refers by termination by combination while Eq. 9.5.8 refers to termination by disproportionation. The relative rates of these two reactions affect the molecular weight distribution.

If it is assumed that:

1) kinetic stationary-state assumption is valid
2) velocity coefficients are independent of chain length
3) long chain approximation
4) volume change is negligible
5) chain transfer to dead polymer is negligible

The mass balance of free radicals is given by:

$$\frac{d[R^\cdot]}{dt} = R_I - (K_{tc} + k_{td})[R^\cdot]^2 \text{ with } R_I \simeq (k_{tc} + k_{td})[R^\cdot]^2 >> \frac{d[R^\cdot]}{dt} \qquad 9.5.9$$

where

$$[R^\cdot] = \sum_{r=1}^{\infty} [R^\cdot]r \qquad 9.5.10$$

R_I = rate of initiation = $2f_{kd}[I]$

[I] = initiator concentration

From 9.5.9

$$[R^\cdot] = \sum_{r=1}^{\infty} [R_r^\cdot] = [\frac{R_I}{k_{tc} + k_{td}}]^{1/2} \qquad 9.5.11$$

The rate of polymerization in moles of monomer consumed per unit volume per unit time is given by

$$R_P = -\frac{d[M]}{dt} = k_p[M][R^\cdot] \qquad 9.5.12$$

This is by applying the long chain approximation (monomer consumed in reactions other than propagation is negligible).

From 9.5.12 and 9.5.11:

$$R_P = -\frac{d[M]}{dt} = k_p[M][\frac{R_I}{(k_{tc} + k_{td})}]^{1/2} \qquad 9.5.13$$

$$[\frac{R_P}{k_p[M]}]^{1/2} = \frac{R_I}{k_{tf} + k_{tc}}$$

$$R_I = R_P[\frac{k_{tc}R_P}{k_p{}^2[M]^2} + \frac{k_{td}R_P}{k_p{}^2[M]^2} \qquad 9.5.14$$

If we call:

$$\frac{k_{td}R_P}{k_p{}^2[M]^2} = \alpha$$

$$\frac{k_{tc}R_P}{k_p{}^2[M]^2} = \beta$$

$$R_P = \frac{R_I}{\alpha + \beta} \qquad 9.5.15$$

The mass balance for $[R_i]$ may be written as:

$$[R_i] = \frac{R_I + k_{fM}[M][R^{\cdot}]}{k_p[M] + k_{fM}[M] + k_{fI}[I] + (k_{fc} + k_{td})[R^{\cdot}]}$$

and for $r \geqslant 2$

$$[R^{\cdot}_r] = \frac{k_p[M][R^{\cdot}_{r-1}]}{k_p[M] + k_{fM}[M] + k_f[I] + (k_{tc} + k_{td})[R^{\cdot}]}$$

$$[R_i] = \phi[R_{r-1}]$$

therefore

$$[R_i] = \phi[R_i]$$

In general:

$$[R^{\cdot}_r] = \phi^{r-1}[R_i]$$

If we define:

$$T = \frac{k_{fM}}{k_p} + \frac{k_{fI}[I]}{k_p[M]} \quad \text{and} \quad \tau = t + \alpha \qquad 9.5.16$$

therefore

$$\phi = \frac{1}{1 + \tau + \beta}$$

$$[R_i] = \frac{(R_p/k_p[M])(\tau + \beta)}{(1 + \tau + \beta)}$$

The mass balance equations for the dead polymer:

$$\frac{d[P_r]}{dt} = R_p\tau(\tau + \beta)\phi^r + R_p\,\frac{\beta}{2}(\tau + \beta)^2 r\phi^r \qquad 9.5.17$$

The instantaneous differential molecular weight distribution (DMWD) may be written as

$$W(r) = \frac{r[P_r]}{\int_0^t R_p dt} = \tau(\tau + \beta)r\phi^r + \frac{1}{2}\,(\tau + \beta)^2 r^2 \phi r \qquad 9.5.18$$

where W(r) is the weight fraction of polymer of chain length r. The following is a good approximation:

$$\phi^r = (1 + \tau + \beta)^{-r} = \exp(-\,(\tau + \beta)r)$$

Then:

$$W(r) = (\tau(\tau + \beta) + \frac{1}{2}\,\beta(\tau + \beta)^2 r)r\,\exp[-\,(\tau + \beta)r] \qquad 9.5.19$$

Applying the method of moments, it may be readily shown that the instantaneous average chain lengths may be expressed as:

$$\bar{r}_N = (\tau + \frac{\beta}{2})^{-1} \qquad 9.5.20$$

$$\frac{\bar{r}_W}{\bar{r}_N} = \frac{2(\tau + \frac{3}{2}\beta)(\tau + \beta/2)}{(\tau + \beta)^2} \qquad 9.5.21$$

where $\overline{r}_N$ is the number average chain length, $\overline{r}_W$ is the weight average chain length and $\overline{r}_W/\overline{r}_N$ is the polydispersity.

EQuation 9.5.21 shows that the measured polydispersity gives a good idea about the mode of termination. For example:

$$\text{if } \beta >> \tau \quad \frac{\overline{r}_W}{\overline{r}_N} = 1.5$$

Therefore the termination is by combination.

$$\text{if } \beta << \tau \quad \frac{\overline{r}_W}{\overline{r}_N} = 2$$

Therefore termination by combination is negligible in controlling MWD.

If the polydisperisty is equal to 2.0 at all conversion, transfer to monomer is dominant in controlling MWD.